



<https://theses.gla.ac.uk/>

Theses Digitisation:

<https://www.gla.ac.uk/myglasgow/research/enlighten/theses/digitisation/>

This is a digitised version of the original print thesis.

Copyright and moral rights for this work are retained by the author

A copy can be downloaded for personal non-commercial research or study, without prior permission or charge

This work cannot be reproduced or quoted extensively from without first obtaining permission in writing from the author

The content must not be changed in any way or sold commercially in any format or medium without the formal permission of the author

When referring to this work, full bibliographic details including the author, title, awarding institution and date of the thesis must be given

Enlighten: Theses

<https://theses.gla.ac.uk/>
research-enlighten@glasgow.ac.uk

**STRUCTURAL STUDIES WITH THE
ELECTRON MICROSCOPE**

by

Katharine E. Carr,

Department of Chemistry, University of Glasgow.

Intercalation and Oxidation

of graphite with sulphuric acid

Thesis submitted for the degree of

Doctor of Philosophy,

July, 1965.

ProQuest Number: 10984206

All rights reserved

INFORMATION TO ALL USERS

The quality of this reproduction is dependent upon the quality of the copy submitted.

In the unlikely event that the author did not send a complete manuscript and there are missing pages, these will be noted. Also, if material had to be removed, a note will indicate the deletion.



ProQuest 10984206

Published by ProQuest LLC (2018). Copyright of the Dissertation is held by the Author.

All rights reserved.

This work is protected against unauthorized copying under Title 17, United States Code
Microform Edition © ProQuest LLC.

ProQuest LLC.
789 East Eisenhower Parkway
P.O. Box 1346
Ann Arbor, MI 48106 – 1346

ACKNOWLEDGMENTS

Thanks are extended to Professor J. M. Robertson for the use of the facilities of the Chemistry Department and to Dr. I. M. Dawson for his supervision of the work.

Thanks are also due to the technical staff of the electron microscopy unit and in particular to Mrs. Violet Fraser.

(iii)

Introduction - Contents

I. Structure

- (i) Ideal Lattice
- (ii) Possible Defects (a) Stacking Disorder.
(b) Defects in the layers.
- (iii) Band Theory of Graphite.
- (iv) Crystallographic Description of Graphite.
- (v) Diffraction Patterns of Graphite.
- (vi) Double Diffraction and moiré formation.
- (vii) Electron microscopy of layer structures.

II. Intercalation

- (i) General
- (ii) Bisulphate reaction (a) Preparation and properties.
(b) Composition and structure.
(c) Graphite bisulphate residue compound.
- (iii) Graphite oxide (a) Preparation and Properties.
(b) Composition and Structure.
- (iv) Study of Intercalation Compounds by Electron Microscopy and Diffraction.
(a) Lamellar and residue compounds.
(b) Graphite Oxide.

III. Oxidation of Graphite

- (i) General gaseous oxidation.
- (ii) Microscopy of Graphite Oxidation.
- (iii) Oxidation of Graphite by atomic oxygen.
- (iv) Chemical oxidation of graphite.

IV. Aim of the Present Work.

INTRODUCTION

I. STRUCTURE.

(i) Ideal lattice. The crystal structure of graphite has been extensively studied using X-ray techniques since the work of Ewald (1914) and Bernal (1924). The material is found to have a layer structure with a distance of 3.3538\AA (Franklin, 1951a) between successive layers and much work has been done on this dimension by Franklin (1950, 1951b) and Bacon (1951, 1958a and b).

The layers themselves are composed of infinitely large, flat sheets of fused, benzenoid carbon rings, with the atoms bound by sp^2 bonding. The carbon-carbon distance in these rings is quoted by Trezbiatowski (1937) as 1.413\AA , and more recent work on the variation of this dimension has been done by Bacon (1950, 1958a and b), Bacon and Franklin (1951) and Bacon and Warren (1956) and this is discussed by Bacon (1958b) using the random-layer explanation.

The layers of carbon atoms are arranged regularly relative to each other as well as being stacked in a parallel fashion. Two main stacking methods have been accepted. The first, or hexagonal form, suggested by Bernal (1924) has the well-known ABAB stacking. The other type of idealised stacking, suggested by Laidler and Taylor (1940) and Lipson and Stokes (1942a and b) and

termed the rhombohedral form, consists of ABCABC stacking, where the third layer of carbon atoms has the same orientation with respect to the second as the second has to the first. That both of these modifications exist in natural graphite was shown by Finch and Wilman (1936) and Boehm and Hofmann (1955) and it has been proved that mechanical treatment (Bacon, 1950, 1952) heating (Boehm and Hofmann, 1955) and chemical treatment (Laidler and Taylor, 1940 and Lukash, 1951 a and b) are able to convert one form to the other, presumably by promoting slip of the layers relative to each other. The relative ease with which the layers can glide over each other is indicated by the low stacking fault energy as given by Baker, Chou and Kelly (1961).

(ii) Possible defects in such an ideal structure.

These defects are of two main types (a) defects in the relative positions between the layers (or stacking disorder) and (b) defects in the structure of the sheets themselves (Ubbelohde and Lewis, 1960).

(a) Stacking disorder. It is possible for the perfect graphite layers to be arranged in a parallel fashion but to be displaced from the ABAB or ABC ideal stackings. This stacking, or turbostratic, disorder has been studied

using X-ray techniques by authors such as Warren (1934), Franklin (1951c) and Bacon (1951) since it was found that the interlayer spacing is dependent on the degree of stacking disorder present in the crystal. Various empirical equations have been described defining d , the mean overall layer spacing in terms of p , the probability of an error of stacking between successive planes (Franklin, 1951c and Bacon, 1950, 1951, 1952, 1958b).

Such stacking fault disorder can be caused by the presence of interstitial atoms which may be carbon atoms knocked out of their sites during irradiation (Bollmann, 1960, 1961a,b,c) or intercalated atoms (Heerschap, Delavignette and Amelinckx, 1964). Alternatively, stacking faults are formed in graphite by the dissociation of perfect dislocations into partials, with fractional Burgers Vectors. The region between such partials is then a stacking fault (Read, 1953 and Friedel, 1964).

(b) Defects in the layers. In this type of defect, the aromatic carbon sheets can be altered or broken in places, leading to the formation of a new bond, for example with an impurity such as oxygen, or forming some type of hole defect (Ubbelohde, 1952, Ubbelohde and Lewis, 1960).

Such vacancies can be caused by irradiation of the graphite, which knocks one or more carbon atoms out of place, leaving hole defects. Another type of defect

present in the layer is the twin plane which is produced by tilting of the layer planes, and can be introduced during growth. They have been studied by X-ray and electron microscope techniques (Lukesh, 1950, Freise and Kelly, 1961, Freise, 1962, Freise and Kelly, 1963, Thomas, Hughes and Williams, 1963, and Baker, Gillin and Kelly, 1965).

Many of the defects described here are most conveniently studied with electron microscope techniques and the extensive work done on this subject will be dealt with more fully in Section I (vii) of this Introduction.

(iii) Band Theory of Graphite. According to the work by Coulson (1947) there are two basic kinds of electrons in graphite, those in the plane of the layers, forming sp^2 hybridised bonds which give the valence band, and the mobile or conduction electrons which are not localised and thus give graphite its metallic characteristics. The π band is symmetrical and falls to zero in the middle. The complete band has 2 electrons per atom, but since there is only one π electron available per atom for graphite, this band is exactly half full. Since there is a zero energy gap between the full and empty parts of this band (Wallace, 1947, Coulson, 1947) it is very simple for electrons to be promoted into the conduction band (Carter and Krumhausl, 1953 and Coulson and Taylor, 1952). Thus at $0^\circ K$ the conduction band is empty, and at room temperature promotion

can take place from the valence band, making graphite an intrinsic semi-conductor and explaining many features of its physical properties (Mrozowski, 1950a, b, Kmetko, 1951, Mrozowski, 1952a, b, Tyler and Wilson, 1953, Hove, 1955, Hooker, Ubbelohde and Young, 1963). The further importance of this band structure of graphite will be discussed in Section II, in relation to the formation of intercalation compounds.

(iv) Crystallographic description of graphite. The graphite lattice has hexagonal symmetry and four reference axes are generally used, three (a_1 , a_2 and a_3) in the plane of the layers at 120° to each other, and the fourth (c) perpendicular to the layers. Four Miller indices are therefore used (h , k , $\overline{h+k}$, l) although the third is technically unnecessary since any plane can be defined by the other three, and is only used because it makes clear some of the symmetry relations of graphite which would otherwise not be obvious. For indexing planes, the unit length along any a axis is taken as one side of the carbon hexagon and the c axis unit is defined as twice the distance between the layers for the ABAB hexagonal stacking.

There are two main types of planes of importance in the diffraction patterns of graphite: a) ~~hk $\overline{h+k}$ l~~ planes, such as $10\overline{1}0$ and $11\overline{2}0$ which are parallel to the c axis, their lattice spacings giving information only about distances

inside the layers themselves and b) oool planes such as 0002, which are in the plane of the layers, their d spacings giving the distance between the layers.

The projection of the crystallographic unit cell on the basal plane is shown in Fig.(i) and is that originally proposed by Bernal (1924). The cell is ABCD, with $AB = 2.45\text{\AA}$, giving the crystallographic 'a' of 2.45\AA , which is not identical to the hexagon side 'a'.

(v) Diffraction patterns of graphite. The typical electron diffraction pattern as described by Finch and Wilman (1936) when the beam of electrons is perpendicular to the layers, consists of a spot pattern from single crystal material, with the $10\bar{1}0$ and $11\bar{2}0$ reflections strongest. The pattern from polycrystalline material shows the same planes, this time in typical ring form. These in-plane diffraction patterns have been described by Dawson and Follett (1959) using an electron microscope for the diffraction.

When the diffraction pattern is obtained from X-ray powder photographs planes of both type a) and b) described in (iv) above reflect and there is a spectrum of about twenty lines starting from 0002 which gives the distance between the graphite layers. The subject of X-ray powder diffraction of graphite has been well reviewed in a report by Bacon (1958b).

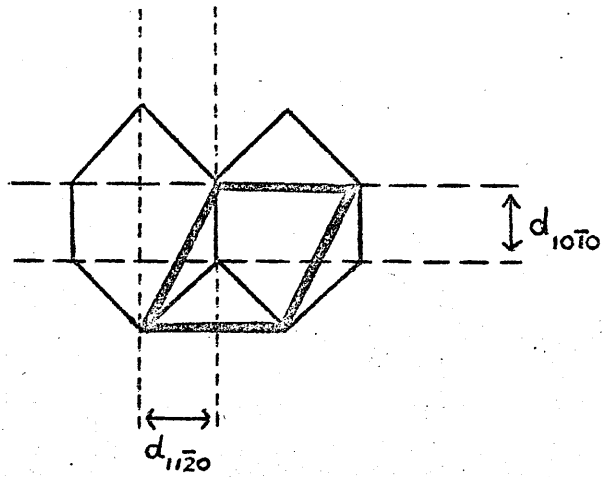


FIGURE (i)

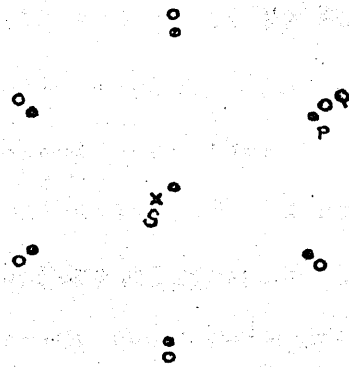


FIGURE (ii)

(vi) Double diffraction and moiré formation. In 1956, Menter showed that the image of a crystal lattice can be formed in the electron microscope by interference in the image plane between the direct, zero order beam and the first order diffracted beam arising from the set of planes resolved. He thus imaged directly planes of copper and platinum phthalocyanine. A similar interference explanation has been given for the formation of moiré patterns. These patterns, consisting of parallel lines or arrays of spots, were first seen in the electron microscope image of graphite by Mitsuishi, Nagasaki and Uyeda (1951). They were noticed also on sericite by Seki (1953), mica by Rang (1953), iron oxide by Hillier (1954), boron nitride by Goodman (1957), molybdenum oxide by Dowell, Farrant and Rees (1958) and on polyethylene by Agar, Frank and Kelly (1959). The explanations that they were moiré patterns, arising from match and mismatch of two overlapping lattices (Hillier, 1954) or interference fringes arising from interference with the zero order beam were brought together by Dowell, Farrant and Rees (1954, 1958) and both explanations were shown to be linked. In the paper of Bassett, Menter and Pashley (1958) the theories are given for two types of moiré formation. The first is formed by fortuitous lattice overlap giving an angle of rotation (α) between two crystallites. It is found that if the lattice spacing

is d , then the moiré pattern spacing will be d/α , thus showing that the pattern gives a magnified image of planes present in the crystal. The second type of pattern is formed by the superposition of two lattices with different spacings d_1 and d_2 , as described by Pashley, Menter and Bassett (1957) using gold combined with copper, nickel, platinum, cobalt and palladium. The spacing finally obtained by the superposition of parallel reflecting planes is given by $d_1 d_2 / (d_2 - d_1)$.

The explanation as given by Bassett, Menter and Pashley (1958) will be summarised briefly for the latter case. Fig. (ii) shows the diffraction pattern from two superposed lattices. Two sets of spots are seen, corresponding to the two crystal lattices. One example of a third type of spot is also seen (S), which has been diffracted in opposite senses by each of the two lattices in turn so that the spot, instead of appearing at P will be diffracted to give a final spot at S. Thus a set of doubly diffracted spots will appear round the zero order beam and will interfere with it to give the moiré pattern associated with the two lattice spacings. If these extra spots round the centre are cut out by a small aperture then the pattern will disappear, as shown by Dowell, Farrant and Rees (1958).

A useful optical analogue is described by Bassett, Menter and Pashley (1958) for the formation of a spot moiré

by superimposing two spot gratings. The diffraction pattern shows the extra spots around the central beam as described above, and if these two interfere, a moiré pattern consisting of dots is formed. Lattices can give a spot moiré in the same way and the final pattern is shown by Dowell, Farrant and Rees (1954, 1958) to be related to the Patterson distribution for that lattice. Thus for a spot moiré the final pattern is related to the positions of the atoms in the lattice instead of the positions of planes as for a line moiré.

(vii) Electron Microscopy of layer structures, such as graphite. A compound composed of parallel sheets such as graphite lends itself well to the preparation of thin flakes for transmission microscopy by cleavage with adhesive tape (e.g. Boswell, 1961) or preparation by thin section cutting (Dawson and Follett, 1959). One of the most distinctive features of graphite is the appearance of moiré patterns on thin specimens examined with the electron microscope, as observed originally by Mitsuishi, Nagasaki and Uyeda (1951), Grenall (1958) and Dawson and Follett (1959). The last-named authors reported the appearance of extra terminating half-lines in the pattern and, in agreement with the general cases discussed by Hashimoto and Uyeda (1957) and Menter (1958), they related this to the presence of a dislocation in the lattice.

This interpretation has, however, been criticised by Williamson and Baker (1960a). The use of moiré patterns, particularly using dark field illumination, for producing an image of various types of defects in the graphite structure after irradiation, has been discussed by Bollmann (1960, 1961a,b,c), Williamson and Baker (1961a), Williamson (1961) and Baker (1962).

Such applications of moiré patterns, though leading to interesting results, are fundamentally indirect methods of examining a crystal and its defects. A direct and powerful method for observing dislocations with the electron microscope depends on diffraction contrast effects arising from the interaction of the electron beam with the displaced atoms in the strain fields round dislocations. This technique is based on the papers of Hirsch, Horne and Whelan (1956), Whelan and Hirsch (1957a,b), Whelan, Hirsch, Horne and Bollmann (1957), Hirsch, Silcox, Smallmann and Westmacott (1958), Hirsch, Howie and Whelan (1960) and the theory has been reviewed by Howie (1961), Howie and Whelan (1961) and Gévèrs (1963). These ideas have been applied to the study of dislocations in graphite by Tsuzuku (1957), Grenall (1958) and Grenall and Sosin (1960). The last-named authors used ciné photography in conjunction with electron microscopy to record the extensive movement of dislocations when subjected to either the stresses of

heating in the microscope, or the presence of contamination.

The interaction of dislocations with crystal step edges and impurities has been described by Bacon and Sprague (1961b) and Siems, Delavignette and Amelinckx (1962) and the interaction of two sets of dislocations, appearing as arrays of parallel lines in the micrographs, to give nets which often have hexagonal symmetry has been reported by Boswell (1961) among others.

This study of dislocations and their interactions for graphite has been dealt with thoroughly by Williamson and Baker (1958, 1960a,b, 1961b) Amelinckx (1956), Amelinckx and Delavignette (1960a,b,c), Delavignette and Amelinckx (1960, 1961) and Bollmann (1962). The subject has been reviewed by Amelinckx (1963), Amelinckx and Delavignette (1961, 1963) and Gèvers (1963) who summarise the many previous publications.

The splitting of perfect dislocations into partials is one of the important features of this theory. The region between the two partials is a stacking fault corresponding to a thin strip of material where the stacking sequence has been altered, for example, ABCA instead of ABAB: this is borne out by the fact that rhombohedral graphite diffraction patterns are observed when the concentration of dislocations is large, for example on heavily ground graphite (Bacon, 1950, 1952). These partial dislocations can interact with each other to produce a

central triangular region of stacking fault seen by its different contrast characteristics and containing an extended node and also a contracted node where the partials actually cross.

The dislocations described above are all observed in the form of lines, but the electron microscope has been used to examine dislocation loops (Williamson, 1961) and vacancy and interstitial clusters (Reynolds, Thrower and Sheldon, 1961, Reynolds and Thrower, 1964 and Bollmann and Hennig, 1964). In the review paper of Amelinckx (1963) the applications of this technique to the investigation of some of the properties of layer structures is described. In particular, the Burgers Vector of a dislocation can be determined by finding under what conditions it is invisible in dark field (Hirsch, Howie and Whelan, 1960). Since the dislocations are visible by virtue of their effect on the intensity of the Bragg reflections, if the displacements around the defect are parallel to the strong reflecting plane used for dark field illumination, the dislocation will lose its effect on the illuminating beam and will disappear. Thus by finding the diffraction vector of the spot used for illumination when a dislocation becomes invisible, the Burgers Vector can be calculated, since it is perpendicular to the vector of the diffraction spot.

The direct study of layer structures containing dislocations gives information on the situation of any

areas containing stacking faults, and methods have been given (Amelinckx and Delavignette, (1963) for calculating stacking fault energies from the width of the areas of fault separating the partials.

II INTERCALATION.

(i) General. It has long been known that graphite, if put into contact with various reagents, swells, changes colour and eventually disintegrates. The whole class of substances thus made is termed intercalation compounds, a name which describes the insertion of reagent in between the graphite layers, thus increasing the c axis spacing. Many investigations into their chemistry and structure have been made and a large amount of work was done on their preparation by Croft (Croft and Thomas, 1951 and Croft, 1952, 1953, 1956a,b,c,d, 1957a,b) and the subject has been excellently reviewed by Riley (1945a,b), Hennig (1959a), Croft (1960) and Ubbelohde and Lewis (1960).

Hennig's review divides the compounds into three general classes: a) non-conducting, b) lamellar and c) residue.

(a) Non-conducting. In these the bonding is described as covalent, with the layers assuming a wavy form because of the reversion of the carbon bonding to sp^3 hybridised tetrahedral bonding. The resonance in the bond system of

the sheets is removed as a result, leading to the light colour of the compounds (Croft, 1960). As their name suggests, these compounds have lost the conducting properties which are found in graphite and are associated with its electronic structure. The chief example of this class is graphite fluoride (CF_n) prepared by Ruff and Brettshneider in 1934. The c spacing expands from 3.35\AA in graphite to 8\AA (Rüdorff and Rüdorff, 1947a,b) and the fluorine is attached by a covalent bond at the tetrahedral carbon bond normal to the original graphite layers.

Graphite oxide, which will be fully discussed below since it is one of the compounds examined in this work, is sometimes included in this group (Croft, 1960) though there is some disagreement as to the validity of this choice (Hennig, 1959a, Ubbelohde and Lewis, 1960).

(b) Lamellar Compounds. The bonding in this case is described as ionic, although there may also be some electrostatic character, and this bonding is possible because of the electronic structure of graphite. The formation of this type of compound is accompanied by a change in the electrical and magnetic properties (McDonnell, Pink and Ubbelohde, 1951, Hennig and McClelland, 1955, Hennig, 1956, 1960a, Ubbelohde, 1961). Excited electrons in the upper energy levels of graphite may be transferred to the intercalated material, or electrons may be given from the inter-

calate to unfilled graphite bands. This subdivision according to change in electronic structure has been conveniently described by Dzurus and Hennig (1957) as a distinction between **P**- and **N**-type lamellar compounds, using terminology similar to that applied to semi-conductors. Examples of the former are graphite bisulphate and nitrate and examples of the latter are graphite-ammonia. A study of this aspect of intercalation compounds and the possibilities of their controlled preparation by electrochemical means has been made by Bottomley, Parry, Ubbelohde and Young (1963) and Ubbelohde (1964).

The graphite layers in this class of intercalation compounds retain their flat aromatic graphite character and the only change in the structure ρ , as found by the X-ray studies, is that the c-spacing has been expanded at least 2-fold, by the insertion of the layers of reagent. The exact c-spacing of any particular lamellar compound depends on whether there is one layer of reagent to every one, two, three or more sheets of graphite.

(c) Residue Compounds. The lamellar compounds described in (b) are stable only in the presence of excess reagent. When they are exposed to water, heat, or even air in some cases, they lose some of their intercalated material. It is found that a definite proportion of the intercalate is tenaciously retained, however, giving what

are known as residue compounds. The composition of these depends on that of their parent lamellar compound, but the composition of the residue compound obtained, for example, from the fully intercalated lamellar compound is reproducibly constant. The residual reagent in these compounds is supposed by Hennig (1952) and Ubbelohde (1957) to be trapped at crystal imperfections, whereas Maire and Mering (1959) observed X-ray lines of bromine in the bromine residue compound and suggested that there are present single layers of intercalate at the interfaces between perfect and imperfect graphite layer planes.

(ii) Bisulphate reaction.

(a) Preparation and properties. The reaction of graphite with concentrated sulphuric acid containing a drop of nitric acid was first reported by Schafhäütl in 1841. The graphite swells, turns an iridescent dark blue and breaks up. The compound thus formed, called blue graphite, was studied by Thiele (1932) who showed that it could be formed by the reaction of graphite with concentrated sulphuric acid in conjunction with numerous oxidising agents other than nitric acid, for example, chromic oxide. The compound produced is the lamellar bisulphate compound and the reaction is reversed by contact with water or air, to give the residue compound. It was reported by Rüdorff and Hofmann (1938) that cleaning the lamellar compound with

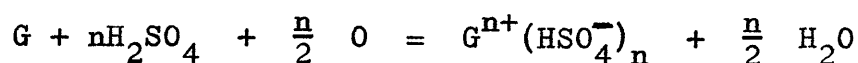
pyrophosphoric acid enabled it to be isolated, without the residue compound being formed.

Graphite bisulphate is a P-type compound and its physical and electronic properties have been studied by Krishnan and Ganguli (1939), Kmetko (1953), Mrozowski (1953) and Hennig (1951). The last author suggests that in graphite most electrons are in one energy band, except for a small number which are excited into a nearby empty one, the current carrier thus being excited electrons in the latter and vacancies in the former. On formation of graphite bisulphate, the lower band is further depleted by donation to the intercalate, but the number of excited electrons in the upper band is depleted to a smaller extent. This change in the electronic structure Hennig correlates with the alteration in the electronic properties, for example, conductivity.

(b) Composition and structure. As described above, Hofmann and Rüdorff (1938) prepared the bisulphate compound using sulphuric and nitric acids and Rüdorff (1939) used chemical, pycnometric and X-ray diffraction means to elucidate the composition and structure. The hexagon layer planes of the graphite are unchanged, but bisulphate ions and sulphuric acid molecules have penetrated between them. It was found there were several stages in the reaction, each with a characteristic formula and X-ray pattern. The final stage, called stage one, had a layer

spacing of 7.89Å, corresponding to alternate layers of graphite and intercalated material and the next stage had a larger C spacing, corresponding to a layer of acid in every alternate row. There are other, similar compounds with a smaller amount of acid intercalated. Hofmann and Rüdorff (1938) suggested that the anions and acid molecules in the stage one compound are arranged in a triangular packing relative to the carbon atoms. From the fact that the $10\bar{1}0$ and $11\bar{2}0$ lines in the diffraction pattern have not changed on the formation of the bisulphate compound, it is presumed that there is no change in the hexagonal sheets of the graphite.

The equation given normally (Riley, 1945) for the reaction is:-



The carbon planes become macrocations. The idealised stoichiometric composition is given as $C_{24}^+ HSO_4^- 2H_2SO_4$. Hennig (1951) reports that a third of the sulphuric acid present is ionised and in the form of bisulphate ion.

(c) Graphite bisulphate residue compound. When the reaction is reversed, the stage one compound is decomposed through the intermediate stages by a process (Rüdorff, 1939) involving redistribution of the sulphate layers. When the reversal process is completed, the residue compound

proper is obtained, with an X-ray pattern identical to that of graphite. According to Hennig (1951) this compound retains approximately one third of the intercalated bisulphate ion and one half of the sulphuric acid present, and the material remaining is trapped in a high state of disorder.

(iii) Graphite Oxide.

(a) Preparation and properties. This substance, originally called graphitic acid (Hofmann and König, 1937, Hofmann and Holst, 1939) was first prepared by Brodie (1859) by oxidising graphite with fuming nitric acid and potassium chlorate and since the work of Berthelot and Petit (1870) this reaction was used to distinguish graphite and graphitisable carbons from non-graphitisable carbons (Maire and Mathieu-Sicaud, 1952, Maire, 1951) since only the former group of compounds will give graphite oxide. Various standard methods of preparation have been used, for example, Staudenmaier (1898, 1899, 1900) and Hummers and Offeman (1958) who report a method of preparing the oxide with only one application of the oxidising agent which in this case was a mixture of concentrated sulphuric acid, potassium permanganate and sodium nitrate.

Graphite oxide is a colloidal material which is yellow when wet and dark brown (Ganguli, 1936) when dry. The preparation is accompanied by colour changes from

black graphite through blue and green intermediate stages to the final yellow compound.

(b) Composition and structure. The material is highly oxidised, as is indicated by the ratios of carbon to oxygen quoted by Boehm, Clauss and Hofmann (1961) as 2.53 to 2.83/1, by Staudenmaier (1898, 1899, 1900) as 2.9/1 and by Hummers and Offeman (1958) as 2.3/1. The material swells in water and other polar solvents (Ruiz, Cano and Macewan, (1955)). For example, when the composition indicates that 8% of the weight is water, the C spacing is 9.2Å, whereas when there is 35% of water present, the spacing has increased to 11.3Å (Hofmann and Frenzel, 1930). The latter value for the layer spacing of the oxide represents the fully hydrated compound and any further washing of the substance with water leads to dispersion of the sheets to form a gel-like mass probably composed of two dimensional macromolecules.

There has been much disagreement as to the bonding of the large amount of oxygen present in graphite oxide and the nature of the carbon sheets. Hofmann and Holst (1939) suggested that some of the oxygen is bound as ethylene oxide and Ruess (1946a,b) suggested that the rest of the oxygen formed occasional tertiary hydroxide groups. This structure was criticised by Clauss, Plass, Boehm and Hofmann (1957) on the grounds that the compound has none

of the properties typical of these groups.

A structure such as this one proposed by Ruess (1946) demands that the carbon-atoms should form tetra-valent bonds, leading to a loss of planarity of the sheets. The detection of this buckling would be difficult using X-ray techniques, since the carbon-carbon spacing obtained from the planar graphite structure is 1.42\AA , while the spacing expected from the projection of the buckled layers is 1.45\AA and workers such as Boehm, Clauss and Hofmann (1961) and De la Cruz and Cowley (1963) conclude that it is difficult to decide the question from such measurements.

The infra-red work of Hadzi and Novak (1955) and Alexanian (1961) indicates the presence of the following bonds:- oxygen-hydrogen (OH), carbon-hydroxy (C-OH), carboxyl (CO_2H), epoxy ($\text{C} \begin{array}{l} \diagup \text{O} \\ \diagdown \end{array} \text{C}$), carbon-oxygen (C-O) and carbonyl (C=O). These results support the theories of Boehm, Clauss and Hofmann (1961) and De Boer and Van Doorn (1958) that the structure contains keto-enol tautomerism, with some epoxy groups. Such a structure would be planar. On such chemical ground therefore the structure (Fig.(iii)) may be that just described.

(iv) Study of intercalation compounds by electron microscopy and diffraction.

(a) Lamellar and residue compounds. The only compound which has been studied thoroughly is the bromine compound.

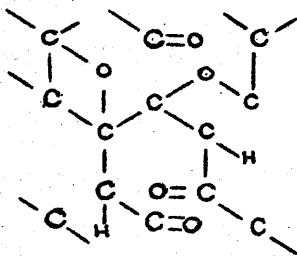
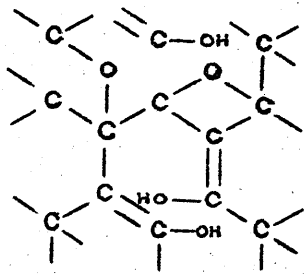


FIGURE (iii)

AFTER CROFT

Eeles and Turnbull (1963, 1965) report that the bromine is intercalated in an ordered fashion and they suggest that in the lower concentration compounds, the intercalate has the form of chains of bromine molecules, in which the interatomic distance is almost identical with that of bromine. They also discuss line and loop defects which moved rapidly and did not seem to be similar to the partials seen in unbrominated graphite. Their findings are similar to those of Heerschap, Delavignette and Amelinckx (1964) who studied the interlamellar compounds of graphite with bromine and iodine monochloride. These authors report the presence of dislocations surrounding areas containing bromine and they describe the further separation of the normal partial dislocations, because of the presence of the bromine. A mechanism is described whereby loops of material are isolated as these moving dislocations pass through the crystal, and the effect of this is often to produce concentric bromine loops in different layers of the material.

A different report is given by Bacon and Sprague (1961a) who describe the intercalation of ferric chloride, bromine and caesium chloride. They show that intercalated material can become trapped at cracks and grain boundaries and the situation they describe is a much more random one than that given by Eeles and Turnbull (1963, 1965),

Turnbull and Eeles (1965) and Heerschap, Delavignette and Amelinckx (1964) but is fairly consistent with the results of the X-ray work on graphite-ferric chloride by Cowley and Ibers (1956).

(b) Graphite Oxide. The electron microscope appearance of graphite oxide was described by Beckett and Croft (1952) as being similar to graphite in that the material consists of thin, flat areas. The oxide, however, contains folds extending in straight lines through even the thickest particles and they suggest that this is caused by a decrease in rigidity of the sheets as the bond order decreases on oxidation.

III OXIDATION OF GRAPHITE.

(i) General gaseous oxidation. The study of the oxidation of graphite by gases such as molecular oxygen using classical means of investigation is a complex one, beyond the scope of this work, but the book of Ubbelohde and Lewis (1960) and the paper of Marsh, O'Hair and Wynne-Jones (1965) summarise the work done on the subject. It is, however, known that the reaction is localised at imperfect parts of the crystal (Watt and Franklin, 1957, 1958) and it is found that the presence of impurities can change the rate of oxidation (Duval, 1961).

(ii) Microscopy of graphite oxidation. Since it is postulated that oxidation is highly localised, direct microscopy techniques are obviously highly suitable for pin-pointing the sites of attack. Early work, for example that of Greer and Topley (1932) using light microscopy, reported that the attack was localised and formed hexagonal holes, which they suggested may have been produced by catalytic attack by impurities. Later work by Presland and Hedley (1962, 1963) studied further the effects of catalysis on oxidation. They reported that there were two main types of attack by molecular oxygen: (a) basic, and (b) catalytic.

(a) The basic attack occurred slowly and irregularly at the edges of crystals, like that reported by Lang, Magnier, Sella and Trillat (1962) and also occasionally produced hexagonal pitting. (b) The catalytic attack was faster, as reported by Jacquet and Guérin (1962) and led to the formation of channels with a catalyst particle at the head. Pits could also be obtained if the mobility of the catalyst particle is reduced. This differentiation into two types of reaction is in agreement basically with the earlier work of Meyer (1938) who studied the kinetics and appearance of graphite after oxidation, using the light microscope. In this case, two reactions are distinguished by the temperatures at which they occur.

At low temperatures a first order reaction is reported, producing carbon monoxide and carbon dioxide in equal proportions and leading to the production of hexagonal holes. At higher temperatures, the kinetics are zero order and the crystals have now been attacked from the edge.

The conclusion of Presland and Hedley (1962, 1963) that crystal defects have no effect on the rate of either of their two basic types of oxidation is not in agreement with that of Sella, Miloche and Trillat (1962). They worked on pyrolytic graphite with oxygen and reported that attack begins at "faults" in the crystal, and proceeds from these points to give hexagonal corrosion figures. However, the faults they mention may well be the grain boundaries and micropores which Dawson and Follett (1963) report as being the site of oxidative attack. These authors describe oxidation on polycrystalline synthetic graphite with air and carbon dioxide for standard material and also material which has been neutron irradiated. They report that the latter reaction rate is "larger" for both oxidants which agrees with the results of Presland and Hedley (1962, 1963). They describe the attack of the unirradiated material as taking place round the micro-crystals of which the crystal is composed, and also at micropores, and this may be fundamentally edge attack which has been catalysed by the presence of impurities. That the impurities are localised in grain

boundaries and pores is reported by Bauer (1961) and the importance of the micropores for oxidation is shown by the results of Lang and Magnier (1963) which prove that, for oxidation with carbon dioxide, the speed of attack increased with the number of micropores. Dawson and Follett (1963) also report shallow pits, similar to those of Presland and Hedley (1962, 1963) but attributed by them to attack at some type of defect. This they confirm from their results for irradiated graphite, which show the whole 0001 layer net to be covered with shallow pits, which are often associated with impurity particles. There is thus difficulty in distinguishing between edge and catalytic attack, and this has been one of the greatest problems in the study of the oxidation of graphite.

This subject has been studied closely by two further schools of research. The first set of papers (Hennig, 1959b, 1960b, 1961, 1962, and Hennig and Kantar, 1960) suggests that the initiation of pits depends on other factors as well as the presence of catalysts. The catalysts are thought to act in conjunction with defects in the crystal. For example, Hennig (1962) states that the catalytic attack in crystals free from defects, takes place mainly parallel to the cleavage surfaces, whereas in crystals containing lattice defects or intrinsic impurities, the attack may be perpendicular to the planes to produce pits on it.

The other set of work deals with the changes in the reaction mechanism with temperature. Hughes, Williams and Thomas (1962), Hughes and Thomas (1962) and Thomas, Hughes and Williams (1963) describe the changes in the shape and orientation of the pits produced as the temperature is changed and correlate this with attack along definite crystallographic planes. In a paper by Hughes, Thomas, Marsh and Reed (1964), evidence is given to show that various defects, for example, c-axis screws can cause pit formation in graphite.

The general conclusion of all these works is that oxidative attack occurs at lattice defects, but that the attack at these specific sites may in some cases be promoted by the presence of catalysts.

(iii) Oxidation of graphite by atomic oxygen. The oxidising agents used in the work described above included molecular oxygen, and it is interesting to discuss here the work of Marsh, O'Hair and Reed (1965) on the use of atomic oxygen. This they produced from a plasma jet and worked outside the plasma at temperatures of 20°C. to 350°C. They report the presence of etch pits and conical hillocks on the surface of the graphite after the reaction and present an oxidation picture quite different from that described in (i) above.

(iv) Chemical oxidation of graphite. All the work described, dealing with molecular and atomic reagents on

graphite, has been concerned with gaseous reactions, usually by employing oxygen or carbon dioxide. Little work has been done on the action of chemical oxidising agents. Matuyama (1952) examined the change in the order of graphite grain structure after reaction with an 8% solution of potassium dichromate in sulphuric acid of specific gravity 1.29. The results of his X-ray examination showed only that crystal structure is most perfect in the inside of the crystals and gave no information on the scheme of the reaction.

A detailed kinetic study of the reaction of graphites with hot sulphuric acid and silver dichromate was done by Oberlin and Mering (1961, 1964) and they distinguish between different structural forms which correspond to four types of elementary carbon layer in a partially graphitised material. They thus use this technique for gaining information on the degree of graphitisation of any particular carbon. This method has been extended by Oberlin, Rappeneau and Yvars (1964) to study the way in which irradiation damage in small doses can influence the reaction in such a way that the rate of oxidation is quite markedly lowered.

IV. Aim of the present work.

The present studies were designed to use electron microscope and diffraction techniques to examine in detail

the oxidation of graphite by sulphuric acid and the aims can be divided into four main headings.

(a) To compare the oxidation of polycrystalline synthetic graphite by sulphuric and nitric acids, both alone and with the addition of catalysts, with the results obtained for gas oxidation of the same material.

(b) To differentiate between the intercalation expected in the formation of the bisulphate residue compound and the oxidation effects of (a).

(c) To examine the electron microscope picture of the graphite bisulphate residue compound and graphite oxide and thus to compare the oxidising power of the reagents used to prepare these two species.

(d) To compare the reaction of sulphuric acid and nitric acid on different types of graphite in an attempt to correlate any difference of oxidation pathway with differences in purity and crystallinity.

EXPERIMENTAL

I. Chemical preparation of Materials.

- (i) Graphite bisulphate residue compound.
- (ii) Vanadium and uranium residue compounds.
- (iii) Graphite oxide.
- (iv) Types of graphite used.

II. Preparation of samples for examination.

- (i) Cleaning.
- (ii) Suspension.
- (iii) Mounting.
- (iv) Shadowing.

III. Electron Microscopy.

- (i) Introduction.
- (ii) Resolution.
- (iii) Double condenser operation.
- (iv) Diffraction in the electron microscope.
- (v) Selected area diffraction.
- (vi) Simultaneous comparative diffraction.
- (vii) Dark field microscopy.
- (viii) Ciné photography.
- (ix) Conditions used in this work.

IV. X-ray Powder Photography.

EXPERIMENTAL

I. Chemical Preparation of Materials.

(i) Graphite bisulphate residue compound. The graphite was ground in an agate pestle and mortar prior to reaction. The reagent used (Brodie, 1859) was a mixture of AnalaR sulphuric and AnalaR nitric acids (70/30 by volume). The impurities present in these acids are given in Table 1.

Table 1.

(a)	<u>Sulphuric acid</u>	<u>% impurity</u>
	Non-volatile matter	0.0025
	Chloride	0.0002
	Nitrate	0.00002
	Selenium	0.001
	Iron	0.0001
	Heavy metals (lead)	0.0002
	Ammonium	0.0005
	Absorbed oxygen	0.00015
	Arsenic	0.00001
(b)	<u>Nitric acid</u>	
	Non-volatile matter	0.001
	Chloride	0.00007
	Sulphate	0.0003
	Iron	0.0001
	Heavy metals (lead)	0.0002
	Arsenic	0.000002

The graphite and acids were mixed in a pyrex test-tube with ground-glass stopper and shaken periodically: the reaction mixture was left at room temperature.

during reaction. The reaction was stopped after periods up to 24 hours when studying intercalation effects, and after periods up to 25 weeks when examining long-term oxidation effects. In both cases the reaction was stopped by abstracting some of the graphite suspension with a broad-bore Pasteur pipette, and adding it to water. As described by Rüdorff (1939) and Riley (1945) this forms the residue compound from the lamellar compound.

(ii) Vanadium and uranium residue compounds. In this case, saturated solutions of ammonium vanadate or uranyl nitrate in the acid mixture described above were used in an attempt to introduce a heavy metal cation. The ammonium vanadate, in solution in sulphuric acid, forms vanadium pentoxide, so the red coloured solution used was a solution of this oxide in acid (Hauser and Lynn, 1940). The preparation of the residue compound was otherwise similar to that used in (i) above.

(iii) Graphite oxide. The method used to prepare the oxide was that of Hummers and Offeman (1958). 5 grams of powdered graphite and 2.5 grams of sodium nitrate were added to a flask containing 115 mls. of concentrated sulphuric acid. 2.5 grams of potassium permanganate were added and an ice-bath was used to keep the temperature below 20°C. The temperature was then allowed to rise and the mixture was left at 35°C. for 2 hours; 230 mls. of water

were added slowly, followed by a further amount of warm water to make the final volume up to 700 mls. 3% hydrogen peroxide was then added to convert the potassium permanganate and manganese dioxide present to soluble sulphates. The solid material remaining was graphite oxide.

(iv) Types of graphite used. Four types of graphite were used: (a) pile grade A, polycrystalline synthetic graphite, (b) spectroscopically pure natural graphite (Spl), (c) single crystal graphite and (d) natural Ceylon graphite. When all four were examined after reaction with acids, it was found that types (b), (c) and (d) all reacted in a similar way, but their reaction differed from type (a). Since less is known about types (c) and (d), these will not be dealt with fully, and the comparison will be made between the polycrystalline synthetic and the spectroscopically pure materials.

(a) Pile Grade A, polycrystalline synthetic graphite. Typical analysis figures for this material are given in Table 2 (Labaton, 1965). The material is composed of many small crystallites which appear in the electron microscope to have an average diameter of 3,000Å (Dawson and Follett, 1959). This point is discussed further in the Results section of this thesis.

Table 2

Typical Range (ppm)

Ash %	0.005	-	0.025
Boron	0.03	-	0.16
Iron	<2	-	16
Copper	<0.01	-	0.5
Phosphorus	<0.1	-	0.2
Hydrogen	15	-	40
Aluminium	0.25	-	2.5
Barium	0.3	-	15
Beryllium	<0.02	-	<0.03
Bismuth	<0.06	-	<0.15
Calcium	7	-	60
Chromium	0.1	-	0.7
Cobalt	<0.01	-	<0.03
Indium	<0.04	-	0.08
Lead	0.04	-	2.5
Lithium	<0.04	-	0.15
Magnesium	0.03	-	1.5
Manganese	0.01	-	0.06
Molybdenum	<0.02	-	1.5
Nickel	0.03	-	8
Silicon	15	-	60
Sodium	<1	-	2
Strontium	0.04	-	1
Tin	<0.02	-	0.08
Titanium	1	-	15
Tungsten	<0.08	-	<0.2
Vanadium	0.4	-	30
Zinc	<0.08	-	<0.2
Dysprosium	<0.008	-	0.015
Europium	<0.004	-	0.008
Gadolinium	<0.005	-	0.015
Samarium	<0.04	-	0.04

Table 3

Typical Range (p.p.m.)

Boron	<.02
Iron	.05
Copper	.04
Aluminium	<.015
Barium	<.015
Beryllium	<.015
Bismuth	<.06
Calcium	<.15
Chromium	<.015
Cobalt	<.015
Indium	<.04
Lead	<.025
Magnesium	<.025
Manganese	<.015
Molybdenum	<.015
Nickel	<.025
Silicon	<.15
Strontium	<.02
Tin	<.02
Titanium	<.02
Tungsten	<.08
Vanadium	<.02
Zinc	<.08
Sodium	<.1
Lithium	<.005

(b) Spectroscopically pure graphite. Typical analysis figures for this material are given in Table 3 (Labaton, 1965). This material is a natural graphite, from Ceylon or Madagascar, and is obviously much purer than the synthetic graphite described above. It also has a larger crystallite size, with particles of 20μ in diameter. It is almost single crystal in character, since it contains only two or three crystallites in each crystal (Walker, 1965).

II. Preparation of samples for examination.

(i) Cleaning. The compounds prepared as in I were suspended in distilled water and cleaned by repeated centrifugation and removal of the supernatant liquid, until the washings had a pH of 7.

(ii) Suspension. The cleaned material was suspended in distilled water and submitted to ultrasonic disintegration for 30 seconds (Dawson and Follett, 1962) to reduce it to a suspension of pieces of a suitable size for examination in the electron microscope. Experiments were also carried out to assess the effects of ultrasonic disintegration alone on graphite.

(iii) Mounting. The normal copper grids of diameter 3.05 mm. were used, having on them a carbon film, prepared by the method of Bradley (1954) by evaporating carbon from

rods under a vacuum of better than 10^{-3} mm. Hg., and using a 30 V. 20 amp. transformer. Alternatively platinum mounts were used, with a diameter of 2.30 mm. with either one 70μ diameter hole, or seven 70μ diameter holes. The mounts required silicon monoxide films, which were evaporated from a molybdenum boat using the same apparatus as for the carbon films, but with a 10 V. 60 amp. transformer. The silicon monoxide film was evaporated on to a Formvar film already on the platinum mounts and this lower film was removed by firing in a porcelain basin.

A drop of a suitable suspension was then placed on the grid or mount, and dried out in a cool oven.

(iv) Shadowing. The shadowing technique is useful for giving information on surface detail and the procedure used was that of Bradley (1959) as described by Kay (1961) for evaporation of carbon and platinum in vacuum when the material to be evaporated was in the form of a carbon-platinum rod. Alternatively a carbon platinum pellet (Kranitz and Seal, 1962) was used, this being balanced between two ordinary carbon rods. A metal screen with an aperture was set up between the source and the specimens to be shadowed to improve the sharpness of the shadow. The system was evacuated as before, and the carbon-platinum evaporated at an angle of 15° to normal, using a 10 V. 60 amp. transformer, with the grids of graphite to be shadowed clamped in a

suitable place to receive the shadow. Elevated parts of the surface shield a small area from the carbon-platinum particles and this area appears less dense in the electron microscope. The usual method of printing micrographs of such material is the making of an intermediate plate which is then used to give a final print in which the shadows are dark, as are shadows cast by visible light. In this work, however, the changes seen on reaction with acid are differences in contrast, and to reverse the image in this fashion would cause further confusion. For this reason the prints are shown with white shadows.

III. Electron Microscopy.

(i) Introduction. The theory and uses of the electron microscope have been fully reviewed (Zworykin, Morton, Ramberg, Hillier and Vance, 1945, Cosslett, 1951, Hall, 1953, and Kay, 1961). The various instruments are fully dealt with in these books of reference and only the particular techniques used in this work will be described here. The instrument used was the Siemens Elmiskop I, which has magnetic lenses with a double condenser illumination system and a projector lens with four different pole pieces, giving magnifications varying from 200 to 160,000.

(ii) Resolution. The precision of any microscope is determined by its resolution which is defined (Cosslett,

1951) by d , the separation of two object points which are just discernible as separate entities in the final image. The Abbé equation describes the factors influencing resolution as $d = \frac{\lambda}{\sin \alpha}$, where λ is the wavelength of the illumination source and α is the angle subtended by the lens aperture. The electron microscope thus has a much better resolving power than a light microscope because of the small wavelength of electrons (3.7 to 6.1×10^{-9} mm. for the Siemens Elmiskop I under operating conditions). The other variable in the Abbé equation is the diameter of the objective aperture, which must be chosen to be of such a size as to minimise confusion due to diffraction. The aperture used in this work for microscopy had a diameter of 50Å.

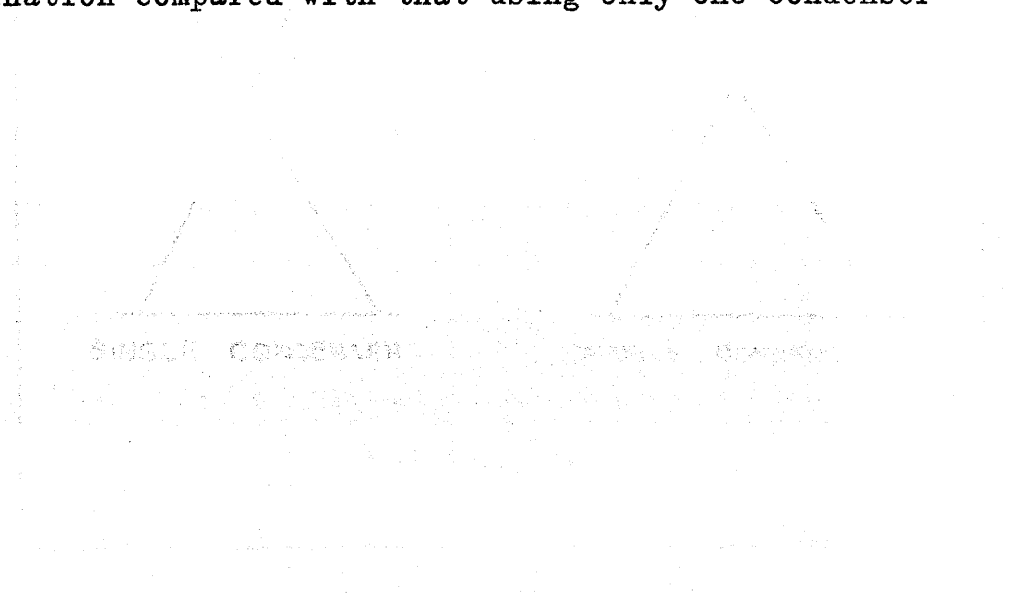
Another factor which must be considered, especially for high resolution work, is the astigmatism of the whole system and particularly of the objective lens. If this defect is present it leads to a deformation of the focussing field from rotational symmetry. In the Elmiskop I any astigmatism in the objective lens is rectified by a stigmator which produces an elliptical correcting field. In many cases, however, astigmatism is caused by dirt somewhere in the column and may be removed by cleaning apertures.

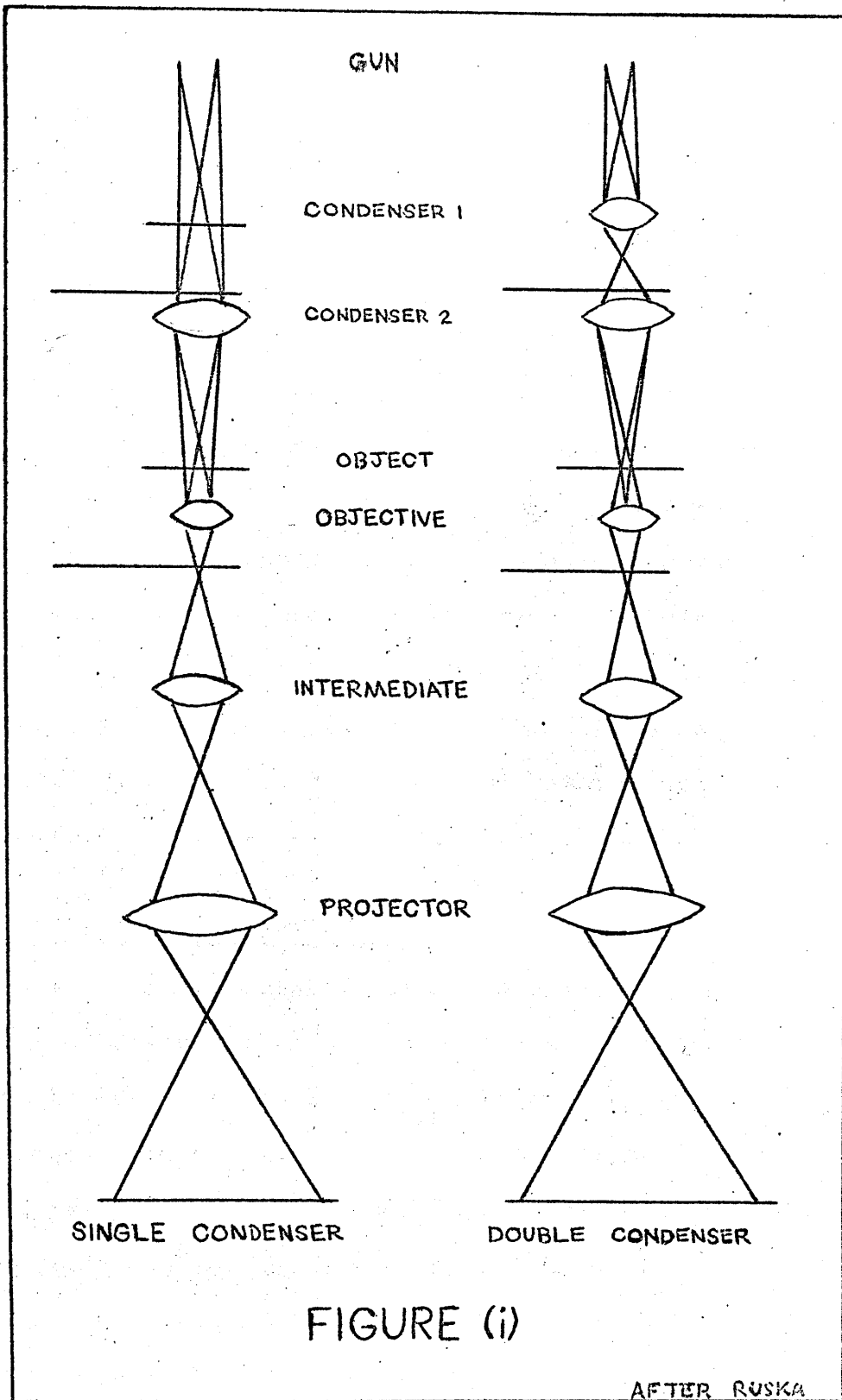
For high resolution work all these factors must be considered, and the illumination must also be chosen to give maximum brightness with minimum damage to the specimen.

To do this both condenser lenses are used together.

(iii) Double Condenser Operation. The first condenser lens, which is switched on in this technique to supplement the second, is a strong lens which forms an image of the electron source at a demagnification of approximately fifty times. The second lens projects this beam of reduced cross-section on to the specimen with a magnification of approximately two. The advantage of this system is that greater brightness is obtained on a smaller area (down to a circle of diameter 2μ) thus decreasing the temperature rise and rate of contamination of the object. When both condensers are used, the first must not be astigmatic, since a point image of the electron source is required: to ensure this a simple magnetic stigmator is used in the Elmiskop I

Figure (i) shows a ray diagram of double condenser illumination compared with that using only one condenser lens.





(iv) Diffraction in the Electron Microscope. To compare the production from a specimen of an image and a diffraction pattern, the wave theory of electrons must be considered (Finch, Quarrel and Wilman, 1935, Thomson and Cochrane, 1939 and Pinsker, 1953). If a plane wave is incident on a row of opaque objects, most of it will travel on in the axial direction to be focussed by the lens system to the corresponding points in the final image. Some of the wave, however, will be diffracted and all rays of a diffracted beam entering the objective lens parallel to each other will intersect at the back focal plane of the lens. This diffraction pattern may then be magnified on to the final screen by the magnifying lenses in the usual way. Figure (ii) shows the ray diagram contrasting the formation of an image and a diffraction pattern.

(v) Selected area diffraction. In this technique, the microscope is illuminated with condenser 2 only, and projector pole piece 3 is put in position. The area of interest in the specimen is defined by an aperture placed in the normal image plane of the objective lens. The intermediate and objective lenses are adjusted until this selector aperture and the specimen are in focus in the same plane. To obtain the final diffraction pattern, the intermediate lens is weakened till the zero order maximum of the final diffraction pattern is as small and

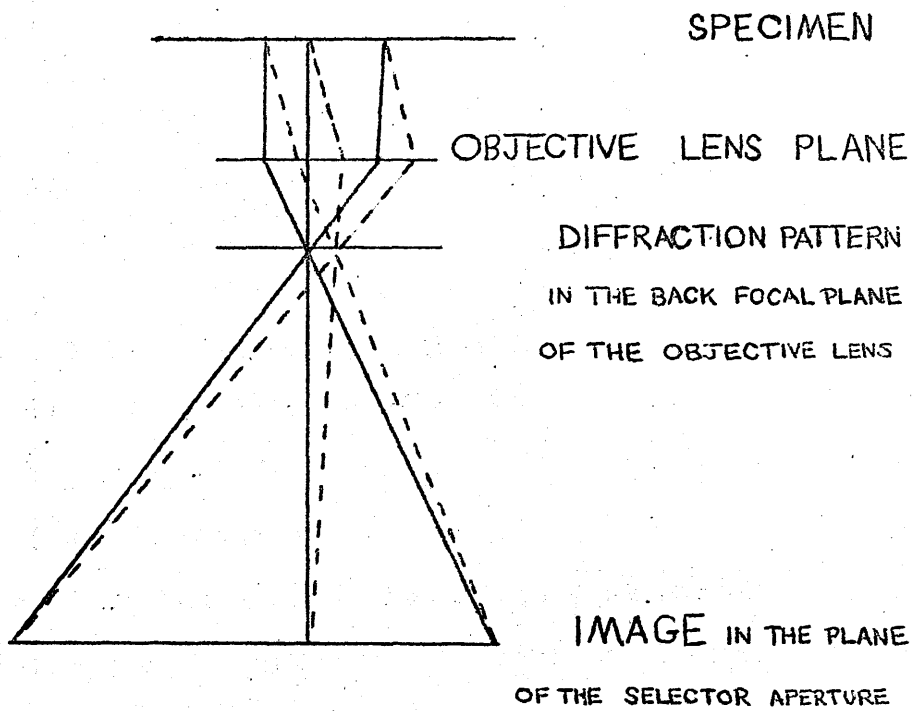


FIGURE (ii)

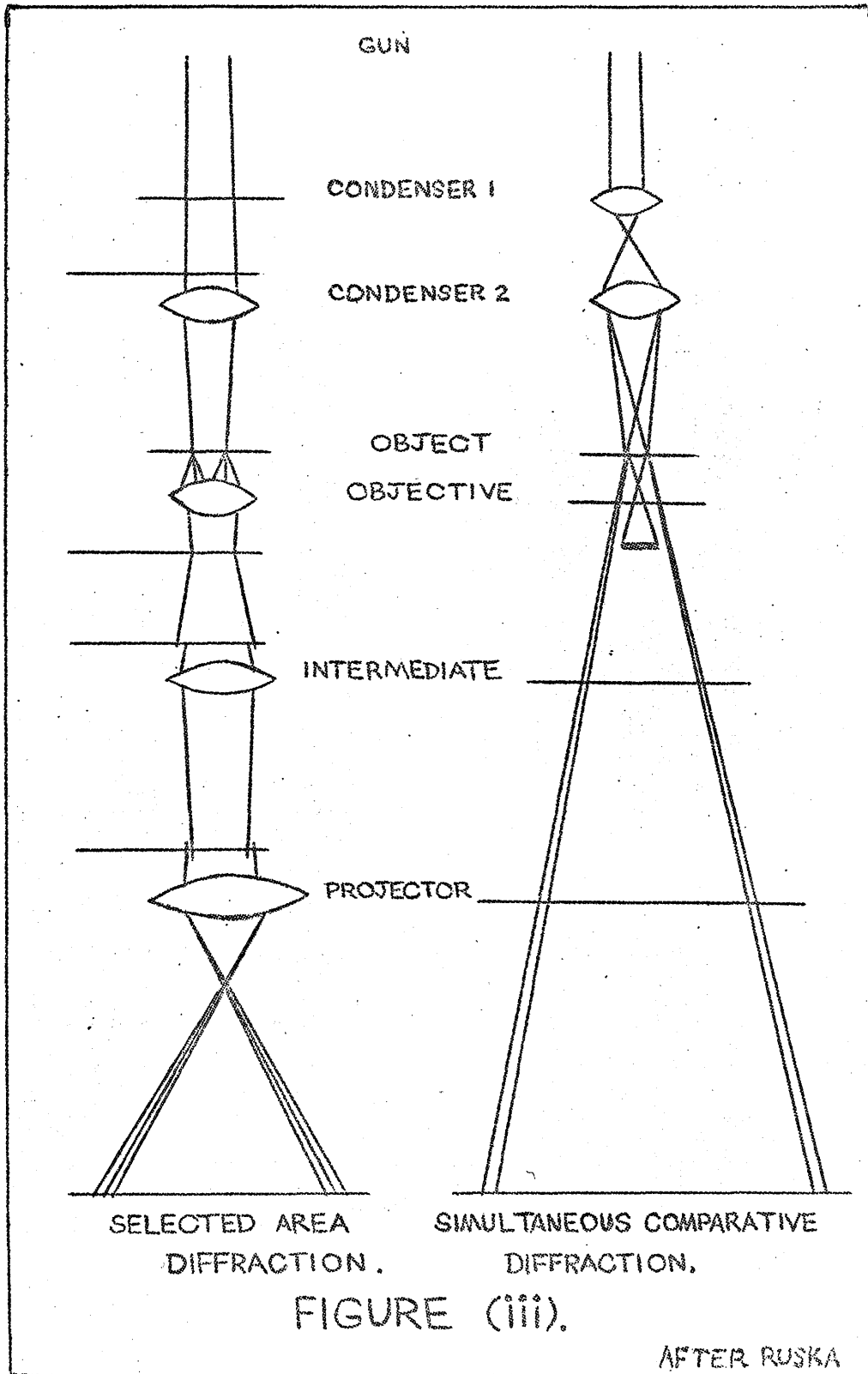
round as possible, and then the objective aperture is removed to show the whole of the pattern. The image of the area diffracted can be seen by re-inserting the objective aperture and increasing the magnification until the selector aperture and specimen are again both in focus. Thus a diffraction pattern and image can be obtained from the same area of the specimen.

(vi) Simultaneous Comparative Diffraction. In the method of diffraction described above, the magnifying lenses are used and a separate diffraction pattern of a standard substance of known lattice spacings (for example thallium chloride) must be taken each time selected area diffraction is being attempted. However, the size of the final image for both standard and unknown substances depends on the focussing of the intermediate lens. A more accurate method is that of simultaneous diffraction as used by Riedmiller (1936) and described by Thomson and Cochrane (1939), where the standard and unknown specimens are mounted together in the same plane in the microscope. A bar below this plane cuts out the overlapping portions of the two diffraction patterns formed, giving a composite picture with half from each material. The illumination from both condenser lenses is focussed on to the final screen and no other lenses are used.

In this work, samples of graphite and graphite oxide were placed on separate, one hole platinum mounts, and a simultaneous diffraction pattern obtained. For comparison with this, a composite pattern from two different concentrations of graphite was also obtained.

Figure (iii) shows a ray diagram comparing selected area diffraction and simultaneous comparative diffraction.

(vii) Dark field. The method used to obtain dark field micrographs was basically that of displacing the objective aperture so that the central, undeviated beam of electrons was stopped. The only electrons used in image formation were therefore those scattered by the object through such an angle that they could pass through the displaced aperture. In fact, the selected area diffraction pattern was first obtained as described in (v) above, then the objective aperture was centred round a spot (or an arc of a ring) of the pattern and this spot was used for illumination instead of the central spot. The magnification was then increased in the usual way and the selector aperture removed. Thus the areas which show bright on the resulting dark field image are those which diffract electrons from the planes corresponding to the spot chosen. After the dark field plate is taken, the objective aperture is again centred round the central undeviated beam and a bright field plate is taken of the same area for comparison.



(viii) Ciné Photography. In order to follow the motion of some of the objects seen in this work, ciné photography was used. The image on the final screen was obtained as usual and focussed at a magnification of 20,000X, and then the brightness was reduced while the ciné camera was focussed on the screen. The condenser and filament current were then both adjusted to give maximum brightness and the ciné film was taken. As the film was taken in this way the resolution is poor since it is restricted by the grain of the final screen of the electron microscope. The resulting film however was satisfactory for screening, but for inclusion in this work the results are presented as a series of stills which were made from the final film by way of an intermediate plate. Due to the grain of the screen and the film used, the final print compares very unfavourably with the standard of ordinary electron micrographs, but the use of stills is a convenient method of quoting the results and can be used to obtain information on particle sizes, distances moved and speed of movement. The ciné film was taken by Mr. Cowper of the University Photographic Department. The camera used was a Paillard-Bolex H16 Reflex camera, with an Angénieux lens ($f=0.95$) and a 5 mm., 1" focal length extension tube. The film used was an Ilford Safety film and the frame speed was 16 per second.

(ix) Electron microscope conditions used in this work.

Routine microscopy was done with the second condenser lens only in action, using projector lens pole piece 2, to give a plate magnification of 20,000X or 30,000X.

Routine selected area diffraction work was done with the second condenser lens only, but using the projector lens pole piece 3. Dark field microscopy was done using one condenser lens with pole piece 2 of the projector lens, even when selected area diffraction was used to choose the spot for illumination.

High resolution micrographs were obtained by using both condenser lenses, with projector lens pole piece 3 in position, to give plate magnifications of 60,000X or 80,000X.

IV. X-Ray Powder Photography.

The material to be examined was prepared and cleaned as for electron microscopy and then it was dried and powdered with an agate pestle and mortar. This powder was then put into a thin glass tube and mounted in the centre of an X-ray powder camera. The X-rays were obtained from a Philips PW 1008 unstabilised X-ray generator, with a copper target and a nickel filter, giving Cu K α radiation with a wavelength of 1.542Å.

- 51 -

The machine was run at 35 KV. and 15 m.amps. for periods of time varying from 30 to 60 hours.

RESULTS

I. INTERCALATION:-

A. Introduction.

- i. General.
- ii. Control of the method used to disintegrate the samples.
- iii. In situ reaction.
- iv. Appearance of standard graphite in the electron microscope.
- v. Standard diffraction patterns of graphite.

B. Transparent discs.

- i. Nomenclature.
- ii. Description.
- iii. Movement.
- iv. Position of the discs in the c-direction.
- v. In situ reaction.
- vi. Structure of the folds.

C. Interference patterns.

- i. Description.
- ii. In situ reaction.

D. Electron dense material.

- i. Introduction.
- ii. Discs.
- iii. Dense mobile particles.
- iv. Adsorption of droplets along straight lines.

E. Influence of heavy metal cations on the reaction.

- i. Addition of ammonium vanadate.
- ii. Addition of uranyl nitrate: a) Analysis
b) Decoration.
c) Crystallites
of uranyl nitrate.

F. Diffraction.

- i. Introduction.
- ii. X-ray powder patterns.
- iii. Selected area diffraction.

G. Bisulphate lamellar compound.

II. The long term effects of acid on graphites.

A. Introduction.

- i. Description.
- ii. Rate of reaction.
- iii. Catalysis.
- iv. Structure of graphite after oxidation.

B. The five stages of oxidation.

- i. The formation of microcracks.
- ii. Stages (a) to (d).
- iii. Break up of the crystals.
- iv. Stage (e).

C. Edge attack.

D. Adsorption of material along crystallite edges and cracks.

- i. Description.
- ii. High resolution plates.

E. Channel Contents.

F. Crystallite size.

III. Comparison of the oxidation of various types of graphite.

A. Introduction.

B. Intercalation.

C. Oxidation: (i) Rate of reaction.

(ii) Channel formation.

(iii) Pit Formation.

IV. Oxidation of polycrystalline graphite to graphite oxide.

A. Introduction.

B. Electron microscopy.

i. Graphite oxide stage (i).

ii. Graphite oxide stage (ii).

iii. Graphite oxide stage (iii) - modification (a).

iv. Graphite oxide stage (iii) - modification (b).

v. Gross oxidation.

C. Diffraction.

i. Introduction.

ii. X-ray powder photographs.

iii. Simultaneous comparative diffraction.

a) Three dimensional order.

b) Nature of the layer planes.

RESULTS

I. INTERCALATION EFFECTS.

A. Introduction.

(i) General. When graphite has been in contact with sulphuric and nitric acids, graphite bisulphate is formed, which gives the bisulphate residue compound when the reaction is reversed by contact with water. Since all the material used in this work was thoroughly washed with water prior to examination, it is the residue compound which is being studied. This section of the Results deals with any effects which are considered to be due to intercalation.

The important features of the residue compound are, firstly, various diffraction phenomena, due to changes in the graphite lattice, and, secondly, dense particles caused by the presence of retained intercalated material. Since the residue compound was broken up for examination by an ultrasonic disintegrator, experiments were carried out to prove that the effects seen were not due to this process.

ii. Control of the method used to disintegrate the samples.

Three types of control sample were examined:-

(a) graphite in its original state with only a minimum of grinding,

(b) graphite after ultrasonic disintegration alone,

(c) graphite after acid reaction alone.

In each case, four types of graphite were examined -

polycrystalline synthetic, natural, single crystal and purified natural materials. In case (a) the polycrystalline material was found to be the most suitable, since the other graphites occasionally contained some of the diffraction effects associated with the intercalation process. Polycrystalline graphite was therefore used in the bulk of this work. In case (b) ultrasonic disintegration caused some of the diffraction effects and was not used for the part of the work dealing with intercalation. The residue compound was simply shaken up with water to disperse it. This is sufficient since the intercalation process breaks down the graphite crystals. In case (c) the acid treatment alone produced all the effects to be described in B to F below, and it is therefore certain that they are due to the intercalation reaction.

(iii) In situ reaction. While most of the material was prepared by bulk intercalation followed by isolation and cleaning of a small amount of the residue compound, in some cases the reaction was followed on a silica film on a platinum mount. An area of graphite can then be examined in its original state and after several successive reactions. For this purpose, single crystal graphite was used, since it contains many flat, thin areas.

(iv) Appearance of standard graphite in the electron microscope. Plate 1 shows a typical area of unreacted

PLATE 1.

Pile grade A, polycrystalline,
synthetic graphite. Standard
sample.

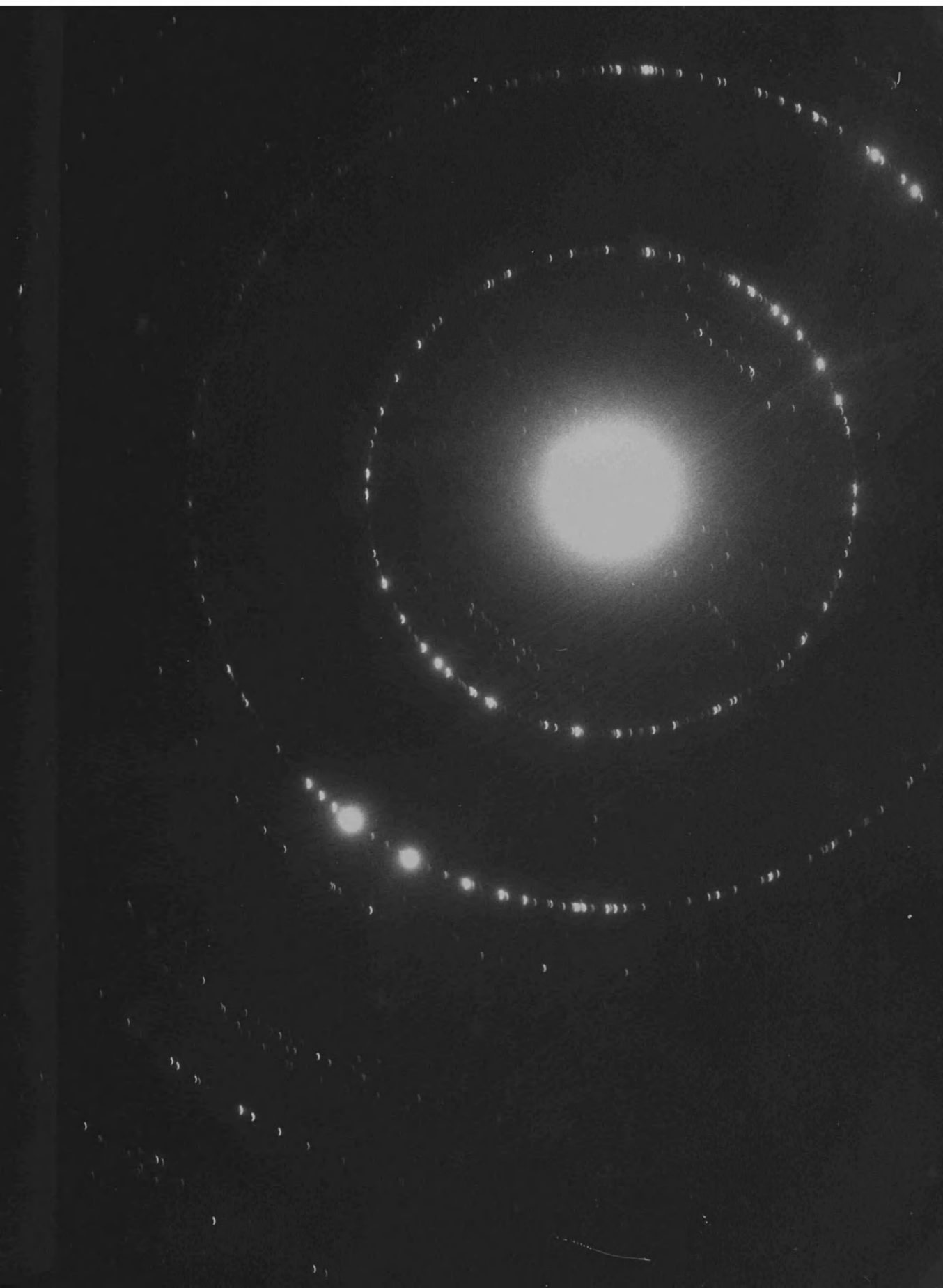
Final magnification - 153,000X.





PLATE 3.

Pile grade A, polycrystalline,
synthetic graphite. Standard
sample. Ring diffraction pattern,
taken using selected area
diffraction technique.



polycrystalline synthetic graphite. Both line (X) and rectangular (Y) moiré patterns are seen extending over a relatively small area and indicating the approximate outlines of the individual microcrystals.

(v) Standard diffraction patterns of graphite. The selected area diffraction technique gives a projection of the (hk0) planes, the (hkl) planes appearing only occasionally if there is much buckling or tilting of the specimen. Plate 2 shows a typical spot pattern obtained from single crystal areas and reveals the hexagonal symmetry of the graphite. The pattern consists of two sets of spots, the inner ones having been diffracted by the $10\bar{1}0$ planes with a spacing of 2.13\AA , and the outer ones by the $11\bar{2}0$ planes with a lattice spacing of 1.23\AA . The second type of pattern, commonly obtained from polycrystalline regions of graphite, is a typical Debye-Scherrer ring pattern (Plate 3). It consists of two rings, corresponding to the $10\bar{1}0$ and the $11\bar{2}0$ planes of graphite.

B. Transparent discs.

i. Nomenclature. The most widespread phenomenon seen on the residue compound is the presence of transparent discs (Plate 4). The term transparent disc is purely descriptive and the structures are probably seen in the electron microscope because of an unusual diffraction

PLATE 4.

Purified natural graphite. After
reaction with sulphuric and nitric
acids for 17 weeks.

Final magnification - 222,000X.

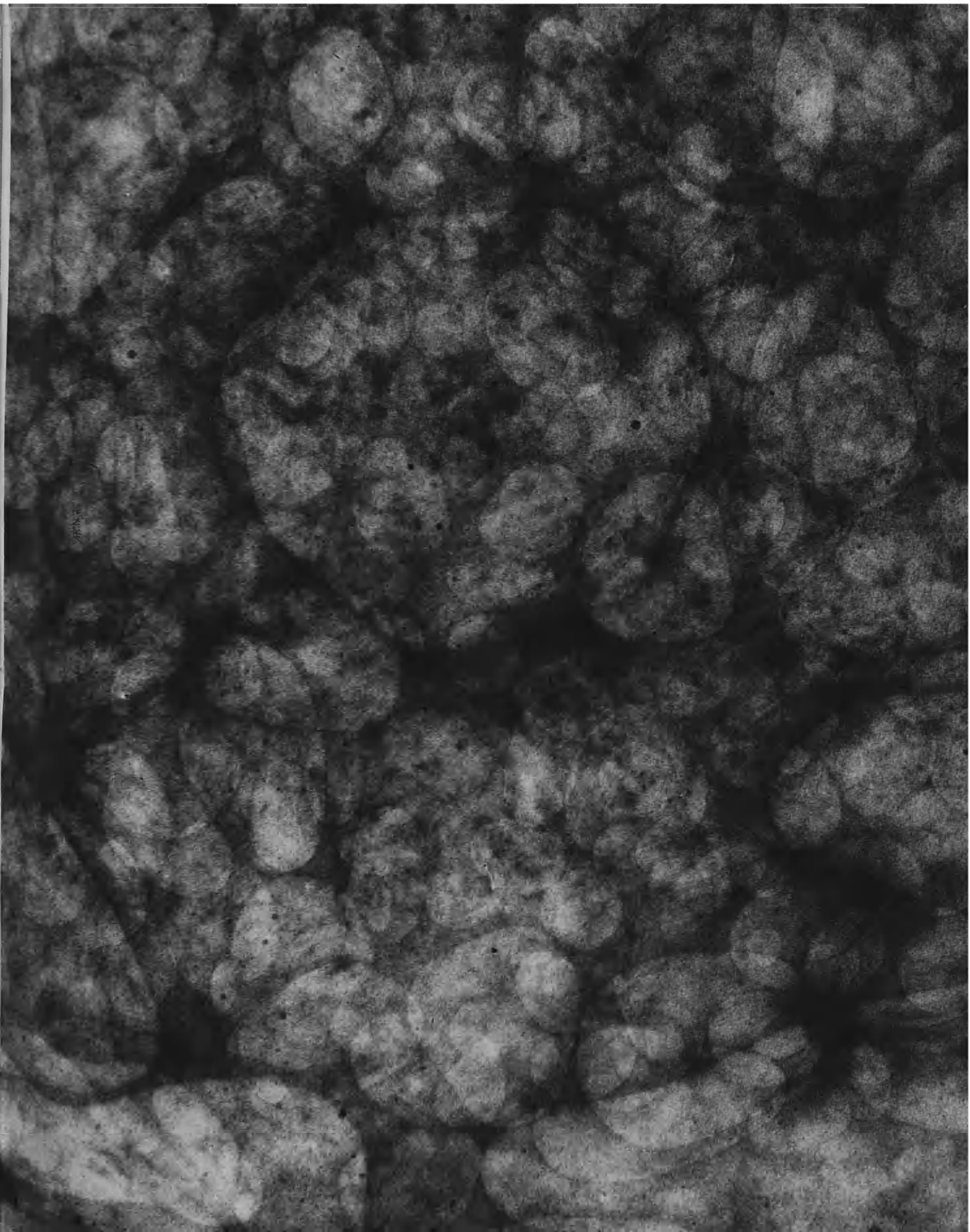


PLATE 5.

Single crystal graphite. After
reaction with sulphuric and nitric
acids for 15 minutes.

Final magnification - 132,000X.

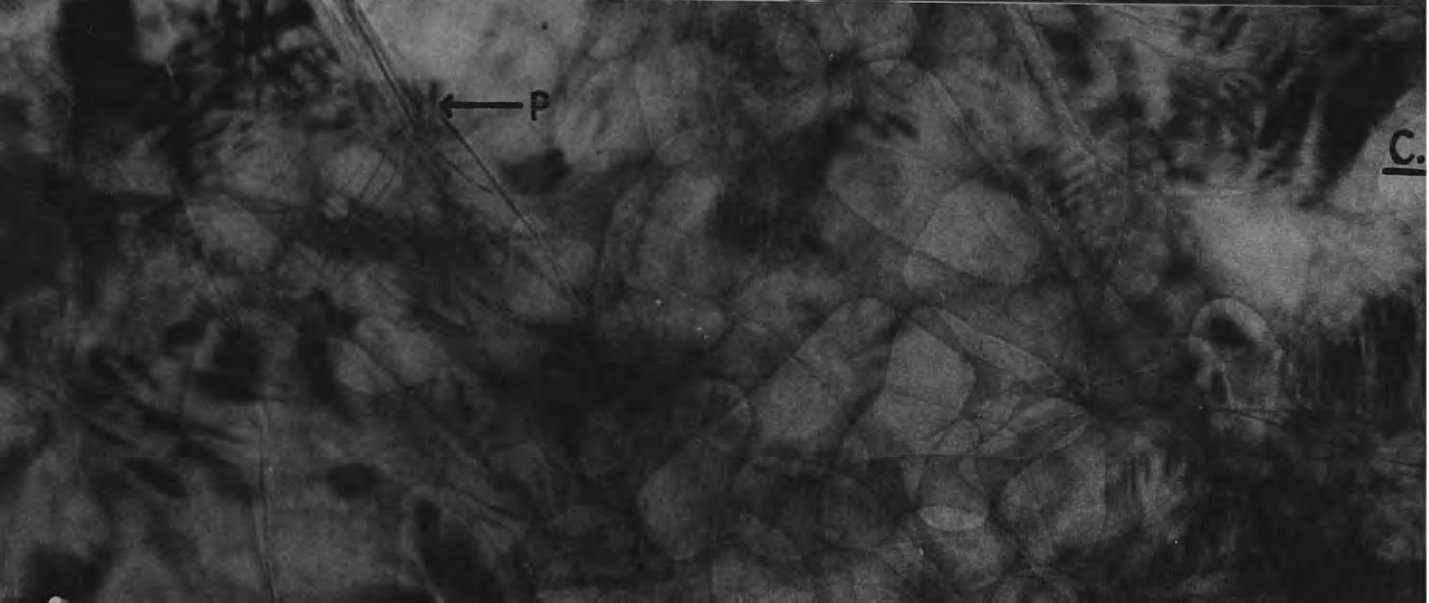
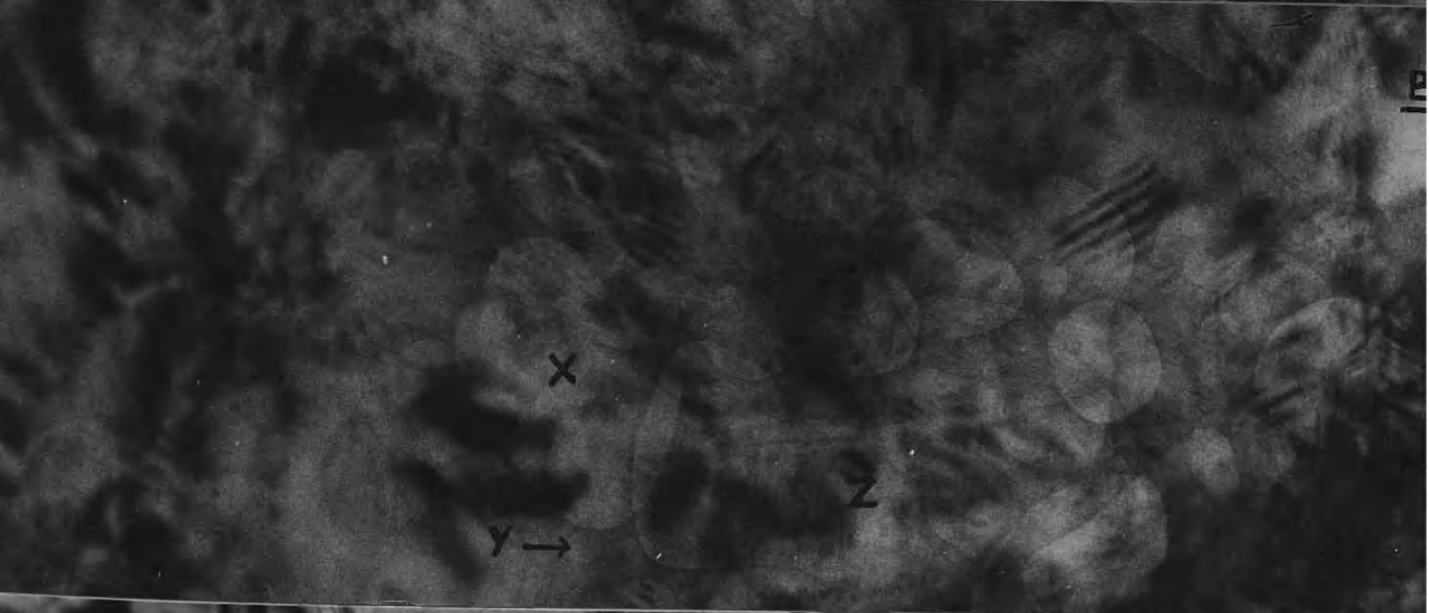
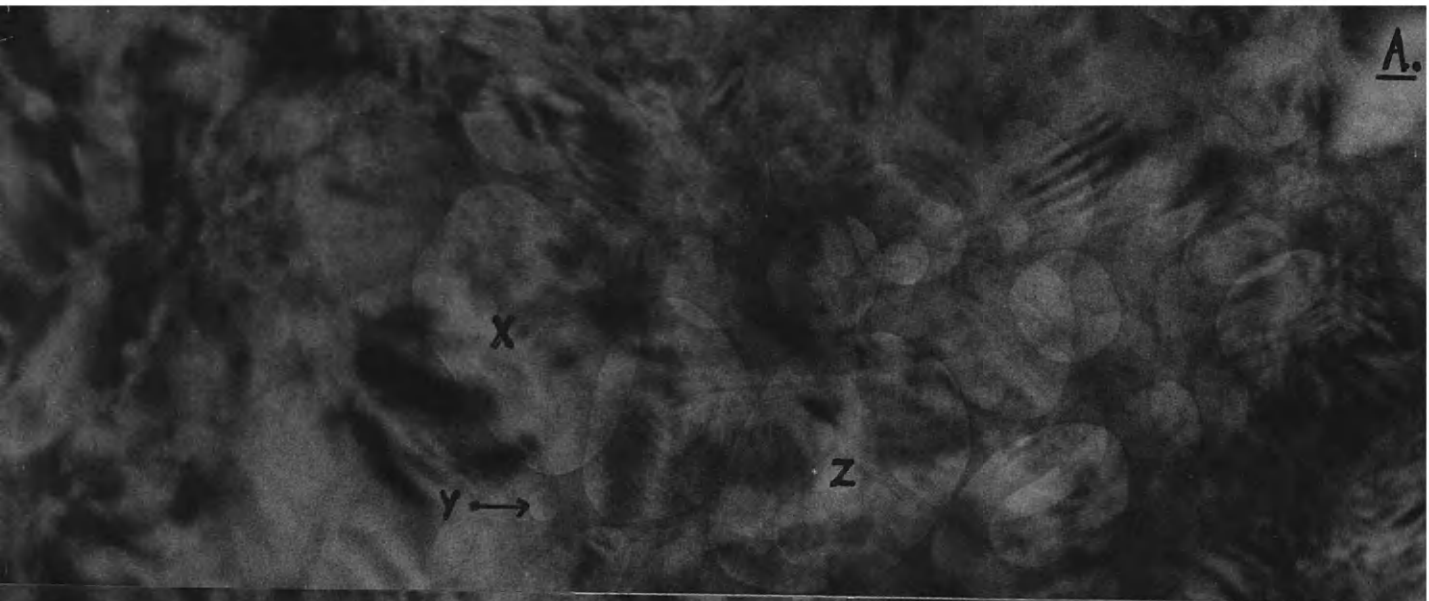


PLATE 6.

Pile grade A, polycrystalline, synthetic graphite. After reaction with sulphuric and nitric acids for 15 minutes. Double condenser illumination.

Final magnification - 306,000X.



PLATE 7.

Same area as Plate 6, after a short
time lapse. Double condenser
illumination.

Final magnification - 306,000X.



process leading to enhanced contrast. There is no indication in the literature of a suitable name for these structures, since the only references to them do no more than describe their appearance (Follett, 1963 and Adamson, 1963). Some of the "bubbles" described by Bacon and Sprague (1961a) may be the same structures and the work of Sella and Trillat (1962) on irradiation effects in mica reported "the interaction of circular Bragg fringes", which have an appearance similar to the transparent discs.

ii. Description. Plate 4, of purified natural graphite after reaction with acid for 17 weeks, shows many of the common features of the discs. They are usually oval, with smooth regular edges, rather like bubbles. They overlap and may extend over the whole area of a thin piece of graphite, particularly in purified natural and single crystal graphites, which contain many flat areas. The discs are from 50\AA - 5000\AA in diameter although those below 400\AA are rarely seen. The outline of the discs has sharp Fresnel fringes when not in focus suggesting that there may be some edge or kink effect diffracting the electrons and causing interference. These focus effects, and indeed the whole appearance of the discs, are quite different from the dislocations reported by Heerschap, Amelinckx and Delavignette (1964) for other intercalation compounds. The discs have a sharper, less diffuse outline and their speed of movement (B.iii, below)

is much faster than that normally associated with dislocations. The dislocation effects reported by Heerschap, Amelinckx and Delavignette were seen in this work but were not prominent.

iii. Movement. An outstanding feature of the discs is their smooth, rapid movement as they obtain energy from the electron beam. This expansion of the discs on heating is seen in Plate 5, where A, B, and C show the same area of graphite with approximately five seconds time lapse between each exposure. The movement is usually one of expansion (X) and the discs may move relative to each other (Y). Discs often disappear during this process (Z) but they may thereafter be replaced by others of a new shape. The movement generally affects the whole of the flat area of graphite which is being examined and the usual end product of this complicated motion is a folded structure (P), which often retains no discs.

The discs are pictured at higher magnification in Plates 6 and 7, which have a five second time lapse between them. The contrast effect seen at the large disc (X) at the top of the field is typical and is similar to the stacking fault contrast described by Baker (1962) and Amelinckx (1963). This dark contrast is most common round isolated discs, but it occurs to a lesser extent in areas containing many overlapping ones. Another feature of the discs in motion is

that they sometimes pass through a stage with straight sides and sharp angles (P). The angles A to F are respectively 120° , 132° , 120° , 120° , 120° , 139° , and it is assumed that this pseudo-hexagonal shape comes from the momentary arrest of the movement by faults or cracks in the graphite lattice. This effect is similar to the pseudo-crystalline shape assumed by boron oxide on graphite (Thomas and Roscoe, 1965).

iv. Position of the discs in the c-direction. Shadowing discs with carbon-platinum at 15° shows that they never cast a shadow. Plates 8 and 9 are of the same area of shadowed material with a time lapse of 5 seconds between the two exposures. The direction of shadowing can be seen at X and the sides of the discs at Y are parallel to this line. The fact that the discs are free from shadow indicates that they are either inside the crystal or that they are so shallow a surface effect that they are not made visible by a 15° shadow. The fact that the discs move (P) and disappear (Q) despite the layer of shadow on the surface supports the suggestion that they are inside the crystal.

v. In situ reaction. The plates which have been discussed so far have all been of separate observations from different experiments. The deductions made have been confirmed by carrying out the reaction on a specimen

PLATE 8.

Purified natural graphite. After
reaction with a saturated solution of
ammonium vanadate in a mixture of
sulphuric and nitric acids for 15 minutes.
Specimen shadowed with carbon-platinum at 15°.

Final magnification - 114,000X.



PLATE 9.

Same area as Plate 8, after a
short time lapse.

Final magnification - 114,000X.



PLATE 10.

Single crystal graphite. A - standard material. B. - same area after reaction with sulphuric and nitric acids for 7 minutes.

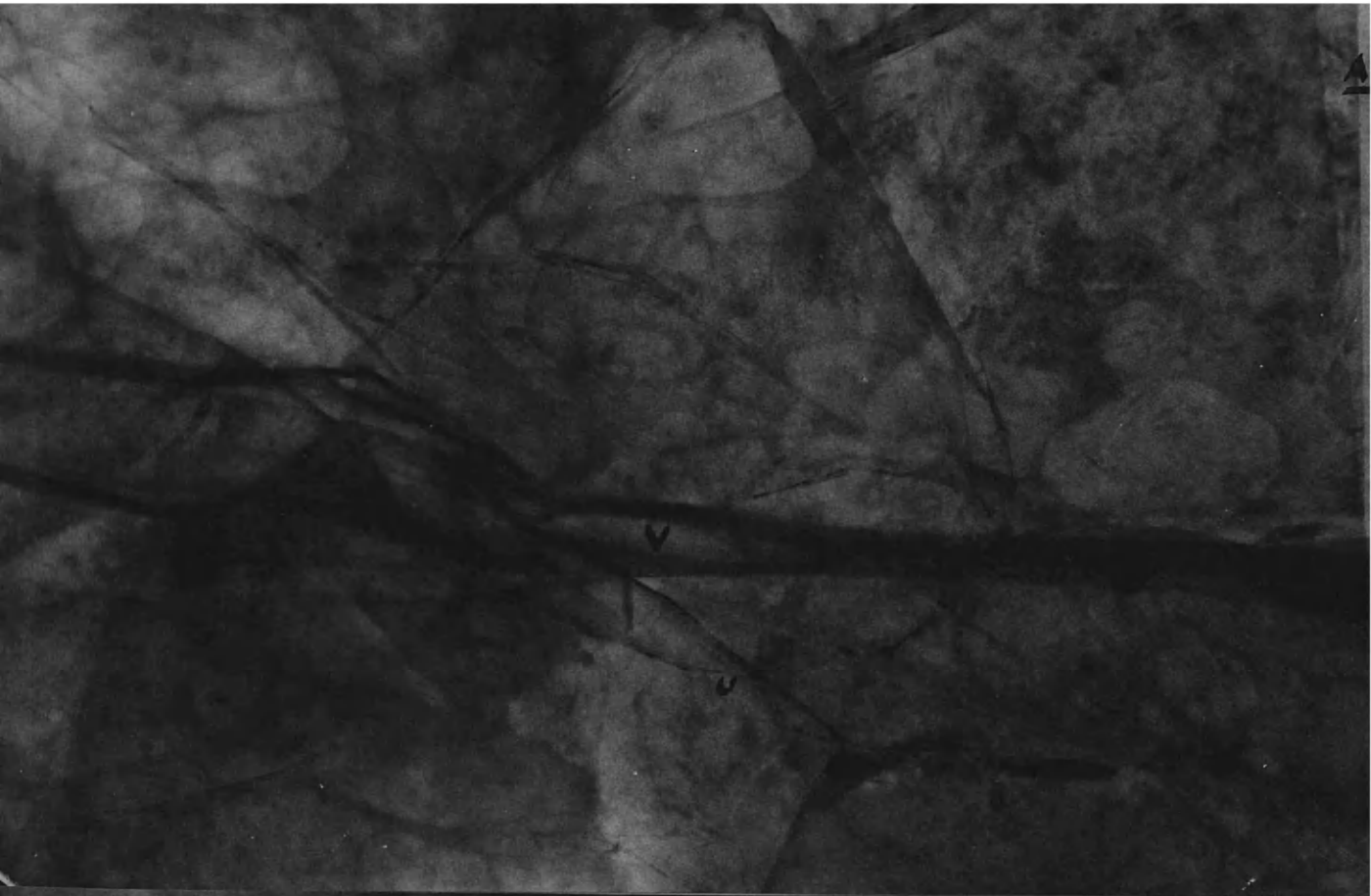
Final magnification - 74,000X.



PLATE 11.

Same area as Plate 10. A - after
reaction for 12 minutes. B - after
reaction for 17 minutes.

Final magnification - 74,000X.



mount and following the course of the intercalation stage by stage. Plates 10 and 11 confirm that the discs and resultant folds are caused by the acid reaction. Plate 10 A shows an area of unreacted single crystal graphite and it is assumed that the material at XY is surface contamination. Plate 10 B shows the same area after 7 minutes' reaction, with XY now marked by an oxidation channel (Section II B, of Results). The moiré patterns have changed and transparent discs have been produced. After 12 minutes' reaction, there are fewer discs, but both thin (U) and thick (V) folds have been formed (Plate 11 A). In this case the folds are being formed from the discs by the action of more acid and not by the heating effect of the electron beam. After 17 minutes' reaction (plate 11 B) the discs have completely disappeared and the folds have changed their position.

vi. The structure of the folds. The folds, formed from the discs by the reaction of either heat or acid, vary in thickness and length. They occur in different layers of the lattice, since they can be seen to overlap and cross (Plate 12). The folded material was examined after carbon-platinum shadowing at 15° (Plate 14). The direction of shadowing is shown at X and the fold parallel to this has no shadow. (Y). Although this is the general

PLATE 12.

Purified natural graphite. After reaction with sulphuric and nitric acids for 6 weeks. The inset shows the diffraction pattern from part of this area and the spots ringed are used to illuminate the dark field (Plate 13).

Final magnification - 171,000X.



PLATE 13.

Same area as Plate 12, but taken with
dark field illumination.

Final magnification - 171,000X.

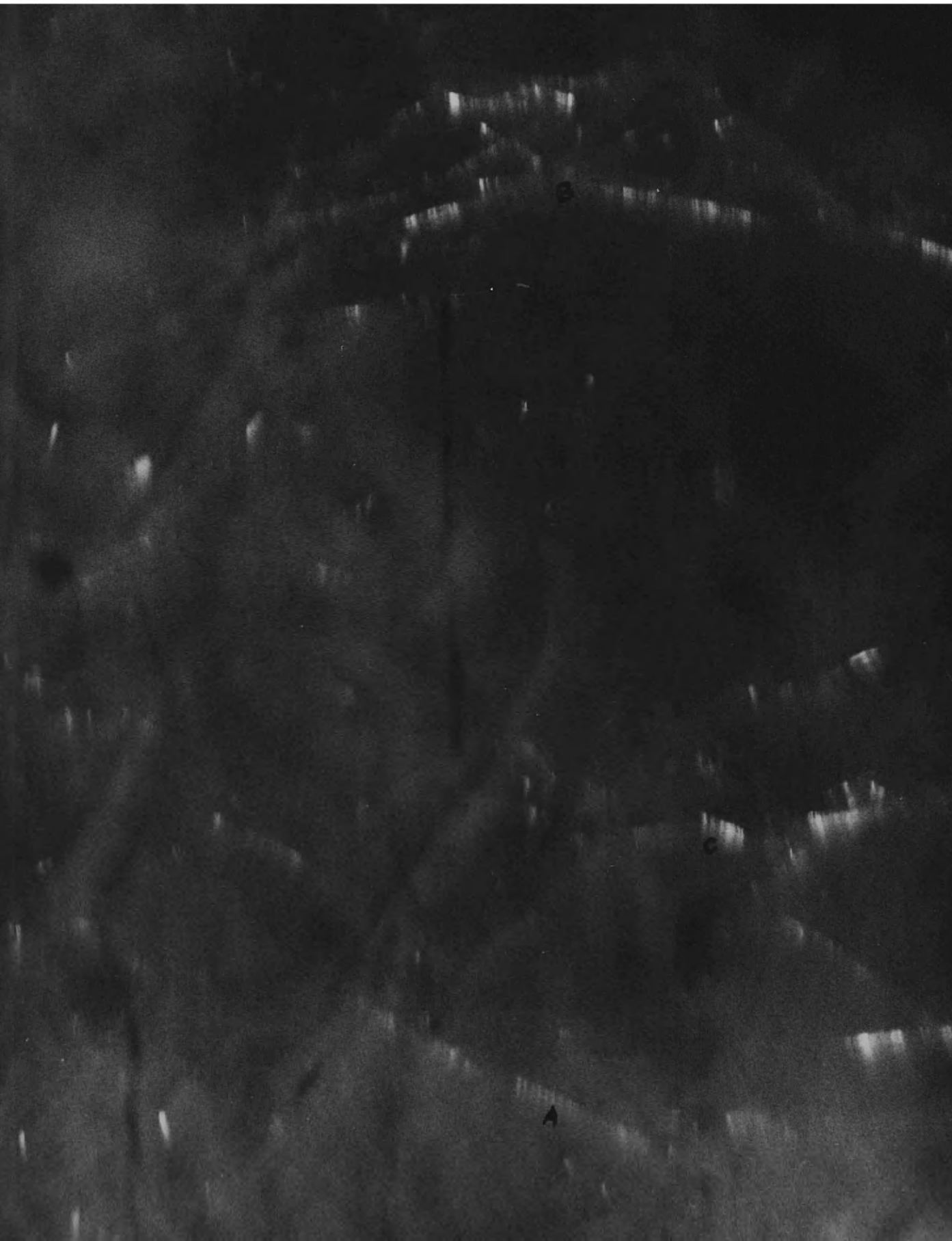


PLATE 14.

Pile grade A, polycrystalline,
synthetic graphite, after reaction
with a saturated solution of ammonium
vanadate in a mixture of sulphuric
and nitric acids for 15 minutes.
Specimen shadowed with carbon-
platinum at 15° .

Final magnification - 318,000X.



picture, occasionally the folds are on the surface and are sufficiently elevated to give a 15° shadow.

Plates 12 and 13 show the light and dark field images of a folded area, with the selected area diffraction pattern in the inset. An extra diffuse ring of spots has appeared in the pattern, with a mean spacing of 3.357\AA , which can be attributed to the 0002 planes of graphite (3.3538\AA , according to Franklin, 1951a). The part of the 0002 ring outlined in the inset was used as illumination for the dark field plate. In this (Plate 13) the folds are brightly illuminated, indicating that they contain 0002 planes. Although there is very good correspondence between the positions of folds in the light and dark field micrographs (A,B,C) they do not all appear in the latter, since some of them diffract to give the 0002 spots not selected for use.

Another feature of the light field image is the production of intensely dark bands (C) which appear as brightly illuminated bands in the dark field image (C). Some periodicity (71\AA at A) is often seen in these bands and this may be an image of regular buckling in the folded areas, or may be some type of extinction band. This effect is similar to the black streaks in the light field image of irradiated graphite, described by Dawson and Follett (1961) who report that they are produced by the strongly diffracting

(0001) planes. Another report of a similar effect is the work, on graphitisation and deformation in carbon films, of Jenkins, Turnbull and Williamson (1962), who observed "bands" or folds when the thin graphite films have been contaminated. These structures give 0002 reflections and also normal extinction contours, similar to those seen in this work. They suggest that the folds, or "kink bands" are the equivalent of twins in single crystal material, but lacking any preferred orientation because of the random arrangement of the crystallites. The folds described above are probably similar kink bands.

C. Interference patterns.

i. Description. Two similar types of interference pattern are seen (Plate 15). The first consists of small dots or concentric rings (X) with either a dark or a light centre. Typical dimensions are 238\AA for the internal diameter and 612\AA for the external diameter. Small dots of this type are often seen connected by streaks (Q) along what may be a fault in the graphite crystal. These dots are similar to those described by Fujita and Izui (1963) and Izui and Fujita (1963) for fission fragment irradiation of graphite and molybdenite and are ascribed by them solely to radiation damage. Similar patterns were, however, seen in the course of this work, on standard natural graphite and this has been reported by Bonfiglioli and

Mojoni (1964). These authors describe the concentric rings as Newton-ring or lenticular defects, and suggest that they are caused by interference due to the presence of cavities in the lattice. For the acid reaction studied here, more patterns of this type were seen after treatment than on the standard material, and it may be assumed that they are the result of the intercalation process. Further proof of this will be given in (iii), below.

The second type of interference pattern, closely related to the first, is a distorted moiré effect (P). In the example shown, the bands are of the order of 55\AA to $1,020\text{\AA}$ in width. These patterns are more extensive in area than any interference effects reported in the literature for radiation damage (Bollmann, 1960, Williamson, 1961, Baker, 1961a, b, and Reynolds and Thrower, 1964). It is obvious that the patterns are moiré fringes when the diameter of the whole defect increases and the lines become more or less parallel, as they are in an undistorted moiré. Although the authors Bonfiglioli and Mojoni (1964) are of the opinion that the concentric circles do not show the same contrast as dislocations, it can be seen (Plate 15, R) that the distorted moirés are sometimes associated with lines similar to the dislocations described by Amelinckx and Delavignette (1961).

These two types of interference pattern are far less common than the transparent discs (B above) but they are

PLATE 15.

Natural graphite after reaction with
sulphuric and nitric acids for $1\frac{1}{2}$ minutes.

Final magnification - 147,000X.



PLATE 16.

Single crystal graphite. A - standard.
B and C are the same area after reaction
with sulphuric and nitric acids for 7
and 12 minutes respectively.

Final magnification - 70,000X.



produced regularly. As the specimen is heated in the electron beam, the contrast may change but there is no overall movement.

ii. In situ reaction. Since there seems to be some uncertainty in the literature about the source of these interference effects, it is useful to report results obtained by observing the reaction stage by stage on a specimen mount. Plate 16 shows the same area of graphite before reaction (A), and after attack with acid for 7 minutes (B) and 12 minutes (C). It is clear that the distorted moirés have appeared and changed their position as the reaction proceeds.

A common feature of line moirés is that they appear and disappear as movement takes place in the lattice, causing a change in the reflecting planes. This effect was never seen with the distorted patterns and it is thus possible to use Plate 16 as proof that they are formed by the reaction of acid.

D. Electron Dense Material.

i. Introduction. Another effect seen in the residue compound is the appearance of dense material. Whereas the transparent discs and interference effects (B and C, above) are thought to be caused by changes in the graphite sheets, the dense material is probably due to the presence of intercalated material. In this section, the plates show graphite treated with acids alone, or with a saturated

solution of uranyl nitrate or ammonium vanadate in acids. The heavy cations were originally used in an attempt to increase the contrast between the graphite and the intercalated material, but it was found that the results were similar in all cases. It is therefore probable that the dense material is retained sulphuric acid or bisulphate ion and the analytical data in E, below, confirms this.

Two main types of dense areas are seen. The first is an interference effect similar to a spot moiré pattern and consists of regular discs. It is thought that these are due to the presence of small areas of crystalline bisulphate compound.

The second type is a direct image of retained intercalated material, which may appear either as highly mobile particles or as adsorbed droplets along grain boundaries in the graphite, and it is thought to be free sulphuric acid. The two types of material will be described in turn.

ii. Discs. Plate 17 is of material which has been treated with acid and vanadium for $1\frac{1}{2}$ hours. There are two sizes of disc, each being located in a different transparent disc. There is a certain amount of uniformity of size in each group: the smaller group has a diameter of 170\AA , with a variation of $\pm 20\text{\AA}$. Plate 18 shows an area containing discs, after shadowing with carbon-platinum at 15° : the direction of shadowing can be seen at X. The fact that

PLATE 17.

Pile grade A, polycrystalline, synthetic graphite, after reaction with a saturated solution of ammonium vanadate in a mixture of sulphuric and nitric acids for $1\frac{1}{2}$ hours.

Final magnification - 267,000X.



PLATE 18.

Pile grade A, polycrystalline, synthetic graphite, after reaction with a saturated solution of ammonium vanadate in a mixture of sulphuric and nitric acids for 15 minutes. Specimen shadowed with carbon-platinum at 15°.

Final magnification - 342,000X.

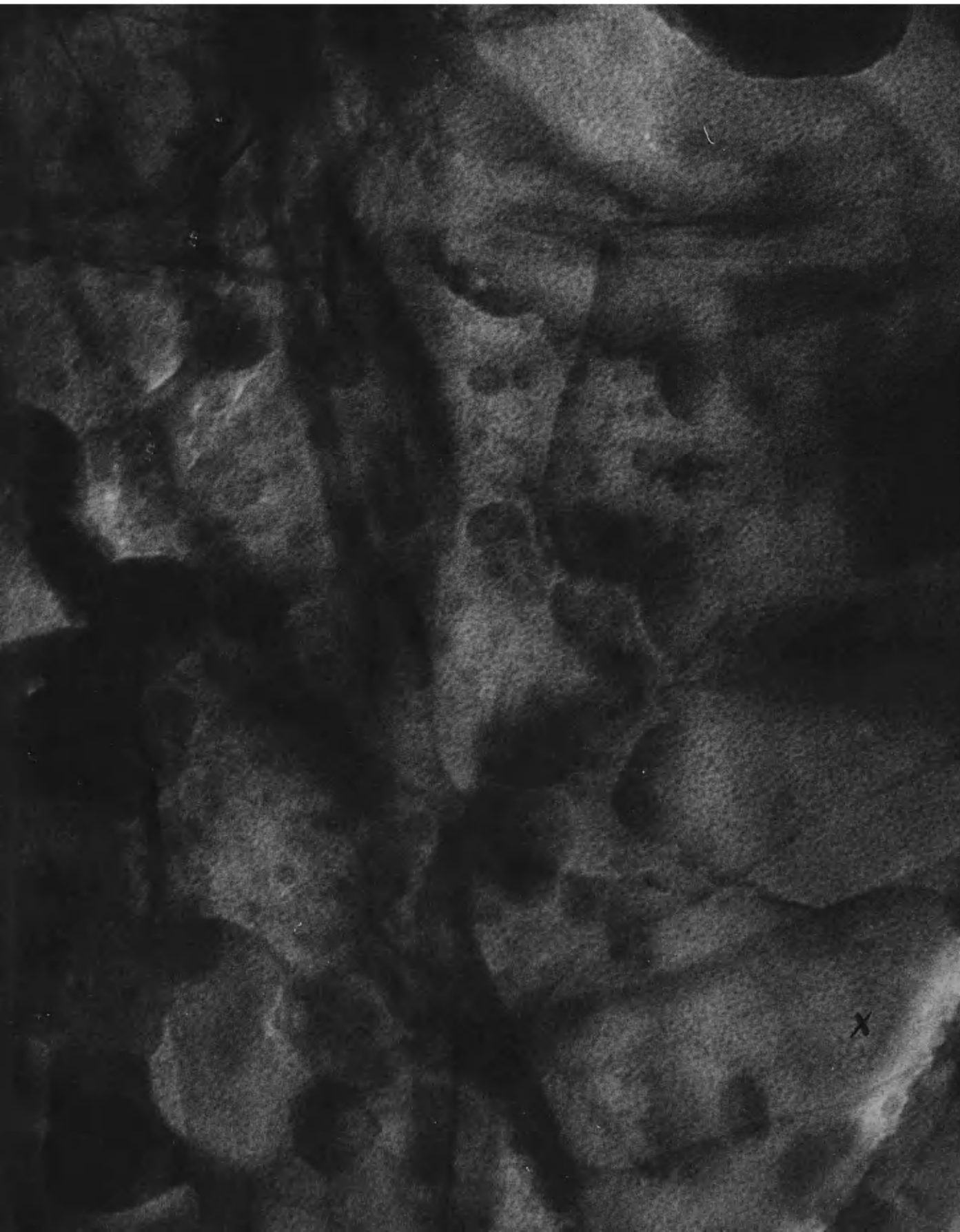


PLATE 19.

Pile grade A, polycrystalline, synthetic graphite, after reaction with sulphuric and nitric acids for 30 minutes. Double condenser illumination.

Final magnification - 327,000X.

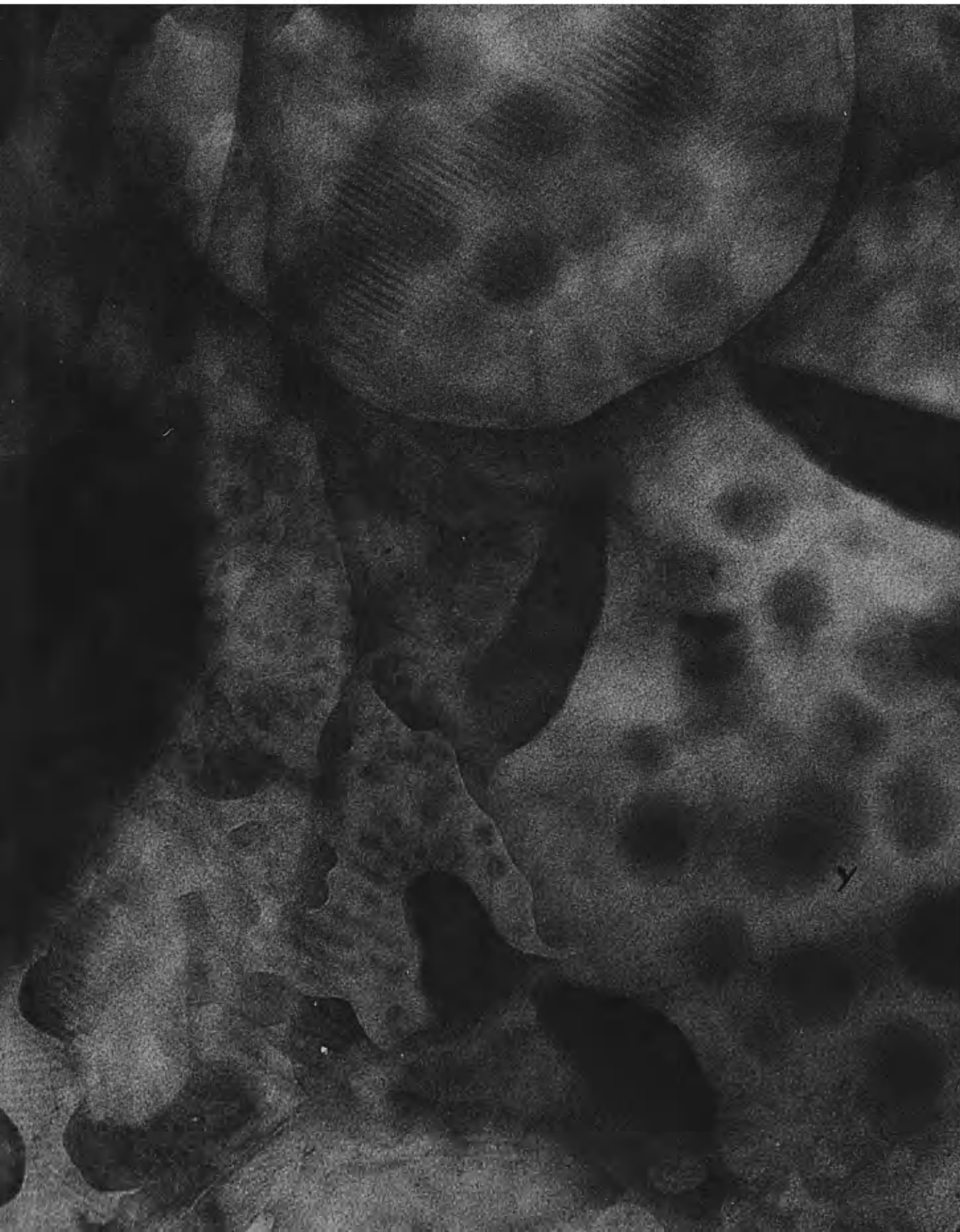
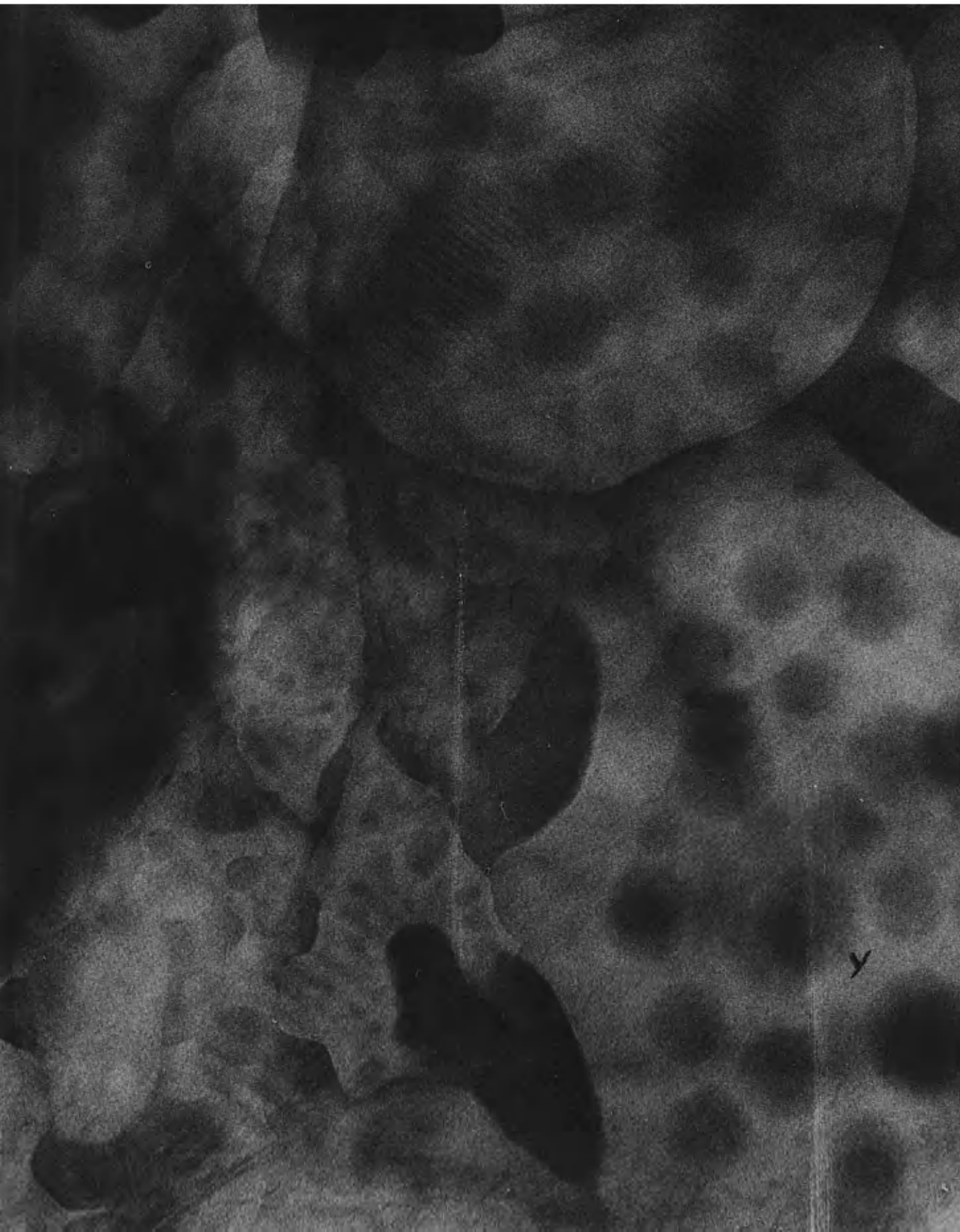


PLATE 20.

Same area as Plate 19, after a short
time lapse.

Final magnification - 327,000X.



there is no shadow on the discs suggests that they are either inside the crystal or are a very shallow surface effect. Since they are often found in association with transparent discs which are almost certainly inside the crystal, it is probable that the dense discs are also a true intercalation effect.

There are two possible explanations for the dense discs: they may either be a direct image of small particles of intercalated material or a diffraction effect similar to a spot moiré. They have the same focussing characteristics as diffraction effects, since they invariably have a diffuse edge, in contrast to the sharp Fresnel fringes which are usually seen round the edge of particles. This suggests that the discs are formed by double diffraction, though the same effect would be seen on the image of a tapering particle with an edge too thin to give Fresnel fringes. However, in Plates 19 and 20, of graphite after attack by acid alone for 30 minutes, the discs are aligned in rows, supporting the suggestion that they are part of a spot moiré pattern, coming from a crystalline part of the residue compound, where bisulphate may still be bound to the graphite lattice. Plates 19 and 20 show the same area, and the discs at Y have moved slowly relative to each other in the small time lapse

between the two exposures. If the discs were a direct image of intercalated material, the motion would probably be faster (iii, below), but if they were formed by interference between the beam diffracted by areas of bisulphate and by the graphite lattice, any slight movement of either layer could cause the slow movement seen. It is therefore concluded that the dense discs are a double diffraction effect.

iii. Dense mobile particles. This type of material is very dense, moves around extremely rapidly, changes its shape and breaks up into smaller pieces which may come together again. Plates 21 and 22, of graphite after contact with acid for one minute, show a typical example of this: the four micrographs are of the same area, with a time lapse of three seconds between the exposures. The whole of the sequence is not shown here, since the particle was originally attached to the transparent disc at A (Plate 21 A) but it moved rapidly round to B before becoming detached. Since the particles can be attached to the transparent discs which are inside the crystal, they must also be a true intercalation effect.

In Plate 21 A the difference between the dense discs and the mobile particles can easily be seen. The discs are smaller and more regular in shape - the diameter of the discs is 280\AA , whereas the mobile particle is approximately

3700Å long and 1300Å broad. The two structures have different contrast characteristics: the discs have diffuse edges, like a moiré pattern, whereas the mobile particle is darker, with a sharp edge round which Fresnel fringes can be seen.

The best method of giving an indication of the movement of these particles is to follow their progress with a ciné film. Plate 23 shows a series of stills from a ciné film taken at an electron microscope magnification of 20,000X, giving a final magnification of 78,000X. The material shown has been in contact with acid and vanadium for 15 minutes. Stills 1 to 4 show a cluster of small, mobile particles oscillating and moving in the typical way. In still 3 a particle (X) is seen at the end A of a microcrack (AB), in 6 and 7 it has moved partly along, in 9 it has reached end B and in 10 it has left the channel completely. The particles often move in this way along microcracks and round the edges of crystallites, following definite paths, as well as oscillating in the centre of the crystallites.

From the set of ciné stills, it is possible to calculate the speed of movement of the particles. The particle X moved along the microcrack AB in stills 5 to 8, comprising 30 frames on the original film, which was taken at a speed of 16 frames a second. The distance AB is approximately 2×10^{-5} cm., so the speed of the particle is 1070Å per second.

PLATE 21.

Pile grade A, polycrystalline, synthetic
graphite, after reaction with sulphuric
and nitric acids for 1 minute. A - standard.
B - same area after a short time lapse.

Final magnification - 99,000X.

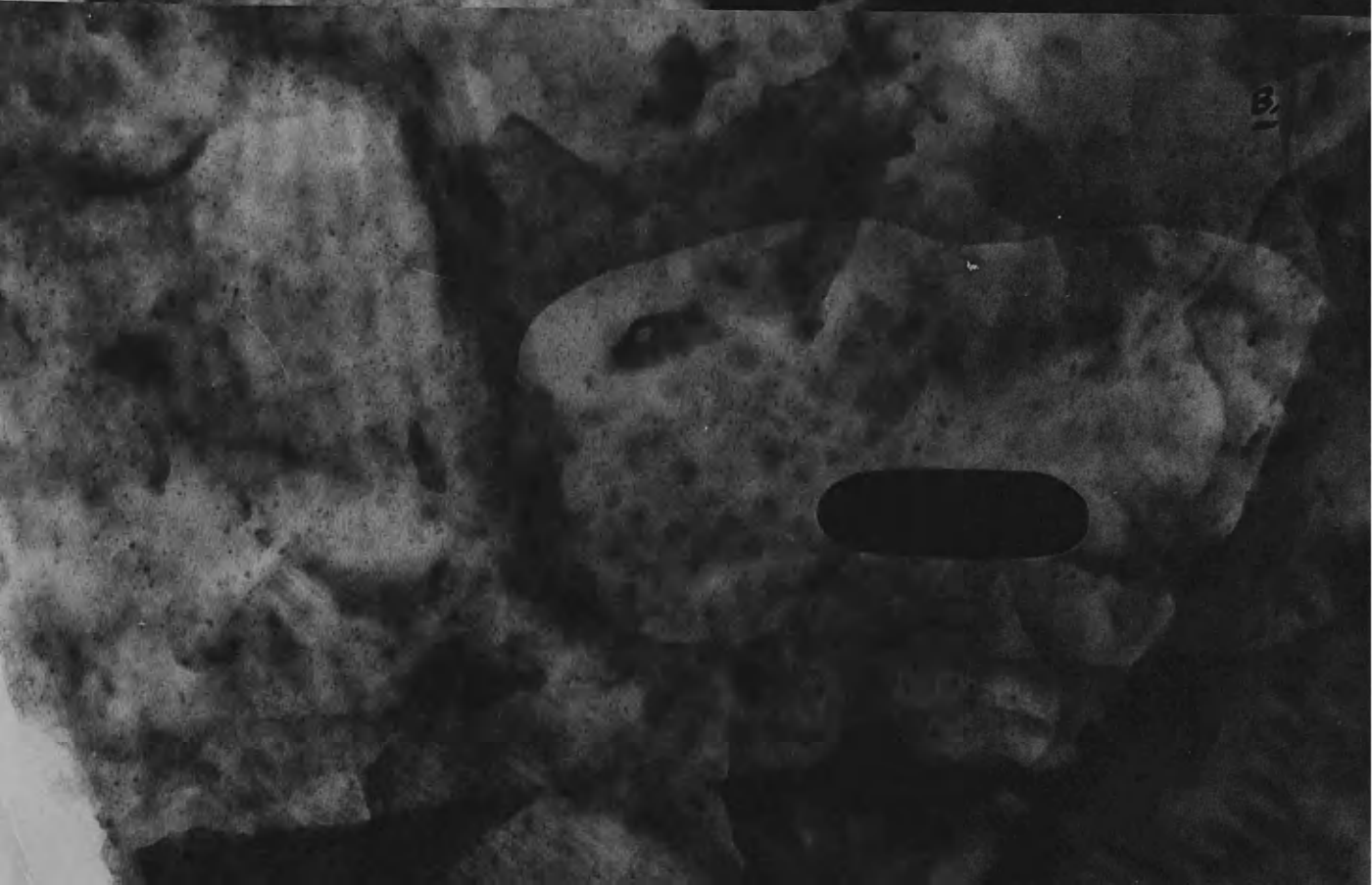
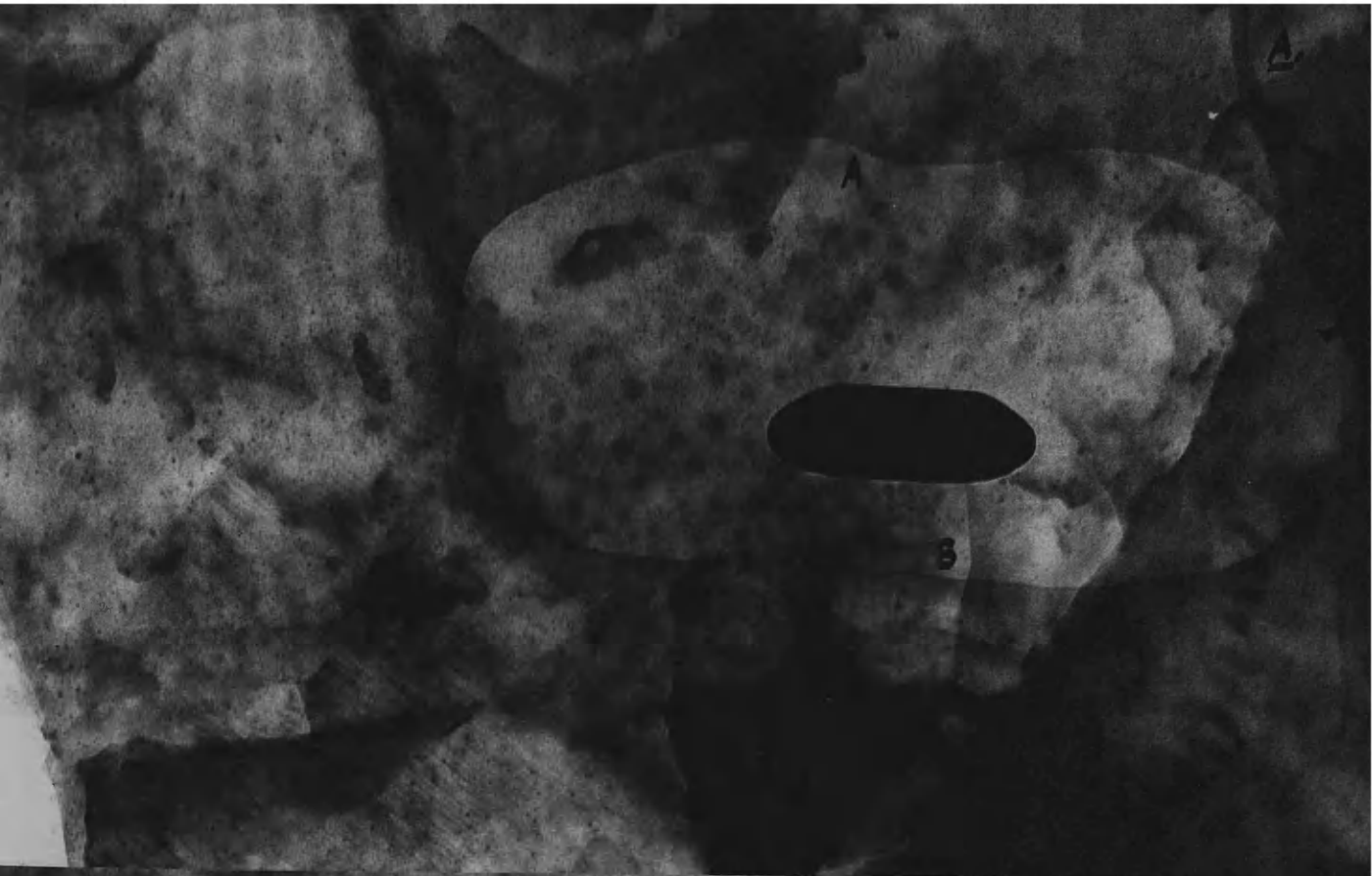


PLATE 22.

Same area as Plate 21. A and B after
two further time lapses.

Final magnification - 99,000X.

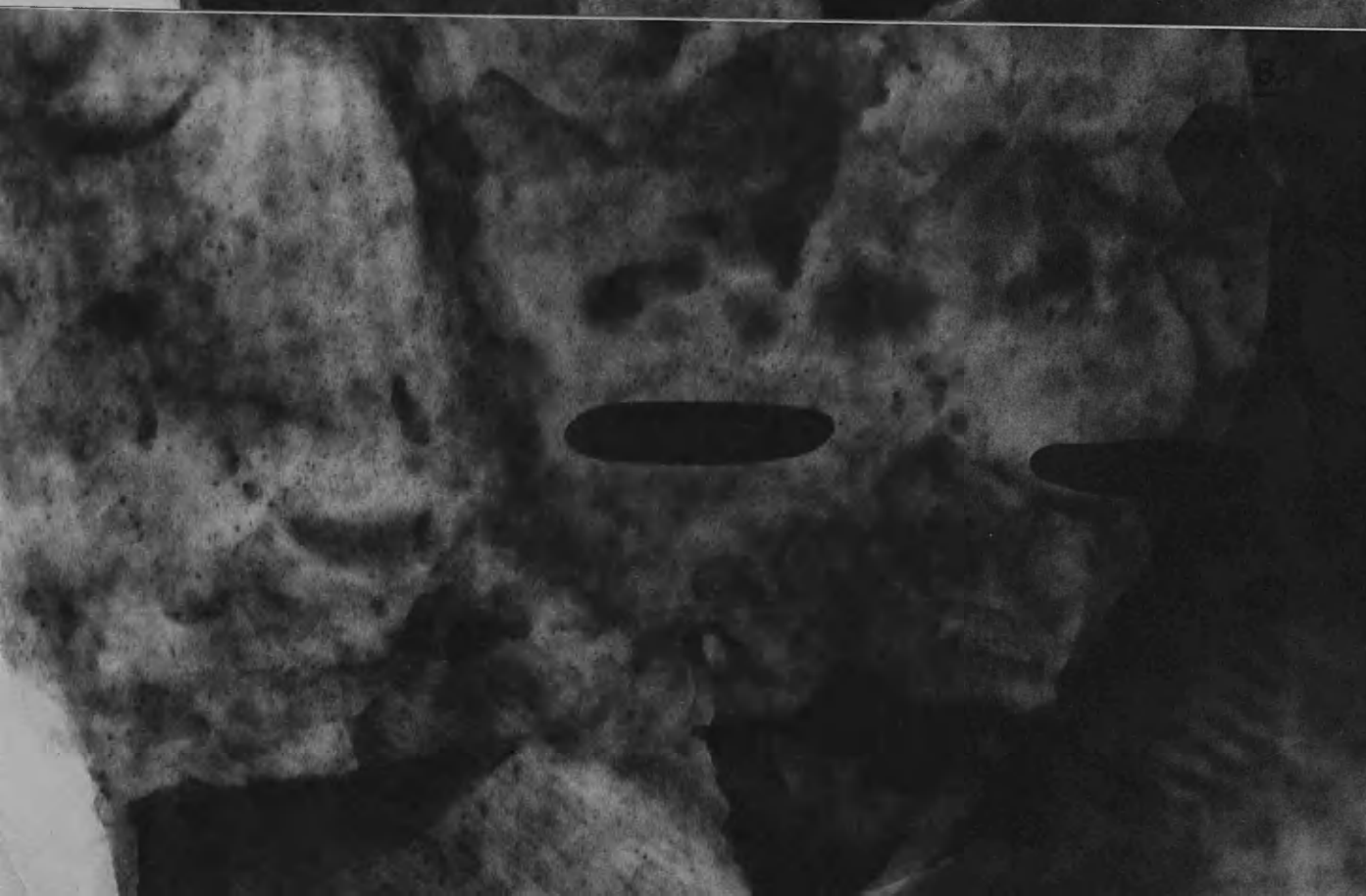
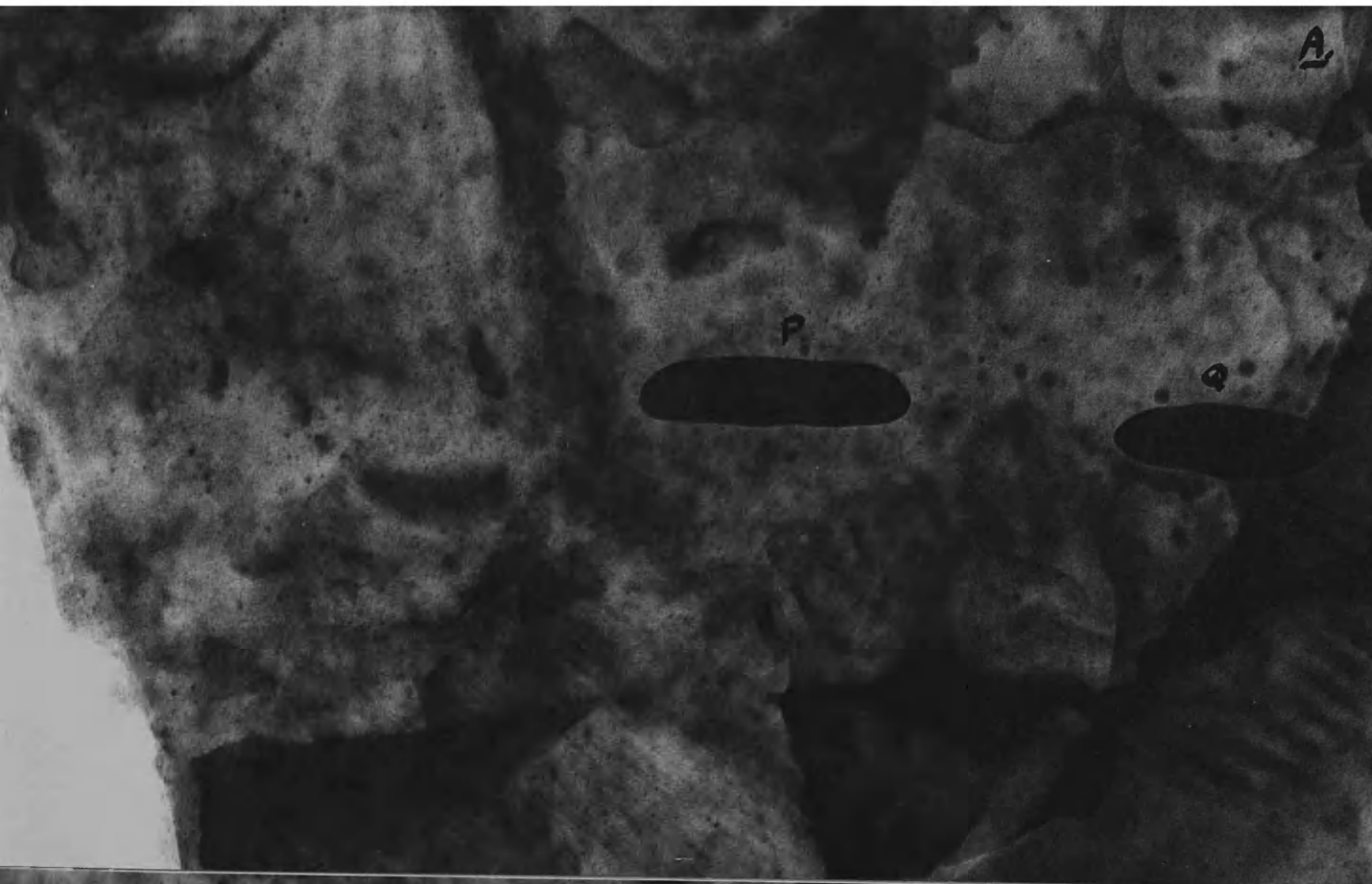
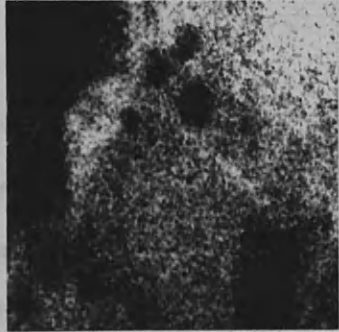




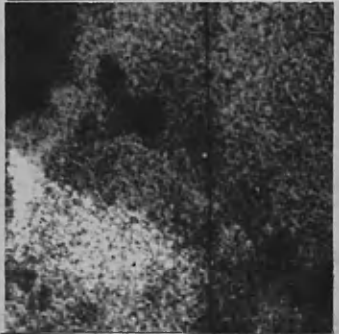
PLATE 23.

Pile grade A, polycrystalline, synthetic graphite, after reaction with a saturated solution of ammonium vanadate in a mixture of sulphuric and nitric acids for 15 minutes. Set of stills from a cine film.

Final magnification - 78,000X.



1.



2.



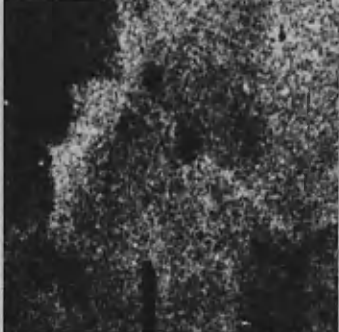
3.



4.



5.



6.



7.



8.



9.



10.

From the micrographs and ciné stills shown, this dense, mobile material has the appearance of liquid particles trapped in the graphite crystals, and it is presumed that the liquid is free sulphuric acid. In some cases, the acid is adsorbed along faults in the lattice to give a row of droplets and this will now be described in detail.

iv. Adsorption of droplets along straight lines. This material has the same focus characteristics as the mobile particles, but it is strung in a regular fashion along straight lines. Plate 24, of purified natural graphite after reaction for 15 minutes with acid and vanadium, shows two sizes of droplet (X and Z). The large droplets (X) are strung along a line leading from a deep fold or pore in the crystal (Y), and the individual particles are joined by a 30\AA thread of material. Trapped sulphuric acid is being piped along a micropore, forming droplets at intervals, presumably at defects in the neighbouring graphite crystallites. At Z, a similar effect is seen, with the droplets in several rows, in almost parallel alignment. This is suggestive of a grain boundary which has adsorbed intercalated material because of its large amount of crystal imperfection. Plate 25 shows an area containing droplets adsorbed in this way, after carbon-platinum shadowing. The lack of shadow on them indicates that they are probably

PLATE 24.

Purified natural graphite, after reaction with a saturated solution of ammonium vanadate in a mixture of sulphuric and nitric acids for 15 minutes.

Final magnification - 291,000X.



PLATE 25.

Pile grade A, polycrystalline, synthetic graphite, after reaction with a saturated solution of ammonium vanadate in a mixture of sulphuric and nitric acids for 15 minutes. Specimen shadowed with carbon-platinum at 15°.

Final magnification - 597,000X.

inside the crystal, though they may be a very shallow surface effect.

Since it is suggested that liquid sulphuric acid is trapped and adsorbed inside the lattice of the graphite bisulphate residue compound, it is useful to give some facts about the boiling point of this acid. Application of the Clausius-Clapeyron equation shows that sulphuric acid, in contact with a pressure of 2×10^{-4} mm., will boil at a temperature of -35°C . The temperature of the electron beam can be taken as 40°C . to 100°C . (A maximum figure of 130°C . is quoted by Watanabe, Someya and Nagahama, 1962.) When a sample of the residue compound is put in the electron microscope, any sulphuric acid which comes directly in contact with the vacuum in the column will evaporate. Since the mobile dense material described in (iii) does not boil, it must not be in contact with the vacuum if it is sulphuric acid. The mobile particles are seen for all three types of residue compound examined and since the uranyl nitrate also gives a solid precipitate (F, below) and there is almost no vanadium pentoxide retained (G, below), it is almost certain that these particles are free sulphuric acid. Since there must be no direct contact between this and the vacuum in the microscope when the material is being examined, there must be sudden tight clamping of the graphite layers on reversal of the intercalation reaction. There

will, therefore, be a minimum pressure required inside the crystal to prevent evaporation of the acid. By applying the Clausius-Clapeyron equation for the temperature range of 40°C. to 100°C., found in the electron microscope, a pressure range of 3.99 mm. Hg. to 0.0776 mm. Hg. is found for the inside of the graphite lattice.

The changes which take place in the sequence shown in Plates 21 and 22 will now be described in detail, since the difference between the transparent discs and the mobile particles is obvious, on close examination of the changes in size during heating in the electron beam.

(a) The total area covered by the transparent disc increases, since it expands both in length and breadth. The measurements are shown for Plates 21 A and 21 B.

	<u>Length (Å)</u>	<u>Breadth (Å)</u>
Plate 21 A	11820	5657
Plate 21 B	11910	5758
Difference	+90	+101

(b) The mobile particle expands in length but contracts in breadth, suggesting that the volume of material remains unchanged.

	<u>Length (Å)</u>	<u>Breadth (Å)</u>
Plate 21 A	3738	1293
Plate 21 B	3779	1201
Difference	+41	-92

These figures suggest that the mobile material is a definite quantity of trapped intercalate, which must counteract any increase in length with a decrease in breadth. On the other hand the electron transparent disc is some type of fault in the graphite which can increase its area till it meets an obstruction and forms a fold.

(c) After the elongation process, the particle breaks in the middle to give two parts, P and Q (Plate 22 A) and these both become longer and narrower (Plates 22 A and 22 B). The measurements are shown for P only.

	<u>Length (Å)</u>	<u>Breadth (Å)</u>
Plate 22 A	3727	909
Plate 22 B	3748	849
Difference	+21	-60

It is interesting to note that, while the breadth of P is smaller than the original particle, the length has expanded till P is as long as the original (3738Å). There would therefore seem to be a tendency for the particles to expand preferentially in one direction.

E. Influence of heavy metal cations on the reaction.

i. Addition of ammonium vanadate. No electron microscope evidence was found for the presence of vanadium pentoxide in the residue compound prepared by leaving graphite in contact with a saturated solution of ammonium vanadate

in a mixture of sulphuric and nitric acids. This is confirmed by the analysis figures (Lind, 1964), which show that vanadium is present only to the extent of 200 parts per million.

ii. Addition of uranyl nitrate.

(a) Analysis. Extra material was seen in the electron microscope examination of the uranium residue compound and the analysis figures (Lind, 1964) show that it contains 3.75% of uranium. This material was seen in two ways - either decorating lines in the crystal (b, below) or as small crystallites (c, below).

(b) Decoration. This effect is seen clearly in Plate 26. The interrelated material has a more crystalline appearance than the bisulphate and sulphuric acid reported in D, above, and is probably uranyl nitrate, either free or hydrated. The material has been preferentially adsorbed along lines which may be micro-pores, steps or dislocations and has an appearance similar to that reported by Nicholson (1963) for silica particles on dislocations. Many of the lines meet at definite angles; for example at P the mean angle is 145° . These lines are probably decorated crystallite edges rather than dislocations.

This decoration was only seen for the uranium residue compound, but it was not a very common feature and it is reported here only because of its similarity to the effect

PLATE 26.

Pile grade A, polycrystalline, synthetic graphite, after reaction with a saturated solution of uranyl nitrate in a mixture of sulphuric and nitric acids for 30 minutes.

Final magnification - 312,000X.



described by Bacon and Sprague (1961a) for caesium hydroxide intercalated in graphite.

(c) Crystallites of uranyl nitrate. Another feature found only in the uranium residue compound is the presence of large crystalline particles. These are seen in Plates 27 A and 27 B, which show the same area of graphite with a time lapse of five seconds between the two exposures. The crystals change their shape (X in the two micrographs) as the material is heated in the electron beam.

The light and dark field images of these crystals are shown in Plates 27 C and 27 D. The corresponding selected area diffraction pattern is shown in the inset, and the spots marked in the 0002 graphite ring are those used for illumination in the dark field image. Uranyl nitrate has a strong spacing at 3.36\AA (F, ii, below) so that this ring may also contain some spots coming from this compound. The fact that the small crystal (X) is brightly illuminated in the dark field image suggests that it is composed of uranyl nitrate.

PLATE 27

A and B

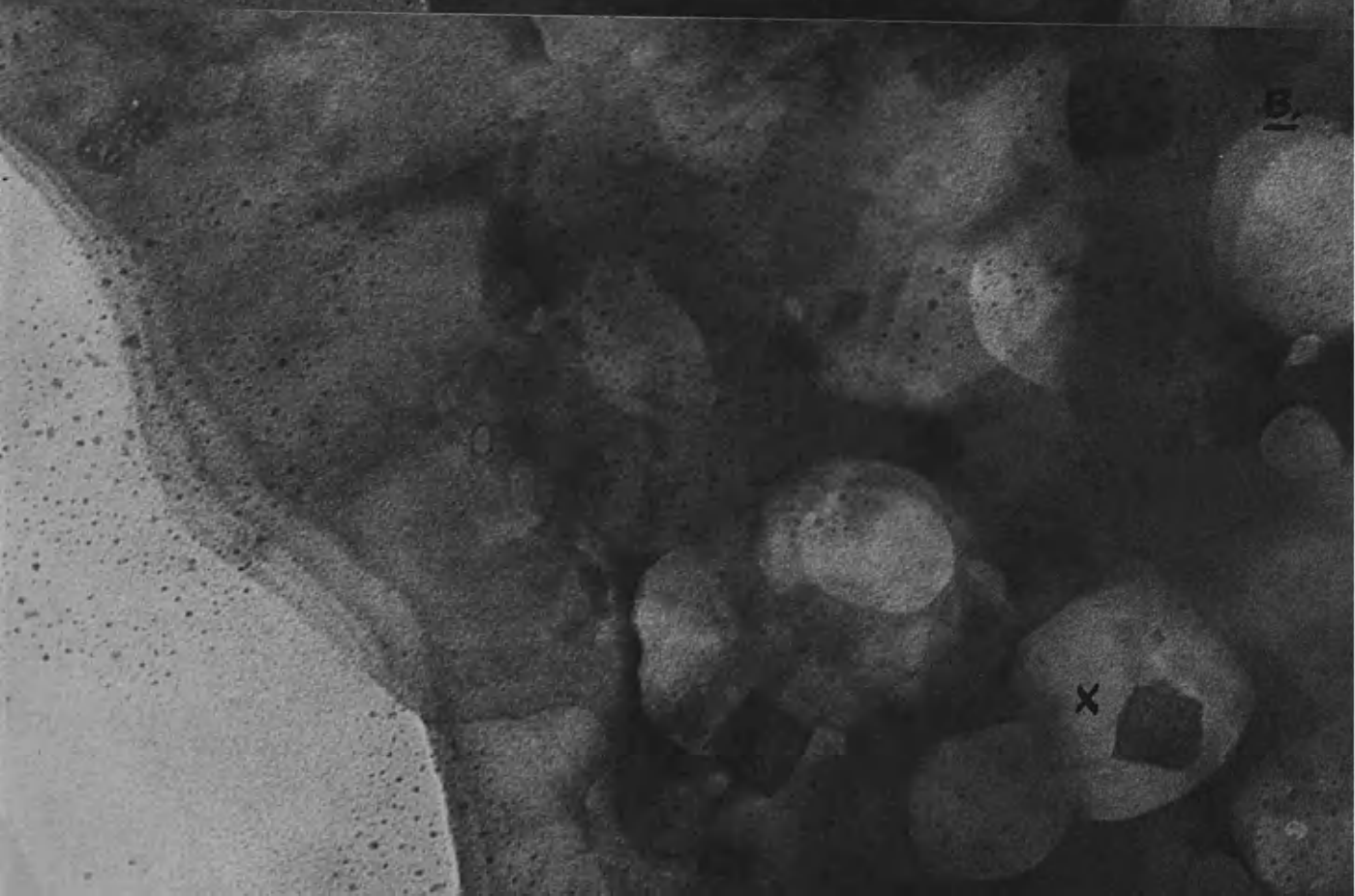
Pile grade A, polycrystalline, synthetic graphite, after reaction with a saturated solution of uranyl nitrate in a mixture of sulphuric and nitric acids for 1 hour. A and B are of the same area with a small time lapse between the two exposures.

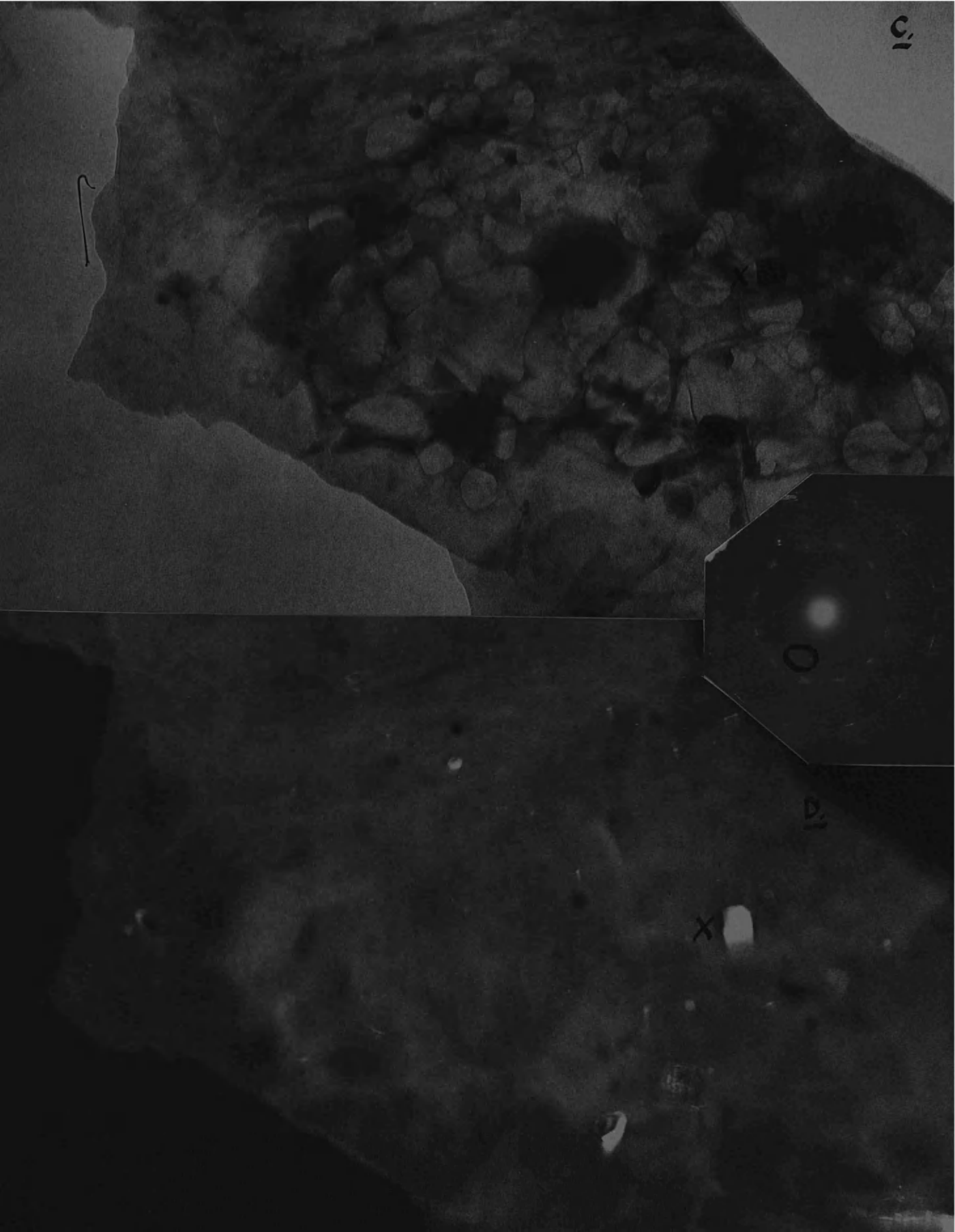
Final magnification - 306,000X.

C and D

Pile grade A, polycrystalline synthetic graphite, after reaction with a saturated solution of uranyl nitrate in a mixture of sulphuric and nitric acids for 1 hour. C, Bright field - D, Dark field image of same area. Inset shows selected area diffraction with (ringed) the spots used to give the dark field D.

Final magnification - 102,000X.





F. Diffraction.

i. Introduction. The intercalation reactions were followed by diffraction and the results confirm the deductions made on the structure of the residue compounds on the basis of electron microscope examination. X-ray patterns and selected area electron diffraction patterns will be discussed in turn.

ii. X-ray powder patterns. The lattice spacings were calculated from the photographs in the usual way. To obtain an indication of the degree of accuracy of the measurements, three patterns of standard graphite were taken, using polycrystalline synthetic material; the mean values and range for the 0002, $10\bar{1}0$, $10\bar{1}1$ and 0004 planes were calculated and compared with the literature values (Hull, 1917).

<u>Plane</u>	<u>Mean d(Å)</u>	<u>Range of d(Å)</u>	<u>Literature value of d(Å)</u>
0002	3.348	3.356 - 3.339	3.37
$10\bar{1}0$	2.122	2.125 - 2.119	2.11
$10\bar{1}1$	2.026	2.029 - 2.025	2.03
0004	1.678	1.678 - 1.676	1.69

The range given here was then used for comparison with the spacings for the residue compounds. The bisulphate and vanadium compounds show no significant changes while the uranium compound has incorporated some of the uranyl nitrate spacings in its diffraction pattern.

a) Bisulphate and vanadium compounds.

Bisulphate	<u>Plane</u>	<u>Bisulphate d(Å)</u>	<u>Graphite d (Range, Å)</u>
	0002	3.352	3.356 - 3.339
	10 $\bar{1}$ 0	2.123	2.125 - 2.119
	10 $\bar{1}$ 1	2.031	2.029 - 2.025
	0004	1.677	1.678 - 1.676

These figures confirm that the bisulphate residue compound has a structure identical to that of graphite (Rüdorff).

Vanadium	<u>Plane</u>	<u>Vanadium d (Å)</u>	<u>Graphite d (Range, Å)</u>
	0002	3.360	3.356 - 3.339
	10 $\bar{1}$ 0	2.125	2.125 - 2.119
	10 $\bar{1}$ 1	2.029	2.029 - 2.025
	0004	1.678	1.678 - 1.676

There is no significant change here, and this is in agreement with the electron microscope and analysis results given in E, above.

b) Uranium compound.

Two sets of values for the powder spectrum of $UO_2NO_3 \cdot 6H_2O$ are given alongside those for the uranium residue compound and graphite (Structure Reports, 1949 and Armour Research Foundation of Illinois, 1949).

<u>Uranium Compound-d(Å)</u>	<u>Graphite d(Å)</u>	<u>Uranyl Nitrate-d(Å)</u>	
		(1)	(2)
R 7.38			
R 6.94		6.72	(6.6)
		6.42	
		5.81	(5.7)
		5.66	
U 4.42		4.34	(4.34)
U 4.13		4.20	
U 3.86		3.80	
		3.74	
		3.61	(3.63)
		3.56	
G:U 3.32	(0002) 3.37	3.29	(3.36)
		3.27	
U 3.03		2.92	(2.93)
		2.84	(2.85)
		2.75	
		2.70	
		2.63	(2.62)
		2.60	
U 2.55		2.53	(2.54)
U 2.49		2.47	(2.46)
		2.43	
		2.37	(2.37)
U 2.34		2.32	
U 2.28		2.29	(2.29)
G 2.13	(10 $\bar{1}$ 0) 2.11	2.11	
U 2.09		2.09	
G 2.03	(10 $\bar{1}$ 1) 2.03		

The spectrum for the uranium residue compound is shown on the left of the table and those lines which correspond to graphite or uranyl nitrate are marked with G and U respectively. The extra lines not explained in this way are marked R and their presence may be due to the fact that the trapped uranyl nitrate has prevented all the expanded layers in the lamellar compound from collapsing completely when the residue compound is formed. This is similar to the effect seen when graphite oxide is formed (Results, IV, C, ii) where extra lines again appear in the X-ray spectrum.

ii. Selected area diffraction. Before reporting the results for areas containing mobile structures and dense discs, some of the difficulties met when applying this technique should be mentioned. For the transparent discs and mobile particles, it is extremely difficult to obtain the relevant patterns since exposures of 30 seconds are required for diffraction plates and a large amount of movement can occur in this time. For the dense discs, the difficulty springs from the lack of contrast between them and the background, since the discs are only visible on the photographic plate and not on the screen of the microscope. The selection of a suitable area is thus a matter of chance and it is difficult to be sure that a typical and significant effect is being presented.

PLATE 28

Pile grade A, polycrystalline synthetic graphite, after reaction with a saturated solution of uranyl nitrate in a mixture of sulphuric and nitric acids for one hour.

Top - diffraction pattern.

Bottom - selected area which gave the diffraction.



PLATE 29

Pile grade A, polycrystalline synthetic graphite, after reaction with a saturated solution of ammonium vanadate in a mixture of sulphuric and nitric acids for 15 minutes.

Top - diffraction pattern.

Bottom - selected area which gave the diffraction pattern.



a) Transparent discs. Many of these areas were diffracted and there was never any significant difference in the pattern, except for the presence of 0002 lines, probably derived from folds which are usually associated with these discs. The usual extra spots from incoherent scattering and double diffraction are sometimes seen, as for standard graphite. A typical pattern with two extra 0002 spots is seen in Plate 28. The $10\bar{1}1$ spots can also be seen on opposite sides of the $10\bar{1}0$ ring, giving the pattern a slightly elliptical appearance: this is due to the tilting of some of the graphite layers and it is sometimes seen in patterns from standard graphite.

b) Dense mobile particles. The typical pattern from these areas is again exactly the same as that of graphite and the failure of this material to give a crystalline diffraction pattern is to be expected, in view of the suggestion that it is liquid sulphuric acid. Plate 29 shows a pattern from this material, with a considerable amount of diffuse scattering inside the $10\bar{1}0$ ring, as is sometimes seen with standard graphite.

G. Bisulphate lamellar compound.

The diffraction results conclude the report on the residue compounds, but a description must be included of attempts to examine the lamellar compound. This material

decomposes even when put in contact with moist air (Riley, 1945) and those liquids which do not decompose it, for example, chloroform, (Ubbelohde and Lewis, 1960), do not act as suitable cleaning fluids. The lamellar compound was therefore examined directly from the acid by blotting it with acid-resistant filter paper and rubbing it on to a grid. The material obtained in this way was very dirty and contained few areas suitable for microscopy. Those that were examined had an appearance similar to the residue compound, with transparent discs and dense mobile material, but the difficulties described made it impossible to carry out a complete study of the compound.

II. The Long Term Effects of Acid On Graphite.

A. Introduction.

i. Description. This was carried out in the same way as the intercalation reaction, but the polycrystalline graphite was in contact with the acids at room temperature for periods up to 25 weeks. Since it is still the residue compound which is being examined, all the intercalation effects are seen, but in addition there is progressive gross oxidation of the graphite. This can be divided into five stages although there is considerable overlap.

(a) Up to 9 hours reaction. After 30 minutes in acid, the microcrystals making up the material are faintly outlined and it is possible to distinguish one from its neighbours.

(b) From 9 hours to 24 hours. The outlining becomes clearer and microcracks appear, both round and across the crystallites. A few fine lines similar to these are seen less frequently on standard graphite and these may be the precursors of the microcracks.

(c) 24 hours to 14 days. The microcracks, which are now more common, have become broader, punctate channels, as though each were formed from a row of fine holes which had not completely joined up.

(d) 14 days to 31 days. The channels are now completely formed and are broader and more numerous than ever.

(e) 31 days onwards. The final sample in this experiment was taken at 25 weeks, and from 31 days till this stage, the channels become deeper and broader. In addition, pits appear as an important feature for the first time.

ii. Rate of reaction. The final appearance of the material is very similar to that described by Dawson and Follett (1963) for graphite oxidised in air. The time taken to reach the same stage of reaction is 15 minutes for air and 5 weeks for acid oxidation: the latter reaction is 3,000 times slower than the former. It is thus more easy to divide the oxidation into the various stages described above.

iii. Catalysis. Since the oxidation of graphite by oxygen is catalysed by many impurities (Dawson, Follett

and Donaldson, 1961; Hennig, 1962; Hughes, Williams and Thomas, 1962; Presland and Hedley, 1962 and Dawson and Follett, 1963), the reaction was carried out with the vanadium and uranium acid solutions used for the intercalation experiments (Section I). The rate of oxidation was increased by a factor of two. Uranium and vanadium have an equally large effect, in spite of the fact that vanadium pentoxide is a particularly good catalyst for air oxidation of graphite (Hennig, 1962).

iv. Structure of graphite after prolonged acid oxidation.

After 25 weeks' reaction, the material still looks like graphite in the electron microscope, in spite of the production of holes and channels: it has high contrast and contains many moiré patterns. This is confirmed by comparing the X-ray powder patterns of graphite before and after 19 weeks' reaction with acid.

Plane	Graphite before reaction-d(Å)	Graphite after 19 weeks' reaction-d(Å)
0002	3.356 - 3.339	3.389
10 $\bar{1}$ 0	2.125 - 2.110	2.125
10 $\bar{1}$ 1	2.029 - 2.025	2.035
0004	1.678 - 1.676	1.674

The correspondence of lattice spacings between the two is not so good as that between those of graphite and its residue compounds (Section I - F), but the two patterns

here were still superimposable. After the reaction, however, it was more difficult to obtain accurate measurements of the ring diameters because of the broadening of the lines due to buckling and breaking down of the crystals.

B. The Five Stages of Oxidation.

i. Formation of microcracks. The next six plates show pictorially the stages described in A above. All the plates in this section are of polycrystalline synthetic graphite, except the first (Plate 30) which is of single crystal graphite and it is included because it is the best example of the formation of a micro-crack. The original piece of graphite (Plate 30A) shows a fine line (AB) which can be seen to be a thin micro-crack at X. After reaction for 12 minutes with acid, AB has been preferentially attacked to give a crack 38\AA broad, which is a typical size for the early stages of the oxidation. Line PQR (Plate 30 B) has not been attacked and it may be a fault without a very high defect content whereas AB is a micro-pore which will be more readily oxidised.

ii. Stages (a) to (d). Plate 31, of graphite after 7 days' reaction, shows many of the features of the first three stages. The outlining of a crystallite is seen at X, where the area surrounded coincides with an independent area of moiré pattern. The outlining at the top of

PLATE 30

Single crystal graphite, A - standard.

B - same area after reaction with a
mixture of sulphuric and nitric acids
for 12 minutes.

Final magnification - 79,000X.

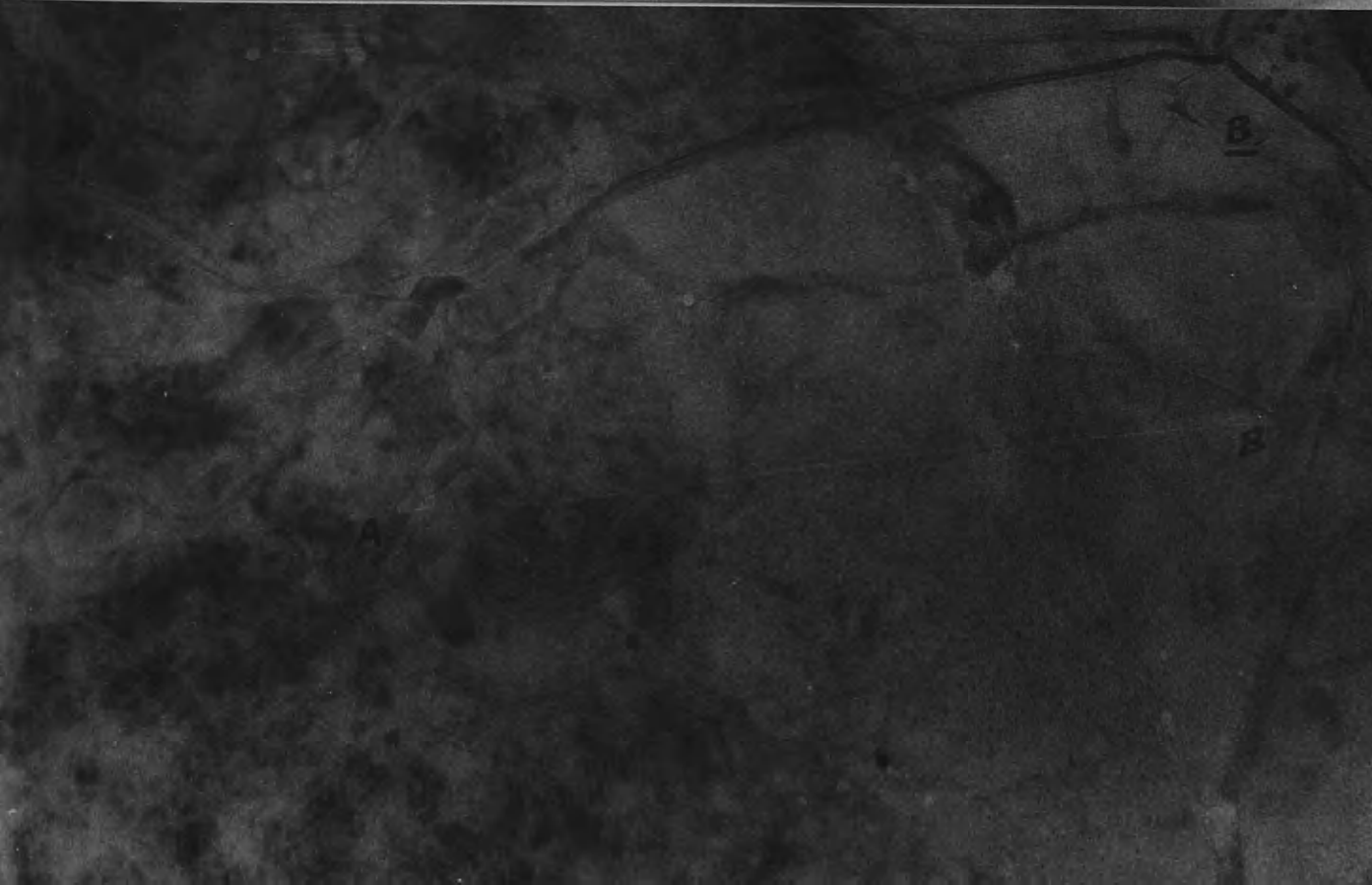
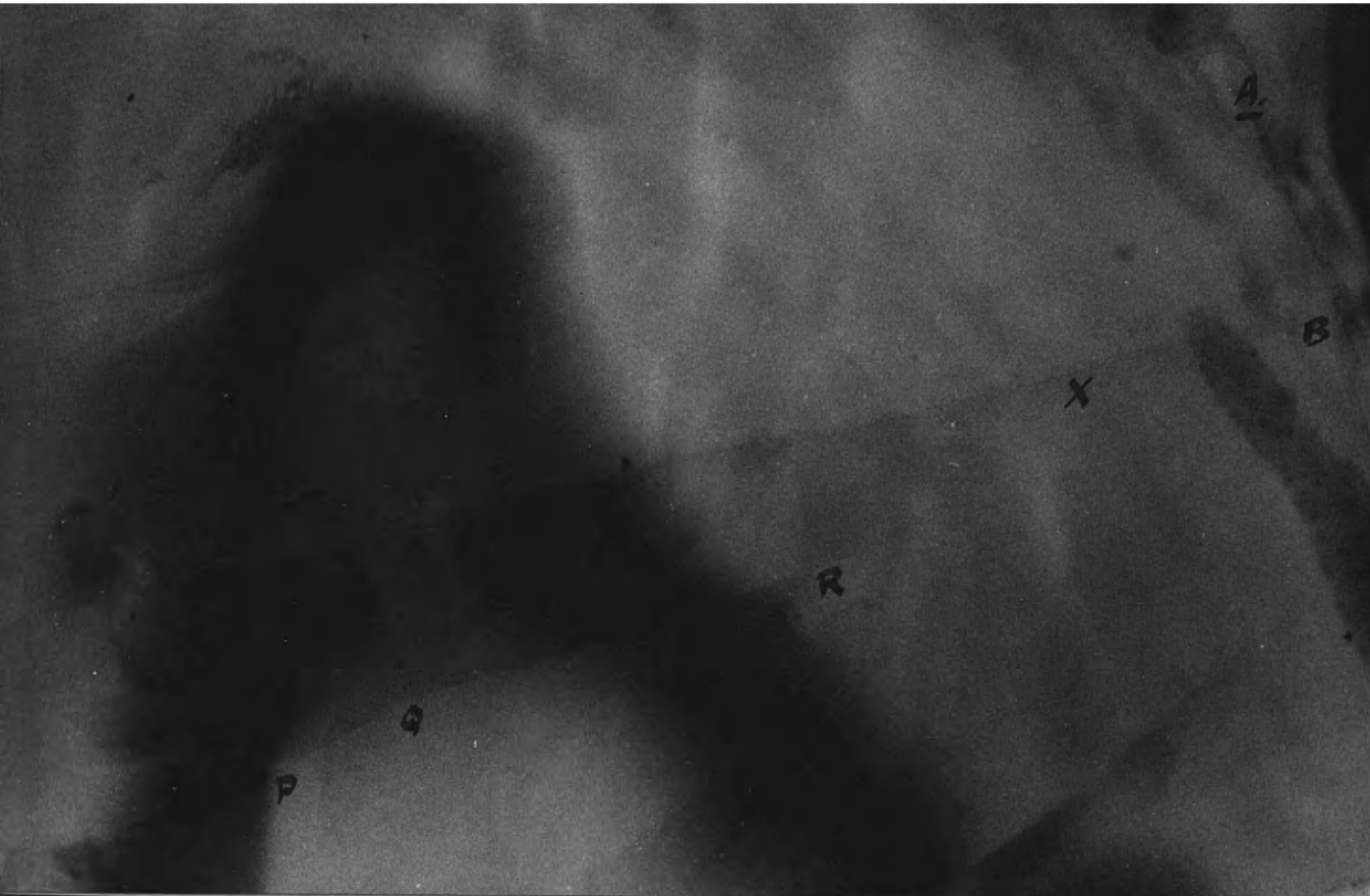


PLATE 31

Pile grade A, polycrystalline synthetic graphite, after reaction with a mixture of sulphuric and nitric acids for 7 days.

Final magnification - 135,000X.



PLATE 32

Pile grade A, polycrystalline synthetic
graphite, after reaction with a mixture
of sulphuric and nitric acids for 3 weeks.

Final magnification - 141,000X.



this crystallite (Y) is typical of the earliest stage (a) where the micro-cracks are barely visible. Stage (b) is represented by the broader channel at Z and at P a punctate channel, typical of stage (c) is seen. This has a breadth of 30\AA , and traces a curved line representing attack at a crystal step or dislocation, not at the edge of a crystallite. The channels can have various depths and in some cases penetrate many layers of the crystal.

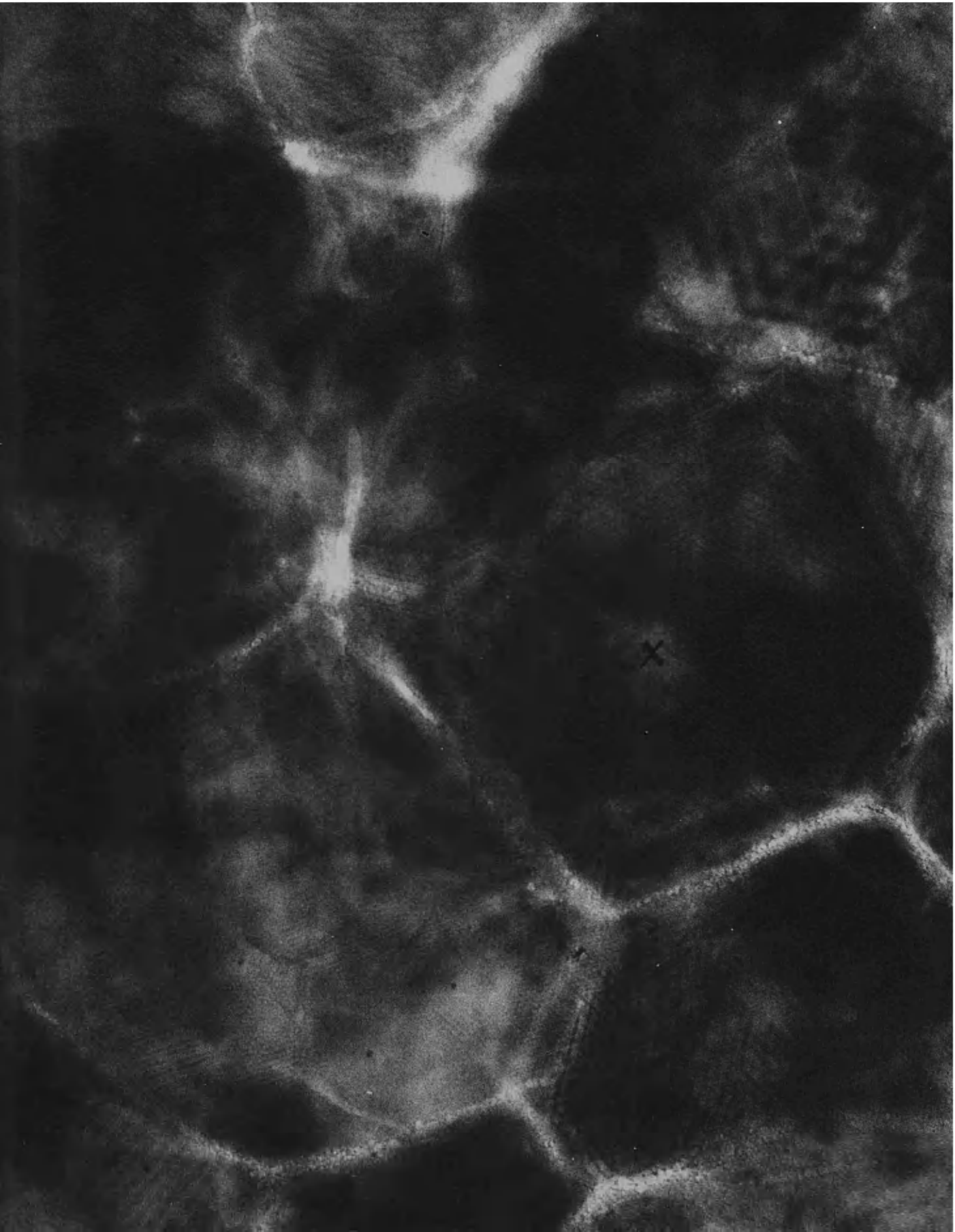
Plate 32, of graphite after 3 weeks' reaction, shows typical stage (d) material. There are more channels present and their breadth has increased from the 30\AA found for the first three stages, to 70\AA . Another feature of this stage is the appearance of a very few small holes, 140\AA in diameter (Plate 32, A and B), which are the fore-runners of the many large pits seen in stage (e).

iii. Break-up of the crystals. At some places in Plates 31 and 32, it can be seen that the cracks meet at definite angles, often in the region of 60° or 120° , which are the angles common to graphite with its hexagonal symmetry. Examples of this are P (Plate 31) with an angle of 115° , and Q (Plate 31) with an angle of 120° . In some cases three channels may meet and cut off a triangular area, again suggesting that attack is taking place preferentially along definite crystallographic directions. This process continues until it is quite obvious that oxidation has

PLATE 33

Pile grade A, polycrystalline synthetic graphite, after reaction with a saturated solution of ammonium vanadate in a mixture of sulphuric and nitric acids for 2 weeks.

Final magnification - 165,000X.



occurred round the edges of the microcrystals, and the remaining sub-units often have a hexagonal shape. This is shown in Plate 33, which gives the typical appearance of the graphite after 4 to 8 weeks in acid. The angles round the crystallite (X) are all in the region of 120° (110° , 124° , 125° , 120° , 128°). In this plate there are signs of complete penetration of the crystal, and this suggests that the crystallites are composed of a stack of layers of roughly the same diameter.

Plate 33 also shows the accelerating effect of an added impurity. Despite the fact that it shows such an advanced state of oxidation, corresponding to a reaction time of from 4 to 8 weeks, the graphite has been in contact with an acid solution of vanadium for only two weeks. The rate is increased by a factor of two when vanadium or uranium is added.

iv. Stage (e). Plates 34 and 35 show the last stages of oxidation. The first is of material which has been in contact with acid for six weeks, and the plate was taken with double condenser illumination at a microscope magnification of 60,000X to give improved resolution. The oxidation features all follow on from the previous stages.

(a) The channels (X) have a diameter of 90\AA to 140\AA , compared with 30\AA for stages (a) to (c) and 70\AA for stage (d).

(b) The channels often have a zig-zag edge, confirming that

PLATE 34

Pile grade A, polycrystalline synthetic graphite, after reaction with a mixture of sulphuric and nitric acids for 6 weeks. Double condenser illumination.

Final magnification - 252,000X.



PLATE 35

Pile grade A, polycrystalline synthetic graphite, after reaction with a mixture of sulphuric and nitric acids for 25 weeks.

Final magnification - 150,000X.

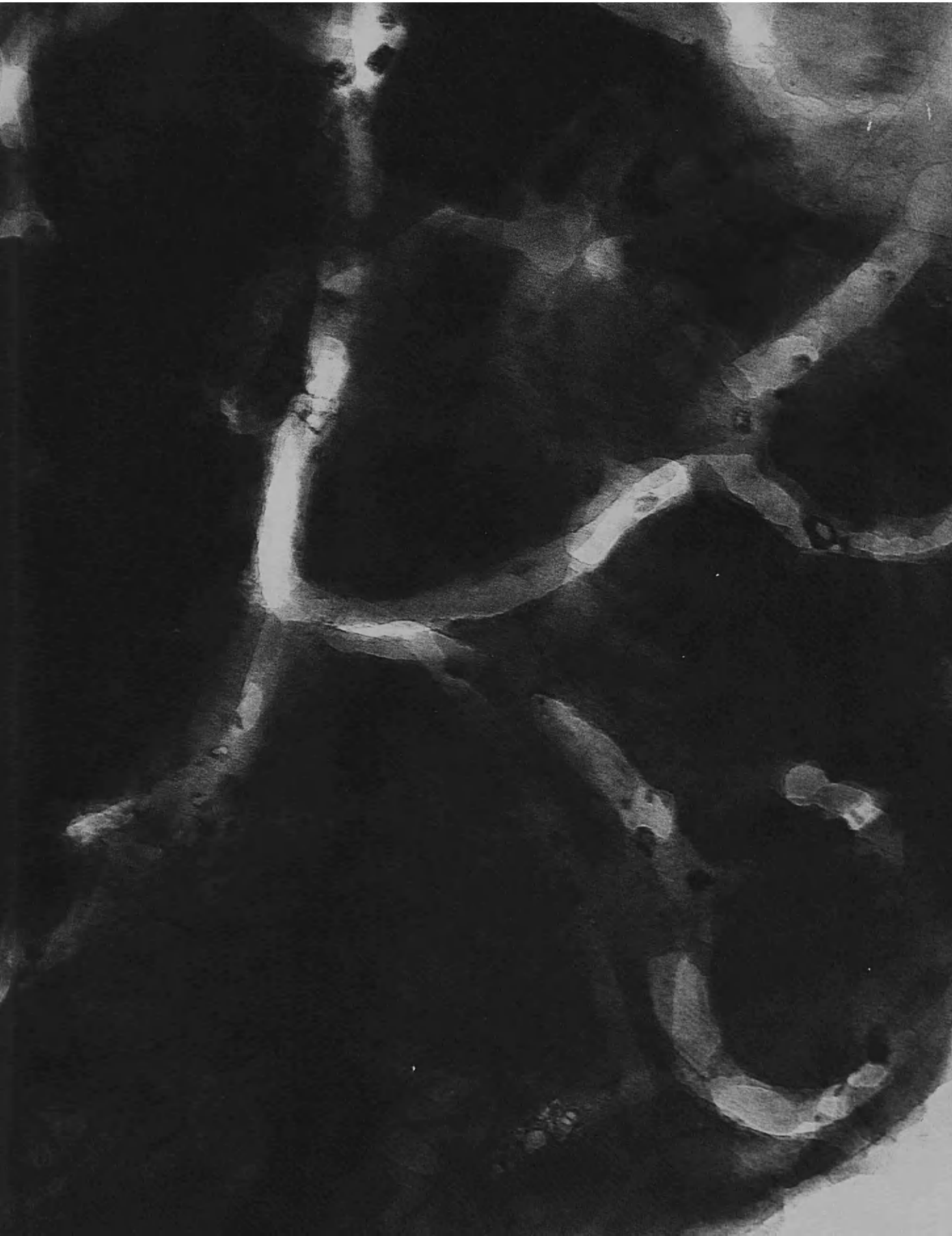
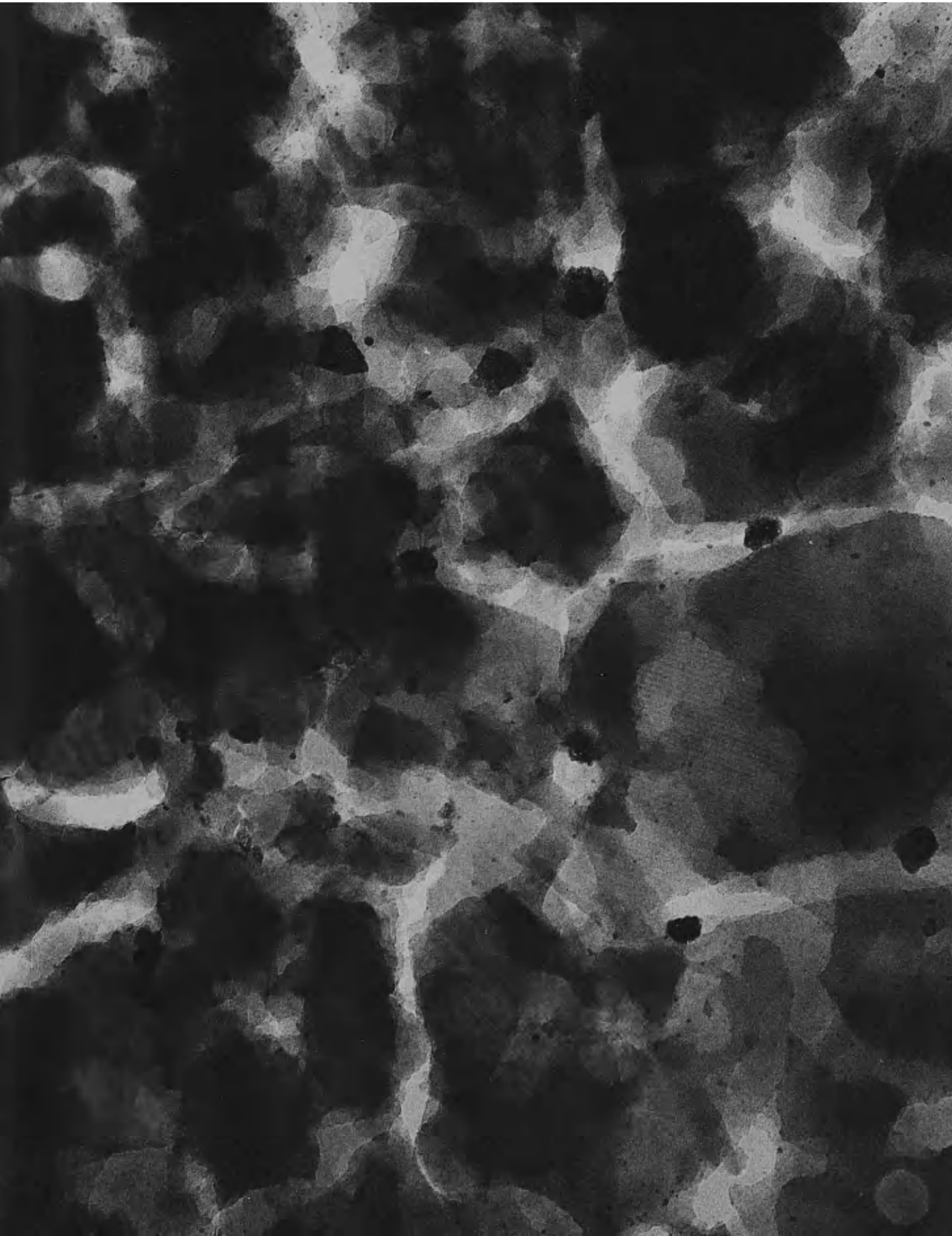


PLATE 36

Pile grade A, polycrystalline synthetic
graphite, after reaction with a mixture of
sulphuric and nitric acids for 25 weeks.

Final magnification - 153,000X.



they are formed by further attack at a punctate line.

(c) Pits are now common and their diameter has increased from 140\AA (stage d) to 260\AA .

Another feature at this stage is the production of shallow pits which sometimes have a certain amount of regularity in their sides. At R (Plate 34) eight sides can be distinguished and at S there are six sides.

Plate 35 shows the final appearance of the graphite when the reaction was stopped after 25 weeks. There are no further changes, except that the diameter of the channels has further increased to 600\AA . Impurity particles are often seen in association with pits and channels and these are particularly common in this plate. In contrast with the reports on catalytic channels in gas oxidation of graphite (Hennig, 1962 and Presland and Hedley, 1962, 1963), there is no tapering along the length of the channels.

C. Edge Attack.

The oxidation described so far is thought to be catalytic in origin. Another, slower type of attack is described by Preland and Hedley (1962, 1963) as basic or edge oxidation, and a similar distinction can be found in the acid reaction. Up until a reaction time of eight weeks, the edges of the graphite crystal remained quite smooth. After this stage, occasional evidence of basic attack is seen and the edges are sometimes irregular.

Plate 36, of graphite after 25 weeks, shows extensive edge attack as well as catalytic oxidation, and the appearance of the material is similar to the examples of the basic reaction of Presland and Hedley (1962, 1963). It is, however, impossible to be certain that there are no small particles of impurity present at the edges and this point will be dealt with further (D, below) in connection with the adsorption of acid around the micro-crystals.

D. Adsorption of material along crystallite edges and cracks.

i. Description. The description of the oxidation given so far is of preferential attack leading to the formation of channels and pits. Another localised effect was seen for graphite which had been treated with acid alone or with acid containing added heavy metal cations. This is the heavy outlining of crystallite edges and steps. It is heavier than the outlining referred to in A and B, above, and is not so common. Plate 37, of graphite reacted with acids alone for 7 days, is a typical example, where the outlining bands vary in thickness from 32\AA to 64\AA . This plate is fairly close to focus, but some out of focus effects can be seen at areas such as A, B, C and D. These give fringe widths of 13\AA , 16\AA , 20\AA and 16\AA , respectively (Kay, 1961) and this is a measure both of the

resolution and of the fringe width of the particular micrograph. The fact that the dense bands have breadths of up to 64\AA suggests that they are real structures, although the out-of-focus effect does of course enhance the contrast and makes the bands more readily apparent. The fact that the dark bands often appear without an accompanying white fringe confirms that they are not merely a focus effect.

At P a crystallite is outlined, whereas at Q crystal steps on the surface or dislocations inside the crystal are decorated, since the lines have adopted a parallel array. While this effect is decoration of some type, it is quite different from that shown in Section I,E above, and from the effect described as decoration in the literature (Hedges and Mitchell, 1953a and b; Bacon and Sprague, 1961a; Mitchell, 1961 and Hennig, 1964a,b,c), where the decorating material is obviously particulate. In the case of the bisulphate outlining, the individual particles are not resolved.

The interest of this outlining with respect to the study of the oxidation is that it often appears on either side of the thin channels (Plate 37, R). This is seen more clearly in Plate 38, where a channel is outlined by a band with a sharp edge. The microscope magnification of this set of plates was only 20,000X and a further set of high resolution plates is included.

PLATE 37

Pile grade A, polycrystalline synthetic
graphite, after reaction with a mixture
of sulphuric and nitric acids for 7 days.

Final magnification - 156,000X.

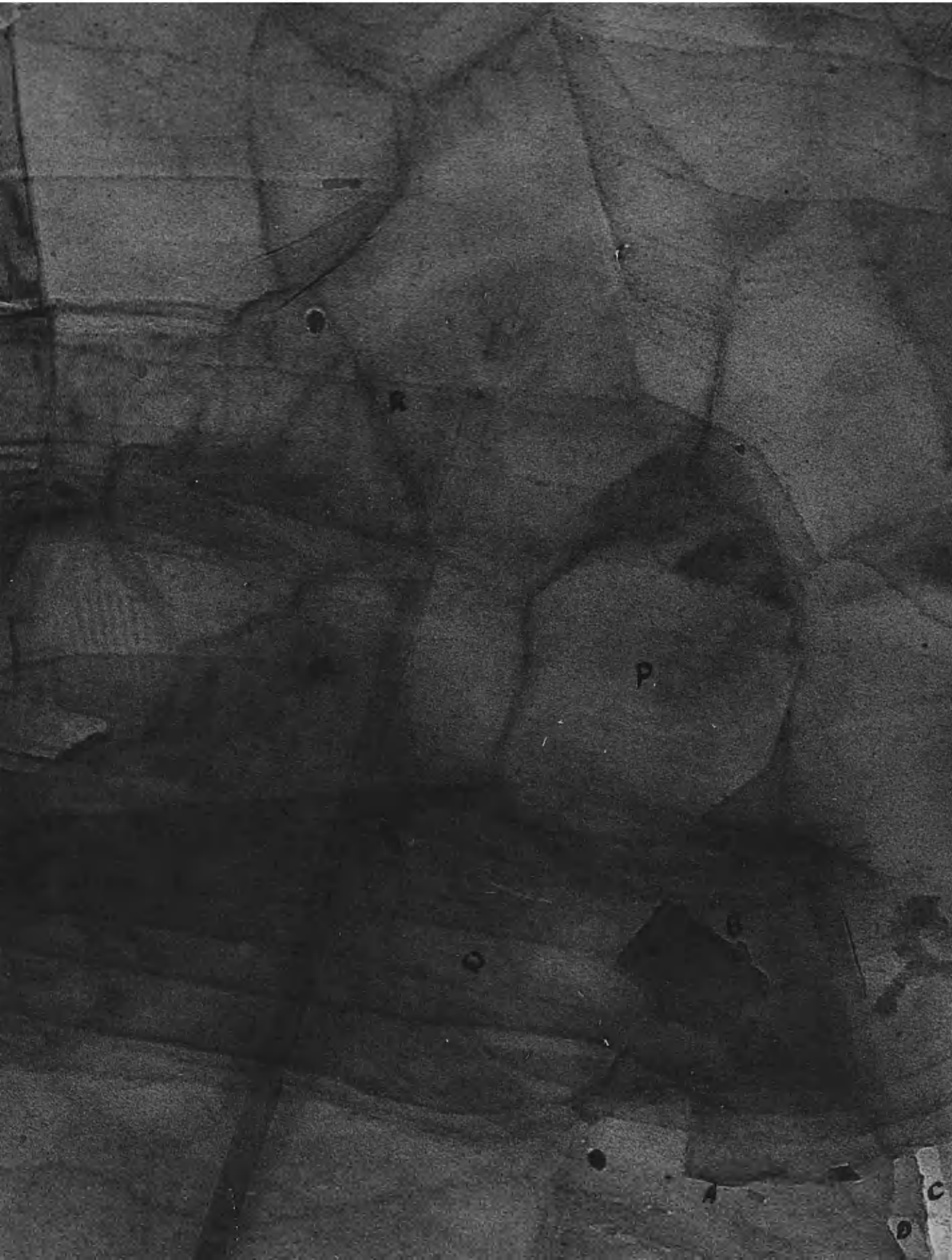


PLATE 38

Pile grade A, polycrystalline synthetic
graphite, after reaction with a mixture
of sulphuric and nitric acids for 3 weeks.

Final magnification - 195,000X.



ii. High resolution plates. Plate 39, of graphite after reaction with acid and uranium for one week, was taken with double condenser illumination at a microscope magnification of 80,000X. It shows an outlined channel (X) which had the same appearance at low magnification as the areas of Plates 37 and 38. The channel is 26\AA broad and is surrounded by a dense band of 58\AA on the left side and 95\AA on the right side, and this lack of symmetry confirms the suggestion that the broad bands cannot be simply an effect caused by the plate being out of focus. The bands are probably areas where there is disorder in the lattice, and they are seen by a scattering process similar to that whereby stacking-faults are made visible (Amelinckx and Delavignette, 1963). Since the bands are seen in material which has been reacted with acid alone as well as with the heavy cations, the disorder may be due to the adsorption of sulphuric acid as particles which are too small to be individually resolved. Alternatively, it could be due to the formation of an oxidation intermediate which would disrupt the regularity of the graphite lattice.

In addition to the broad bands in Plate 39, the edges of the channel (Y) and its accompanying band (Z) are marked by an even denser line, varying in width from 7\AA to 22\AA with a mean value of 14\AA . Plate 40 shows another area from the same plate. At A there is a shallow channel,

PLATE 39

Pile grade A, polycrystalline synthetic graphite, after reaction with a saturated solution of uranyl nitrate in a mixture of sulphuric and nitric acids for 1 week.

Double condenser illumination.

Final magnification - 688,000X.



PLATE 40

Different area from the same plate as Plate 39.

Double condenser illumination.

Final magnification - 592,000X.

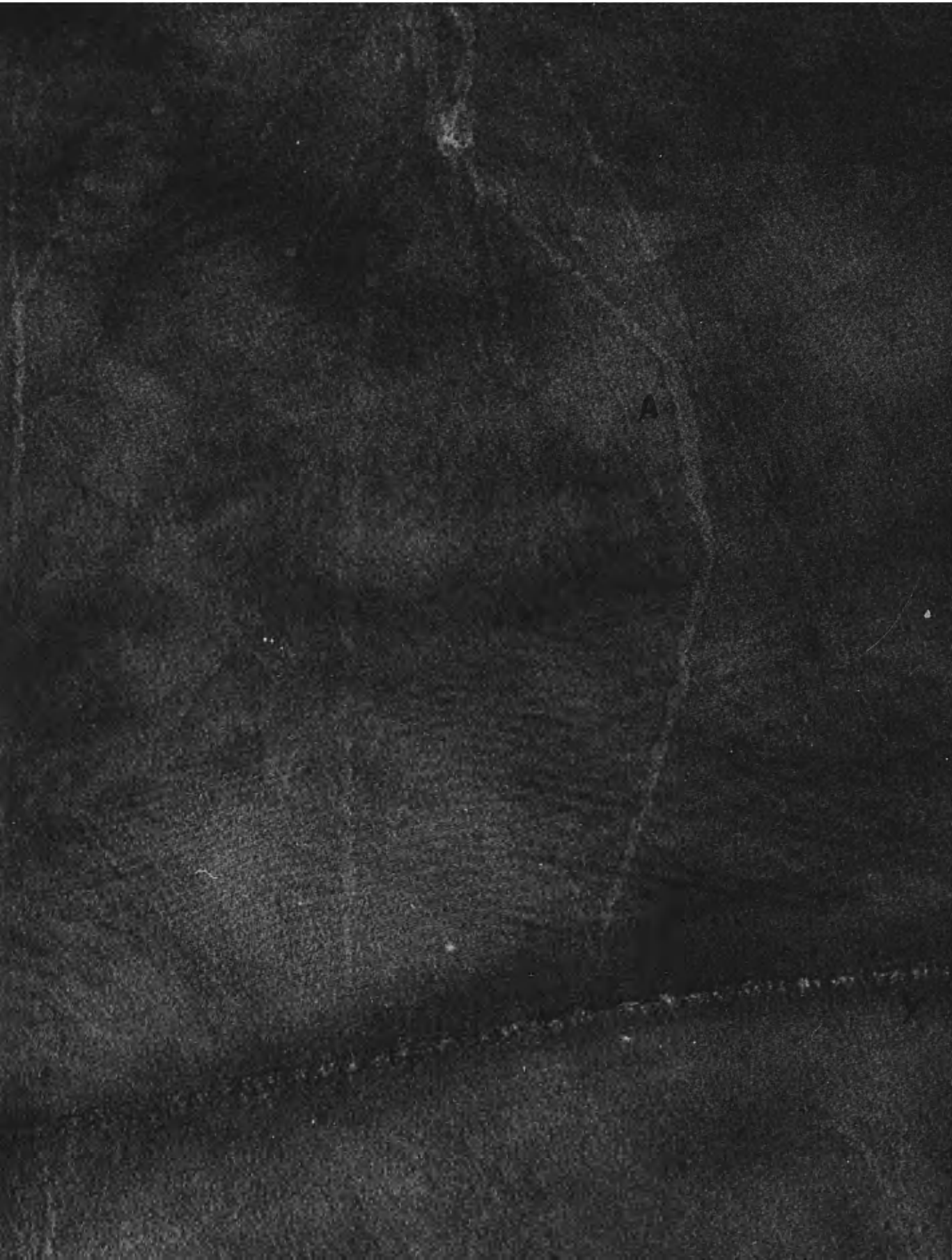


PLATE 41

Two plates of area A from Plate 40, from
successive plates in a through-focal series.
Double condenser illumination.

Final magnification - 592,000X.

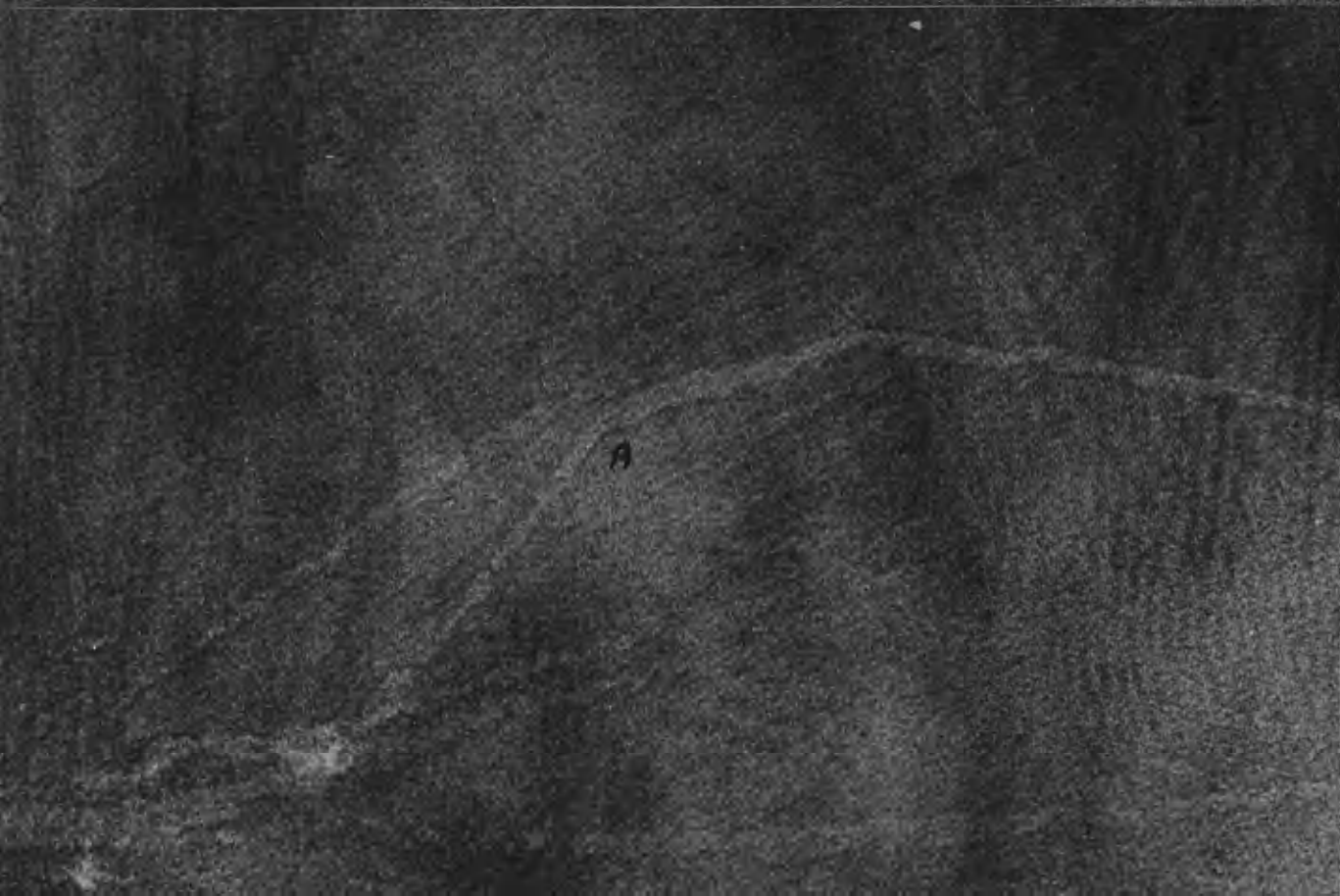
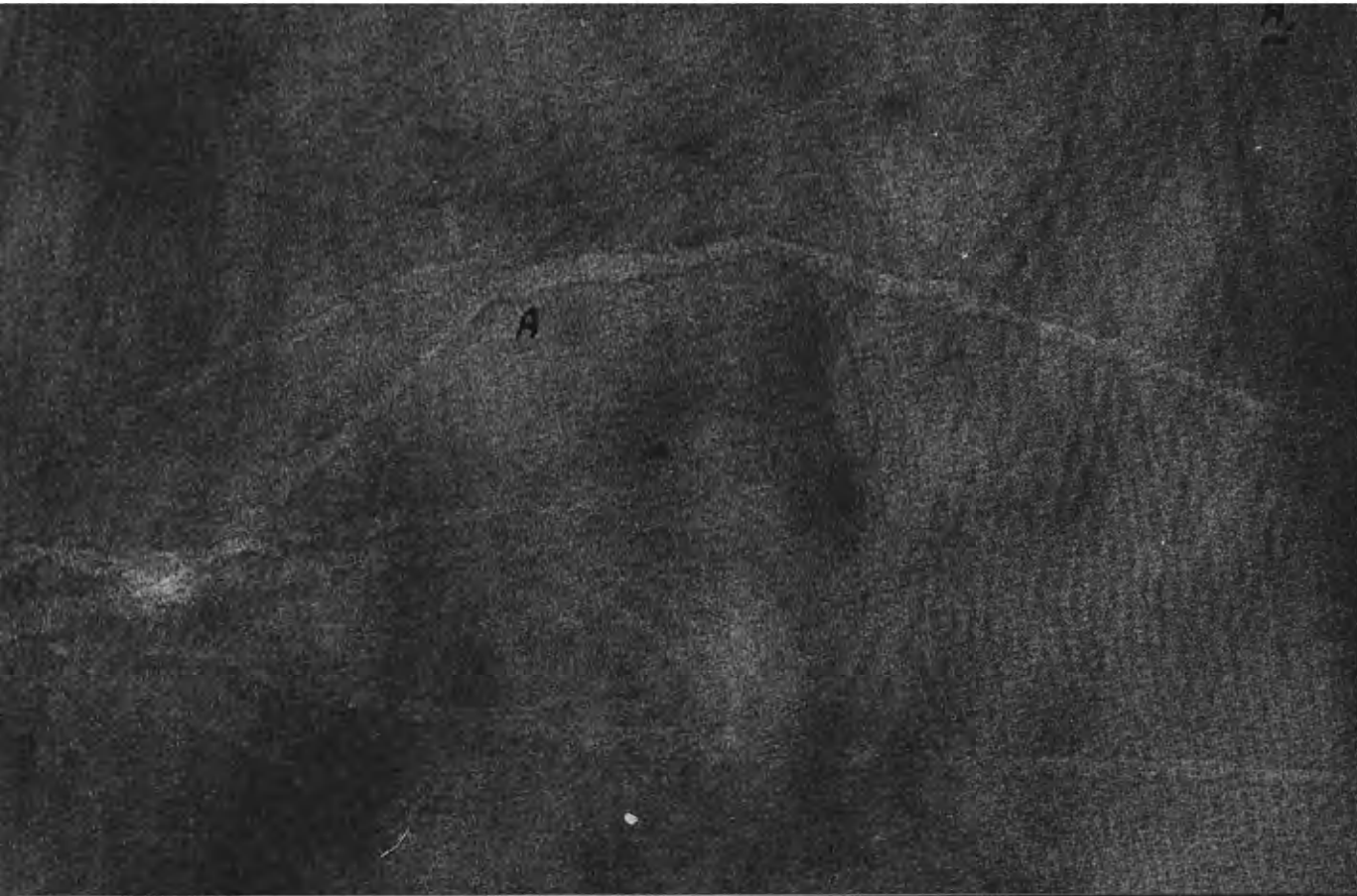


PLATE 42

Pile grade A, polycrystalline synthetic
graphite. Standard sample. Double
condenser illumination.

Final magnification - 520,000X.



60 \AA broad, which has a thin dense line along its edge with a thickness of 9 \AA . When dealing with high resolution micrographs, it is important to distinguish between lines of material and Fresnel fringe effects, particularly for graphite which occurs in layers at different levels. In this case the 9 \AA line (Plate 40, A) does not change in a series of plates taken at successive planes of focus: to demonstrate this, two plates from the through focal series are shown in Plate 41. At some points (Plate 40, A) the individual particles making up the line can be distinguished, suggesting that it is not a fringe effect and it is concluded that the line is the image of a row of particles adsorbed along the crack.

It is useful at this stage to compare Plates 39 and 40 with a micrograph of unreacted graphite, taken in the same high resolution conditions (Plate 42). While there are no deep, broad channels of the type seen after reaction, there are several fine cracks (X) with a breadth of around 17 \AA . At some edges these have a dense line with a diameter of 9 \AA , which is the same as the value quoted for the material after reaction.

The outlining is thus made up of (a) a thin dark line which can be seen before and after reaction and (b) a broad band which appears only after oxidation and which is probably due to a local disorder in the lattice caused by the

oxidation process. In view of the fact that the channels are formed by the gradual widening of a thin crack, it is suggested that the attack takes place by catalytic oxidation in a direction perpendicular to that of the channel.

This could arise if there were a thin line of impurity adsorbed along the crack, which could either be already present in the graphite, since polycrystalline graphite has a high impurity content, or could be adsorbed from the acid reagent. In this case, the 9\AA line seen in the micrographs will be the image of this adsorbed impurity. Since the outlining is seen at the edge of crystals as well as along channels it is probable that the oxidation described as basic attack in C above is caused by a similar adsorption of catalyst particles, leading to preferential attack.

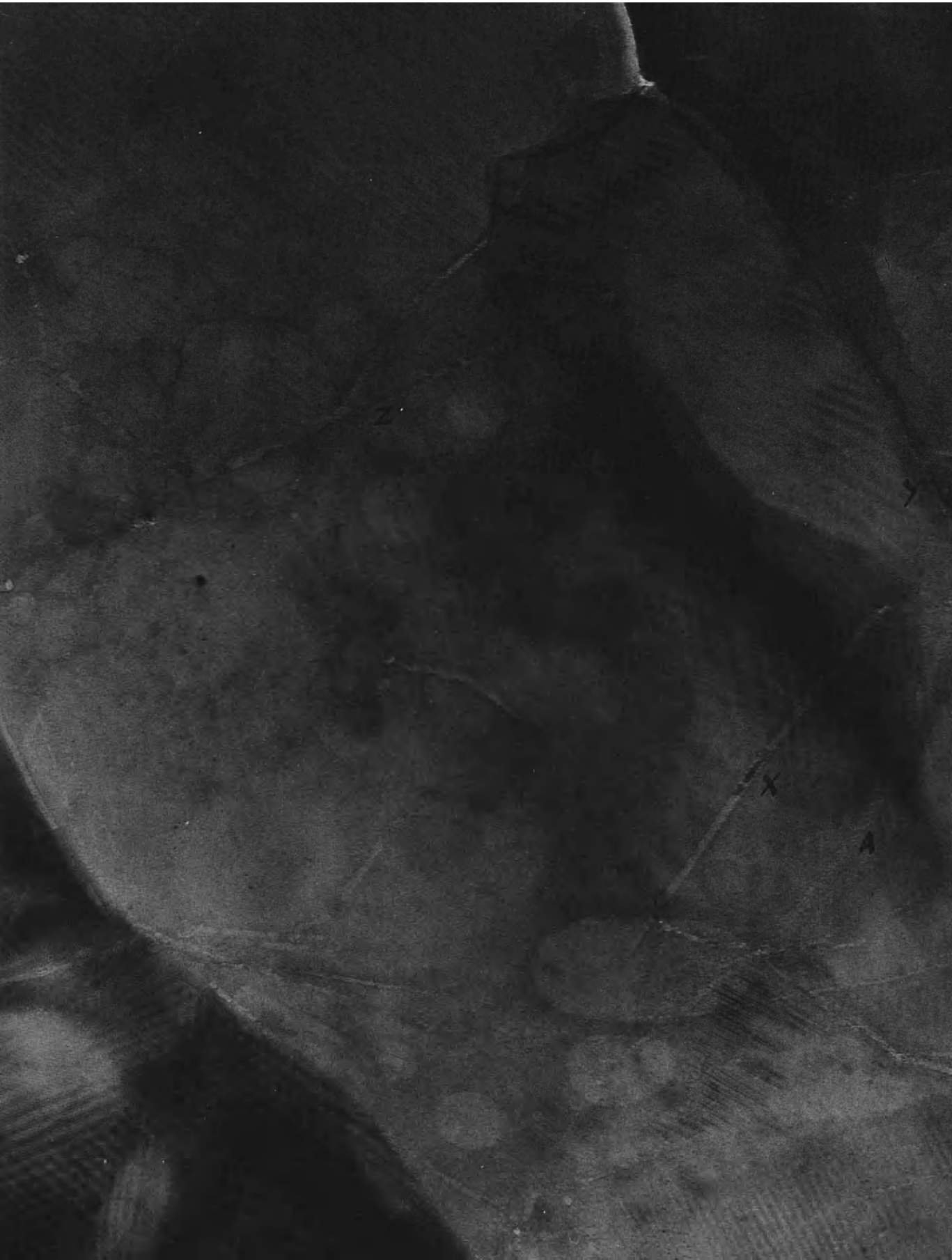
E. Channel contents. Many of the channels are not empty and it is thought that the material that they contain is an oxidation intermediate. Plates 32 and 43 show this clearly. There are three stages, corresponding to different degrees of separation of the edges of the channels from their contents.

(a) At X (Plate 43) a channel of breadth 125\AA is seen, containing material 900\AA long and 90\AA broad. There is a gap of 16\AA on either side and the material stands out

PLATE 43

Pile grade A, polycrystalline graphite,
after reaction with a mixture of sulphuric
and nitric acids for 3 weeks.

Final magnification - 153,000X.



sharply from the channel edges. Similarly, at Y (Plate 43) there is a piece 400\AA broad which has been retained in an enlarged part of a channel.

(b) At Z (Plate 43) the material fits closer to the edges of the channel and tends to obscure it. This may be because they are still connected or simply because the channel is shallow and can contain less material.

(c) At A (Plate 43) the channel is barely visible, but on close examination it can be seen to consist of many small punctures mixed with finely divided material such as that seen in the deeper channels. In the high resolution plate (40) material can be seen filling the punctate channel (Y) in pieces of 10\AA to 50\AA in length, with no evidence of a gap between the channel and its contents.

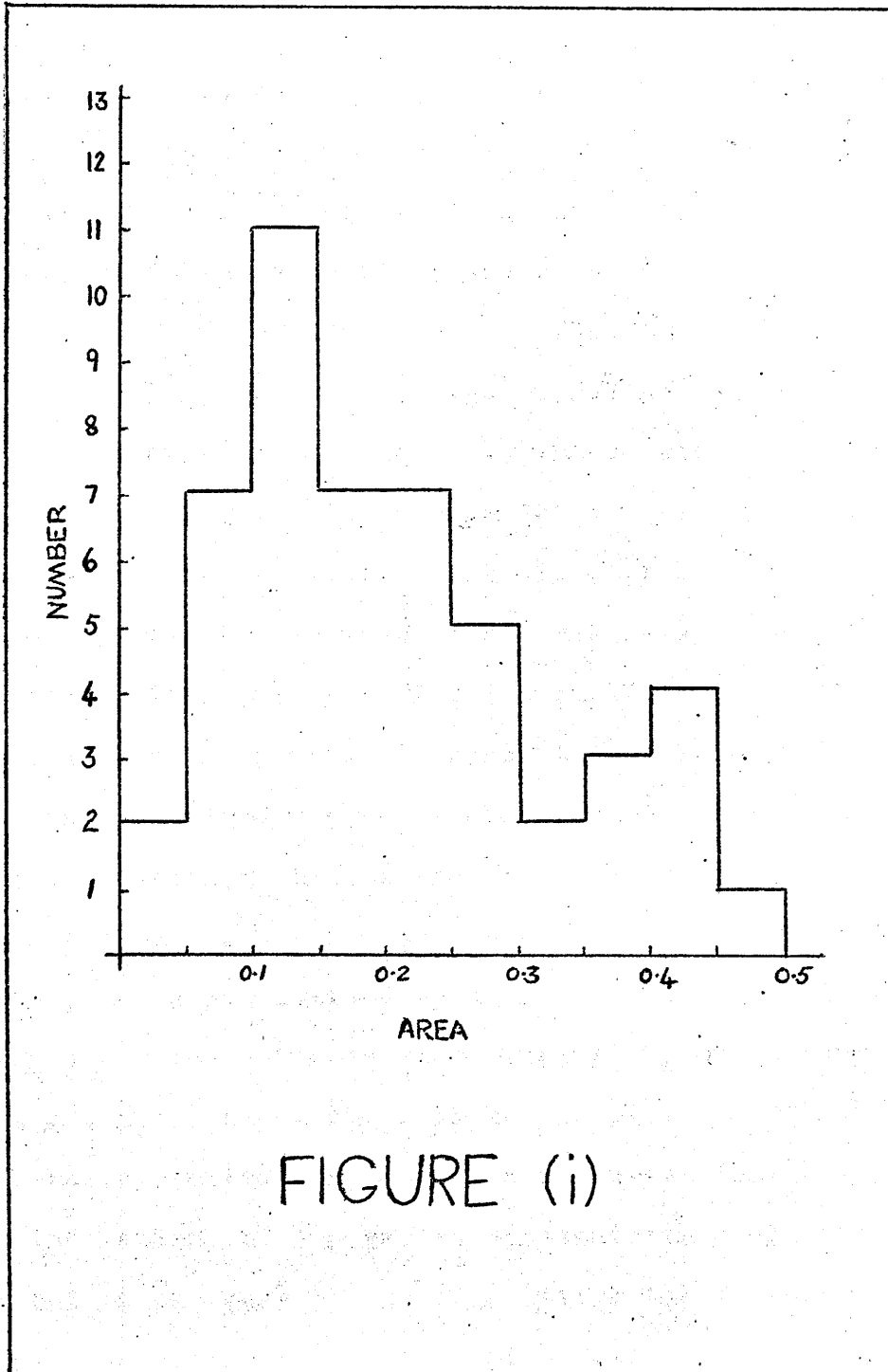
There is no evidence of large amounts of impurity lying on the surface and the material is sometimes caught loosely in the channel: it is therefore unlikely that it is simply dirt, unconnected with the oxidation. The channel contents give a diffraction pattern identical to that of graphite in the electron microscope. In view of the fact that, for the uranium residue compound, the X-ray spectrum contains many uranyl nitrate lines it is surprising that there are no extra spots seen in the pattern from the channel contents. It is therefore

unlikely that they are composed of an oxidation intermediate containing bound catalyst. The channel contents may then be graphite which has not yet been attacked, or an intermediate such as carbon suboxide polymer, which has a diffraction pattern identical to that of graphite (Schmidt, Boehm and Hofmann, 1958, and Smith, Young, Smith and Carter, 1963).

F. Crystallite size.

The overall effect of acid oxidation is to break up the polycrystalline material into its component microcrystals. Figure (i) shows a histogram for the area of 50 microcrystals, using material from stages (a) to (d). There is a large peak at $0.01 - 0.15 \mu^2$ and a smaller one at $0.40 - 0.45 \mu^2$ giving an approximate diameter of 3160 \AA or 6320 \AA . The two areas are related by a factor of 1:4 and the larger one may be a set of four smaller ones holding together tenaciously. These figures are in agreement with those of Dawson and Follett (1959) who quote $3,300 \text{ \AA}$ as the diameter.

The figure obtained in this way does not agree with the results of Bacon (1958b) who calculated the diameters, using X-ray techniques, as $270 \text{ \AA} - 790 \text{ \AA}$. To compare the two techniques using the same specimen of graphite, an



approximate calculation was made in this work using the line broadening of the 0002 line on the powder photograph of the material after 19 weeks' reaction with acid. The equation used was $t = k/\beta \cos \theta$, where t is the size of the crystallite, k is 1.07, considering the particle to be spherical, β is the broadening and θ is the Bragg angle (Henry, Lipson and Wooster, 1951). The figure obtained was 412Å, which falls in the range of Bacon (1958b). While the method used was extremely inaccurate, it nevertheless shows the discrepancy when the two techniques are applied to the same graphite: the diameter obtained by microscopy is almost ten times that from X-ray line broadening. This agrees with the work of Hesketh (1964) who showed that the strains in graphite are 1/10 of their theoretical value and suggested that the unit volume over which the theoretical values should be calculated is not a single crystal, but small groups of crystals. In line with this, the size obtained by X-ray methods is that of the single crystal, whereas that obtained by microscopy is a larger group which stays intact despite the attack of acid. For air oxidation, it could be argued that this was due to the failure of the gas to penetrate into all the pores, but in the case of the acid attack the oxidant penetrates so completely that it also forms an intercalation compound. The failure of the graphite to break up

completely must therefore be due to some inherent lack of reactivity at some of the pores.

III. Comparison of the oxidation of various types of graphite.

A. Introduction. Purified natural, single crystal and natural graphites were all oxidised to compare the results with those for polycrystalline, synthetic material. These three graphites have a similar appearance in the standard state, containing many flat areas and giving an impression of higher crystallinity than the polycrystalline graphite. All three types behaved similarly on acid oxidation, but in a way quite different from that described in II above. The purified natural graphite has been chosen as being representative of the three, since more is known about its crystallinity and purity and it will be compared with the polycrystalline material: this is described in detail in the Experimental Section, (p.35). Plate 44 shows a typical area of standard purified natural graphite, with a very clear line moiré.

B. Intercalation. Exactly the same features are seen for the two types of graphite but the purified natural graphite shows more transparent discs, and these extend over larger areas and move more freely.

PLATE 44

Purified natural graphite. Standard
sample.

Final magnification - 192,000X.



C. Oxidation.

i. Rate of reaction. The rate of oxidation is completely different for the two types of graphite. Since the purified natural graphite is almost single crystal in nature, no outlining or cracks round sub-units appear. Up till 9 weeks' reaction time, there are no signs of gross oxidation, whereas at this stage in the polycrystalline material there are many broad channels. Plate 45, of purified natural graphite after 9 weeks' reaction, shows the first sign of oxidation. Two holes, with a diameter of 380\AA , are seen in a piece of graphite which is otherwise unchanged. From this stage on, holes appear more often and deep-cut channels are seen, but many of the pieces of graphite still have no signs of oxidation.

ii. Channel formation. Only thick channels appear and the attack comes from the edge of the crystal: this is seen in Plate 46 which shows purified natural graphite after 17 weeks' reaction with acid. This is similar to the catalytic attack described by Hennig (1962) for gaseous oxidation, and the channels give the impression of being formed by a catalyst particle, burrowing in from the edge of the crystal. This is confirmed by the fact that the edges of these channels are not zig-zag, as are those of polycrystalline material which are formed by further attack at punctate cracks.

PLATE 45

Purified natural graphite, after reaction with
a mixture of sulphuric and nitric acids for
9 weeks. Double condenser illumination.

Final magnification - 264,000X.



PLATE 46

Purified natural graphite, after reaction
with a mixture of sulphuric and nitric
acids for 17 weeks.

Final magnification - 169,500X.

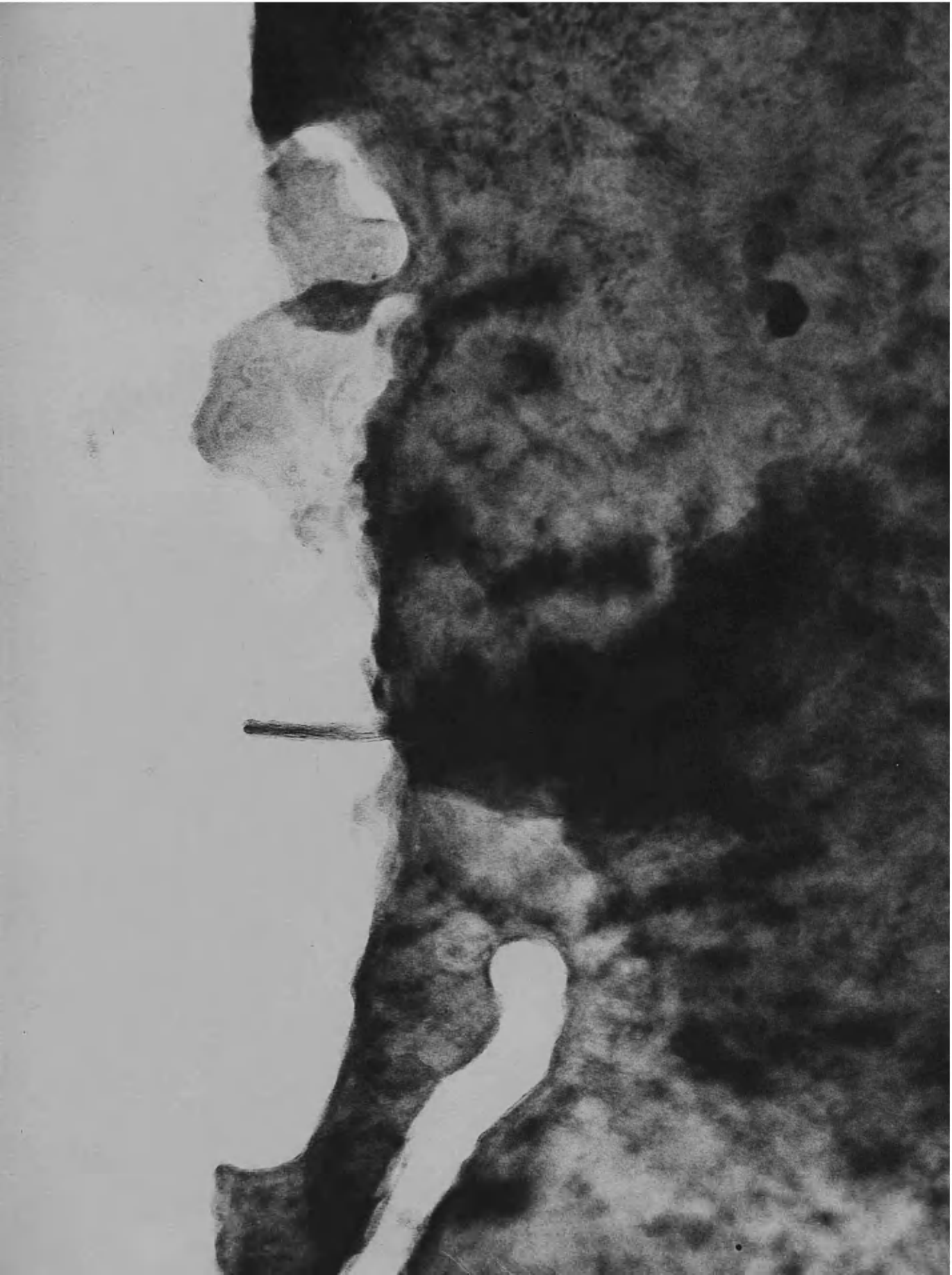


PLATE 47

Purified natural graphite after reaction
with a mixture of sulphuric and nitric
acids for 17 weeks.

Final magnification - 183,000X.



iii. Pit formation. For the purified natural graphite, pits and channels appear at the same stage of oxidation, whereas for the polycrystalline material the pits are seen only in the last stage. For the former type of graphite, both pits and channels are formed by the same localised catalytic attack, and Plate 47 shows an example of extensive pit formation after 17 weeks' reaction. Their diameter is of the order of 710\AA and they occur individually or in clusters, and they vary in the amount to which they penetrate the crystal.

Many of the pits have a small, dense impurity particle associated with them (A and B) and this confirms the suggestion that their origin is catalytic. The particles may well be impurities in the acid oxidant. Another interesting feature of this plate is the dense area at C, which has the same dimensions as a typical channel and may be a channel under the surface which is seen because of a scattering effect caused by local oxidation and disorder at its edges.

IV. Oxidation of polycrystalline graphite to graphite oxide.

A. Introduction. Oxidation to graphite was carried out according to the method of Hummers and Offeman (1958), which is described in section A of the Experimental. Only after three cycles of the oxidation was the graphite

converted to the yellow oxide and sample of this (Graphite oxide stage three) and the two intermediates (stages one and two) were examined by electron microscopy and diffraction.

B. Electron microscopy.

- i. Graphite oxide stage i. The material still has an appearance similar to that of graphite and contains many moiré patterns. There are also transparent discs and Plate 48 shows how similar this material is to the bisulphate residue compound.
- ii. Graphite oxide stage ii. The material is now different from both graphite and the bisulphate residue compound. Every crystal contains transparent discs, which are pinned rigidly, since there is no movement as the heating action of the beam takes effect. The crystallites are outlined but in a different way from that described in II above for the oxidation with sulphuric and nitric acids. Plate 49 shows these two features. An electron dense ridge can be seen round the crystallite at X although the outlining sometimes has a flatter structure (Y). In each case, there are no cracks and it seems to consist of a dense material containing many tiny pores. Plate 50 shows more clearly the structure of these areas, with pores of 60\AA in diameter, and they resemble in many ways the contents of the channels described in Section II and may consist of some kind of oxidation intermediate.

PLATE 48

Graphite oxide, Stage I, from
Pile grade A, polycrystalline
synthetic graphite.

Final magnification - 195,000X.



PLATE 49

Graphite oxide, Stage II, from Pile grade A,
polycrystalline synthetic graphite.

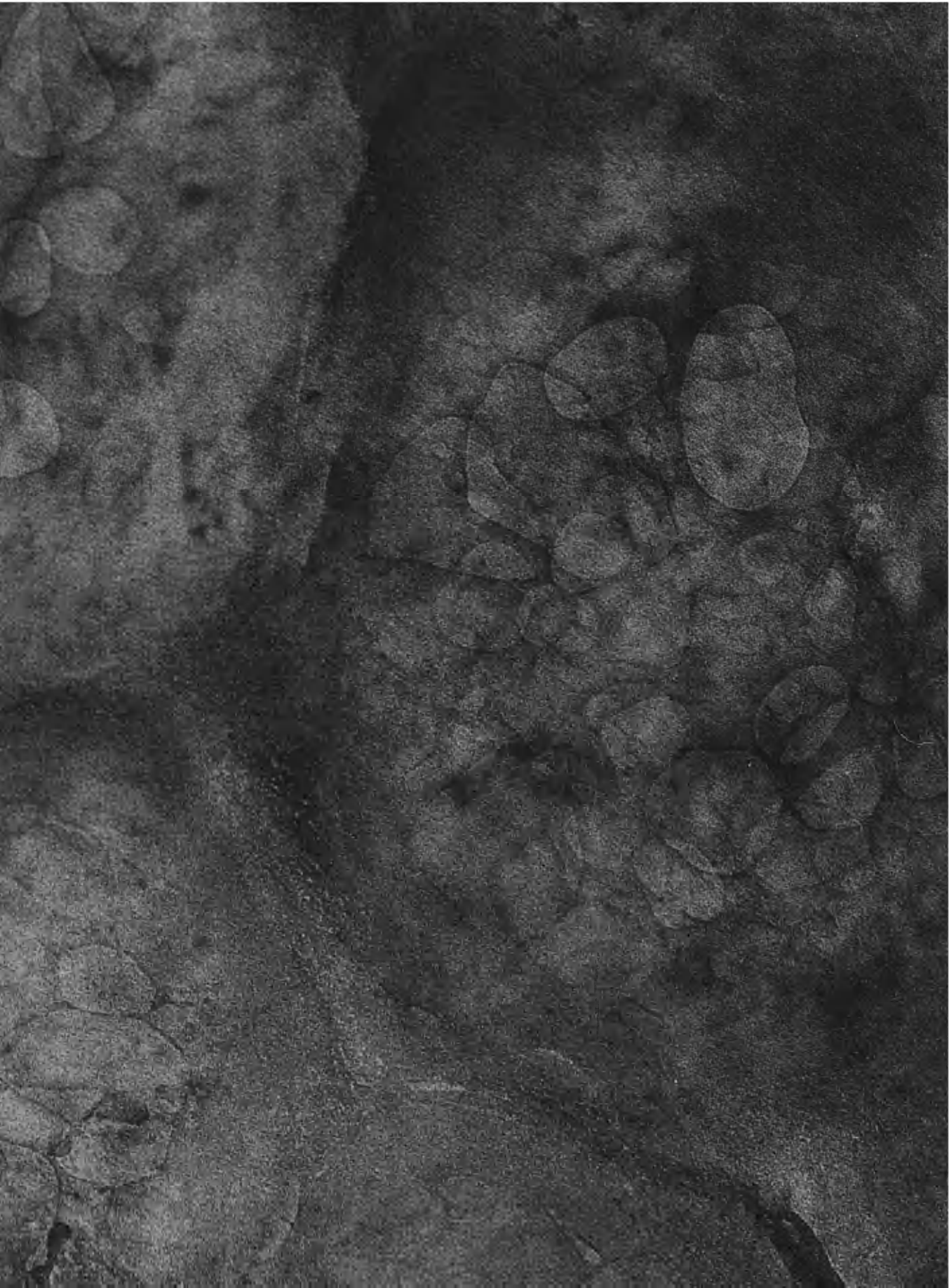
Final magnification - 135,000X.



PLATE 50

Graphite oxide, Stage II, from pile
Grade A, polycrystalline synthetic
graphite.

Final magnification - 156,000X.



The stage ii oxide still contains moiré patterns and there are a few signs of gross oxidation, in the form of occasional shallow channels.

iii. Graphite oxide stage iii - modification (a). Plate 51 shows the appearance of the final yellow oxide. The material no longer looks like graphite since it has a flat structure and has completely lost its moiré patterns.

The transparent discs which were so common in the intermediate stages have also disappeared. Most of the crystals have broken up into individual crystallites of a hexagonal shape and in the larger pieces which remain it is often possible to pick out the component parts of the crystal (Plate 51).

iv. Graphite oxide stage iii - modification (b). Plate 52 shows this kind of material which is seen at all stages in moderate amounts. It is thin and flat, with many small folds (X) and it is non-graphitic since it contains no moirés. It is probably identical to the other modification of stage three graphite oxide and is formed earlier because of its thinness. It resembles the graphite oxide described by Beckett and Croft (1952).

v. Gross oxidation. Channels of various depths appear round the crystallites in stage iii, replacing the dense ridges. This suggests that the ridges are more highly

PLATE 51

Graphite oxide, Stage III, modification (a),
from Pile grade A, polycrystalline
synthetic graphite.

Final magnification - 156,000X.



PLATE 52

Graphite oxide, Stage III, modification (b),
from Pile grade A polycrystalline synthetic
graphite, after only one application of the
oxidant.

Final magnification - 145,500X.

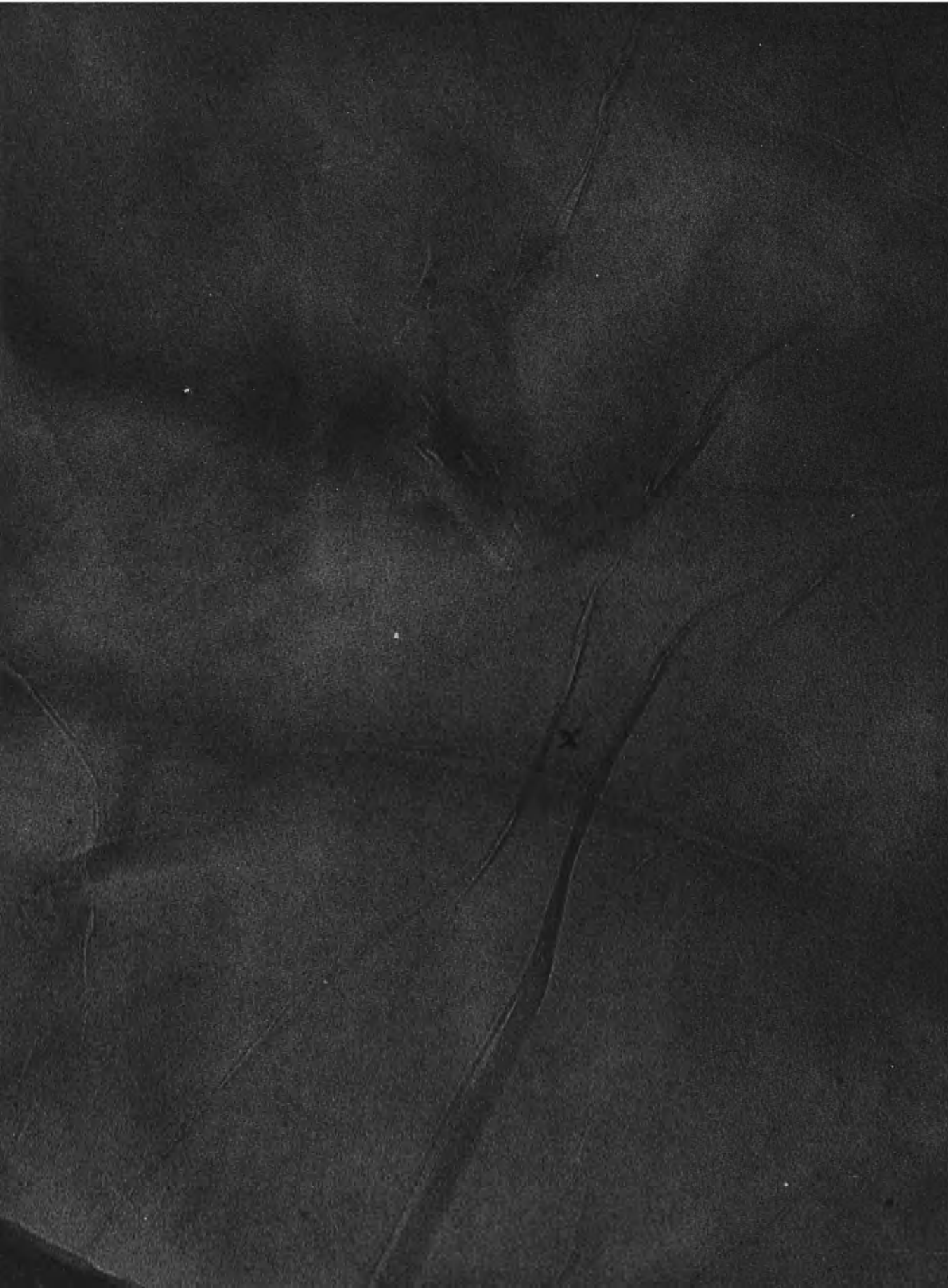
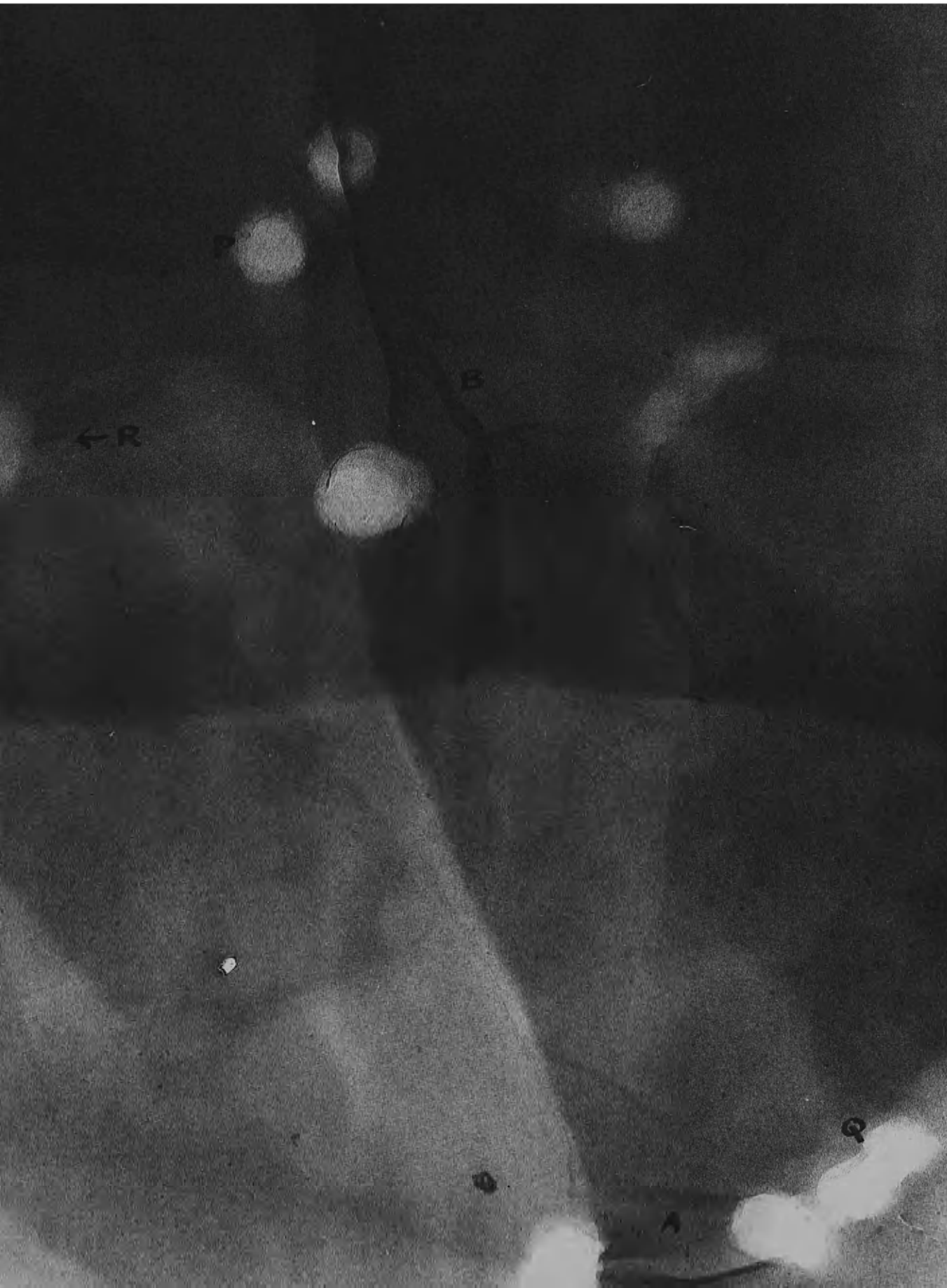


PLATE 53

Graphite oxide, Stage III, modification (a),
from Pile grade A, polycrystalline synthetic
graphite.

Final magnification - 138,000X.



←R

B

Q

A

oxidised at stage ii than the rest of the crystal because of their large concentration of defects. This makes these regions more susceptible to further attack, producing channels at the next stage. The channels are often not on the surface of the material, suggesting that there has been complete penetration of the oxidant inside the lattice (Plate 51).

Plates 51 and 53 show the appearance of pits which occur singly (P), in short lines (Q) and in clusters of three (R). They are often found in association with folds (A and B), which may have trapped impurity atoms when they are formed to give the pits by localised catalytic attack. The combination of pits and lines is reminiscent of the work on etch pits on beryllium by Damiano (1962) who describes the lines as dislocations. In the case of graphite oxide, however, the lines are certainly folds, since it can be shown by carbon-platinum shadowing that they sometimes lie on the surface.

C. Diffraction.

i. Introduction. The selected area diffraction patterns of graphite and graphite oxide are identical, but little stress can be laid on this in view of the lack of accuracy of the technique. X-ray diffraction was used to obtain information on the changes in the layer spacing, and simultaneous comparative diffraction was used to compare

the in-plane lattice spacings in the two compounds.

ii. X-ray powder photographs. The figures for the lattice spacings of the three stages are given, compared with those of graphite.

Graphite oxide stage i.	PLANE	GRAPHITE OXIDE STAGE I - dÅ	GRAPHITE d(RANGE-Å)
		4.912	
		4.326	
	0002	3.360	3.356 - 3.339
	10 $\bar{1}$ 0	2.122	2.125 - 2.119
	10 $\bar{1}$ 1	2.029	2.029 - 2.025
Graphite oxide stage ii.		STAGE II	
		5.003	
		4.884	
		4.639	
		4.347	
	0002	3.808 & 3.723 3.402 & 3.344 2.950 & 2.900	3.356 - 3.339
		2.324	
		2.204	
	10 $\bar{1}$ 0	2.122	2.125 - 2.119
		2.055	
	10 $\bar{1}$ 1		2.029 - 2.025
		1.642	
Graphite oxide stage iii.		STAGE III	
		7.741	
	0002	3.360	
	10 $\bar{1}$ 0	2.124	2.125 - 2.119

The final oxide has a c-spacing of 7.741Å, falling within the range of 6Å - 11Å, quoted by Hennig (1959) which corresponds to various degrees of hydration. The 3.360Å

spacing in the stage iii pattern may be an unchanged graphite 0002 ring or a second order oxide c spacing. The extra spacings in stages i and ii correspond to intermediate structures, which will be formed when the layers react with different amounts of oxygen and are forced apart to different extents.

The only information from this data on the structure of the layers is that the $10\bar{1}0$ line remains constant within the accuracy of the technique, but the $10\bar{1}1$ line has disappeared just as was reported by Matuyama (1954). This represents a loss in the order of the stacking of the layers.

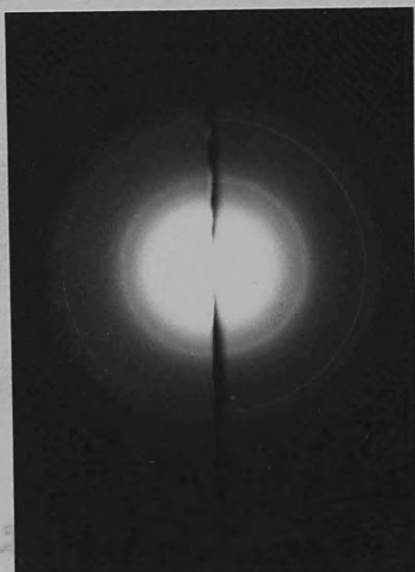
iii. Simultaneous comparative diffraction.

a) Three dimensional order. Plate 54 shows two simultaneous diffraction patterns. A contains a standard pattern, comparing two different concentrations of graphite. Two sets of rings are seen: the inner is the $10\bar{1}0$, $10\bar{1}1$ complex and the outer the $11\bar{2}0$, $11\bar{2}2$ complex. The $10\bar{1}0$ was taken as an internal standard and the spacings of the other three rings calculated and compared with the literature values (Finch and Wilman, 1936).

PLANE	$d\text{\AA}$	EXPERIMENTAL	$d\text{\AA}$	LITERATURE
$10\bar{1}1$		2.032		2.027
$11\bar{2}0$		1.234		1.229
$11\bar{2}2$		1.55		1.154

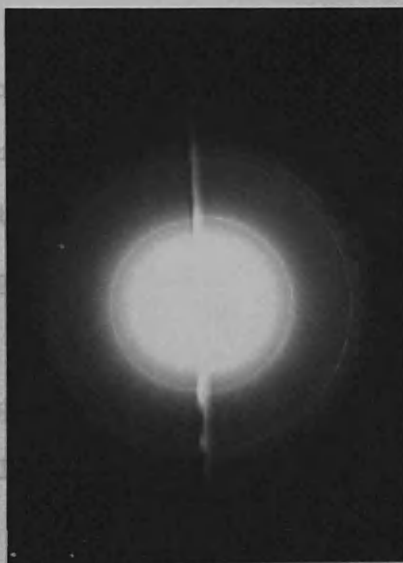
PLATE 54

Pile grade A, polycrystalline synthetic
graphite. Simultaneous comparative
diffraction patterns. Top - Graphite (left)
and a higher concentration of graphite (right)
Bottom - Graphite oxide, Stage III (left) and
graphite (right).



A.

PLATE 54



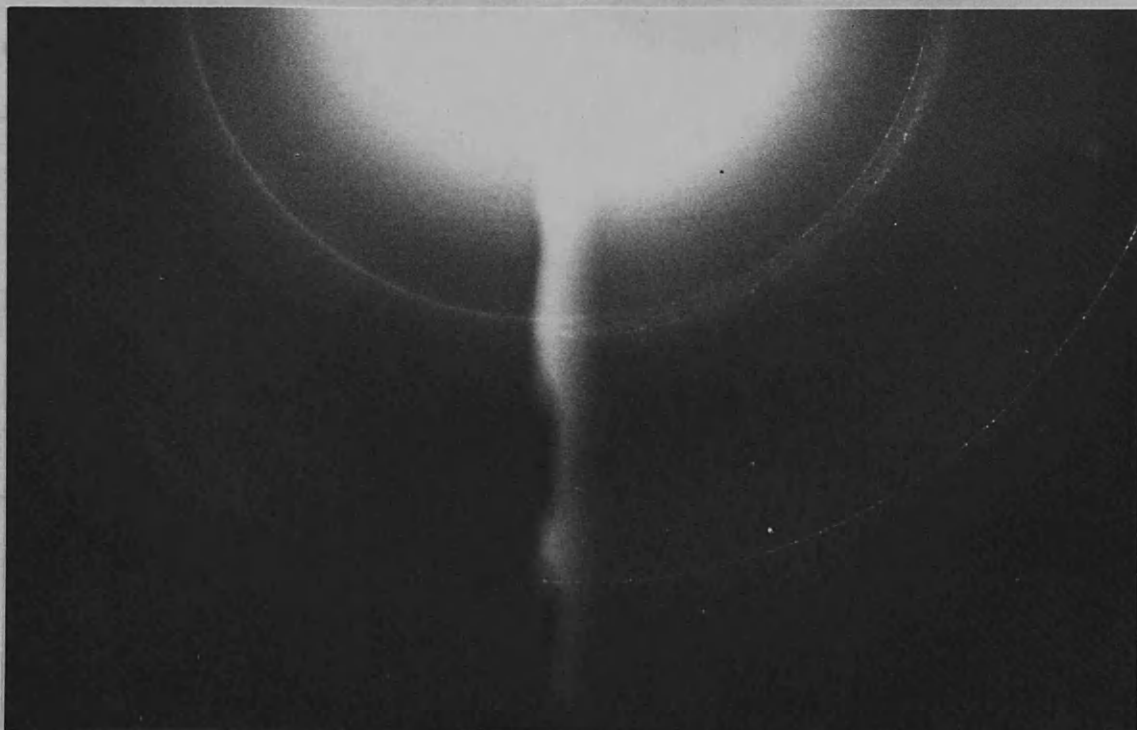
B.

Plate grade A, pyrographite. Similar diffraction pattern as Plate 54, magnified. Graphite (left) and pyrographite (right) of graphite (right) oxide, Stage III.

ation
ite
(right).



A.



B.

This pattern must be compared with 54B, which compares graphite (right) and graphite oxide (left). In the latter, the $10\bar{1}1$ and $11\bar{2}2$ lines have disappeared. This agrees with the X-ray figures (ii) and the results of Matuyama (1954).

b) Nature of the layer planes. Plate 55 shows the overlapping areas of the patterns in Plate 54, printed at a further magnification of 4.2X. As before, A compares two samples of graphite and B compares graphite (right) and its oxide (left). There is exactly the same amount of correspondence between the $10\bar{1}0$ and $11\bar{2}0$ rings for both A and B, suggesting that the layer planes for graphite and its oxide are identical. The X-ray results of De la Cruz and Cowley (1963) report that the C-C spacing in graphite oxide is 1.44\AA and they state that this spacing is compatible with either a flat carbon sheet with a C-C distance of 1.42\AA , or a buckled non-aromatic sheet with a C-C distance of 1.45\AA (Hennig, 1959).

While it is at the limit of any technique to distinguish between these two possibilities, the simultaneous diffraction method does present a good method of comparison of two patterns. The factors limiting the resolution of this method will be listed:

The microscope resolution for diffraction is defined as $d/\Delta d$ where d is a lattice spacing to be measured and Δd

is the difference between it and another spacing from which it is to be resolved (Kay, 1961). In this case for the $10\bar{1}0$ rings, the resolution required is that between two spacings of 2.13\AA (flat layers) and 2.18\AA (buckled layers): this gives a resolution of 42.6. The resolution limit for the microscope for the conditions used here is 1200 (Siemens' technical data) and it should thus be possible to distinguish between the two types of layer for graphite oxide. The emulsion of the plate used has a point resolution of 0.15 mm. (manufacturer's data) and since the resolution required is 0.26 mm., the plate should be sufficiently accurate for the purpose.

In the final print (Plate 55) the difference between the two types of $10\bar{1}0$ ring would be 0.22 cm. in diameter if the oxide had a buckled structure. This size of difference should be noticeable and the fact that the $10\bar{1}0$ rings for graphite and its oxide are exactly the same in diameter suggests that the latter still has the flat unbuckled structure. Because such high resolution results are involved, the final conclusion can, however, be no more than a suggestion.

DISCUSSION.

- I. Structure of the layers in the graphite bisulphate residue compound.
- II. Trapped intercalated material.
- III. Gross oxidation of graphite by a mixture of sulphuric and nitric acids.
- IV. Structural changes during the formation of graphite oxide.
- V. Comparison of the two liquid oxidants.

DISCUSSION

I. STRUCTURE OF THE LAYERS IN GRAPHITE BISULPHATE
RESIDUE COMPOUND.

Information on the changes which have taken place in the lattice during the intercalation process can be obtained by examining the similarities and differences between the residue compound and the parent graphite. The diffraction evidence indicates that the two compounds have an identical structure. The fact that the $10\bar{1}1$ and $11\bar{2}2$ lines appear in the bisulphate diffraction pattern suggests that the stacking sequence of graphite has been retained; this must be contrasted with graphite oxide, where the stacking disorder is reflected in the disappearance of these two lines from the diffraction pattern. In all major respects, therefore, the bisulphate residue compound is identical to the original graphite. On the other hand, the appearance of transparent discs and interference patterns (Results, I, B and C) are considered to be caused by minor changes in the structure which have occurred in the process of the formation and break-up of the lamellar compound.

When the lamellar compound is put in contact with water, the residue compound is formed and this is accompanied by a decrease in the spacing between the layers from 7.89\AA to 3.35\AA , and it is thought that the transparent discs are

are caused by the spontaneous collapse of the layers, giving an amount of local crumpling in the sheets. As the layers come together, most of them must form an ordered ABAB stacking sequence, but the speed with which this is done can leave other parts of the crystal loose and crumpled: an analogous effect is the drying-out of parallel sheets of paper after their immersion in water. The areas containing discs will be crumpled regions of an otherwise regular material, and the fact that the discs sometimes have stacking-fault contrast round their edges confirms this suggestion. These areas may have the rhombohedral stacking, similar to the extended nodes described by Williamson and Baker (1958, 1960 and 1961) and Amelinckx and Delavignette (1963). The edge of each of these areas which is out of register is definite enough to give rise to the interference fringes which are seen as the focussing conditions are changed.

This crumpled material containing discs is the material originally examined in the electron microscope. It is unstable and the movement of the discs is due to the re-arrangement of the badly-fitting parts of the crystal, which will continue until the sheets have become properly pinned in some way. This can be caused by the presence of an impurity, which has been seen in the course of the experiments to halt the movement of the discs. Alternatively, a tight

tight kink can be formed, enabling a stable ABAB stacking to be maintained in the rest of the crystal and these kinks are the folds seen in the electron micrographs (Results, I, B,vi).

It is possible that this crumpling of the sheets is caused by the presence inside the lattice of trapped material which moves as the specimen is heated in the electron beam. If the discs are caused by such inclusion of material, it must be present in the gaseous state, since the spontaneous and almost infinite nature of the expansion of the discs and their failure to join each other or break-up is not typical of the movement of liquid particles. The two possible gases are sulphuric acid vapour or water vapour, the latter entering when the residue compound is formed: such trapped gases could expand quickly as they are heated and cause the layer movements seen in the electron microscope.

Although it is impossible to decide whether the crumpling is caused by the spontaneous collapse of the layers or by the presence of trapped gases, it is more difficult to explain the presence of the other intercalation effects in terms of a residue compound containing gaseous inclusions. It is therefore concluded that the discs are formed by the spontaneous reversal of the intercalation reaction. Further information as to the position of the

the discs can be obtained by counting the number of overlapping discs and comparing this with the number of stacking faults expected (Dawson and Follett, 1959). It was found that two or three discs often overlapped in the less densely populated areas of graphite and that there was an upper limit of about 10 for those areas containing many discs. The numbers of discs which overlapped ranged from 2 to 10 with a peak from 4 to 8. Dawson and Follett (1959) state that their experimental values of 9 to 16 stacking faults agree reasonably well with the theoretical value of 6 to 8 for a typical piece of synthetic graphite. The values calculated from counting the overlap of the discs thus agree well with these two sets of figures and it may be that the areas which contain the disorder leading to the formation of the discs may be those which originally contained the stacking faults.

Another effect which is thought to be due to the spontaneous reversal of the intercalation reaction is the appearance of distorted moire patterns (Results I, C) which are similar to those described by Phillips and Cannon (1960) in graphite, Frankl (1963) in silicon and Fujita and Izui (1963) in molybdenite and graphite. According to Hashimoto (Fujita and Izui, 1963) these Newton-ring defects are due to the presence of vacuum blisters which cause a disorder in the lattice. In the case of the bisulphate

bisulphate residue compound, the ring defects can be due to blisters either of this vacuum type or of intercalated material. In view of the fact that these disordered moiré patterns remain stationary when the specimen is heated, it is probable that they are due to vacuum blisters produced when the sheets collapse on the formation of the residue compound, since all the effects due to the presence of intercalated material can be seen to move on heating. It is thus considered that the discs and the distorted moiré patterns are both a reflection of the fact that the reversal of the intercalation reaction has led to a certain amount of crumpling in the graphite layers. It is interesting to note that the discs often occur in conjunction with ordinary line moirés, but the circular patterns tend to appear on areas free from the usual patterns. Since a moiré pattern is formed by two microcrystals diffracting the electrons in turn, it is clear that the formation of transparent discs or circular moirés occurs under two different diffracting conditions of the component crystals. In the former case, one of the crystallites contains several disordered sheets which are imaged directly as overlapping discs: this one disordered crystallite will not contribute to the formation of a moiré pattern, but those above and below it will act in the usual way. This explains why the discs can be overlaid

overlaid with ordinary line patterns. The disordered and circular patterns must be formed, however, when the crystallite containing the crumpled sheets acts as one of the lattices which contributes to the final pattern. In the optical analogue for the formation of moiré patterns, one of these distorted patterns can be obtained by superimposing an undistorted line grating on a similar one which has been crumpled. This is confirmation of the suggestion that the transparent discs and the circular moiré patterns are both manifestations of the same slight disorder in the graphite lattice.

Another difference between the bisulphate residue compound and graphite can be seen when the movement of the transparent discs is considered - it is obvious that some of the pinning which holds the lattice rigid has been destroyed during the twofold expansion which occurs in the formation of the lamellar compound. Not all of the pinning has been attacked, since the pieces of graphite keep their original shape when the reaction is studied by the in situ technique. The smaller pieces of graphite are left fundamentally intact whereas the intercalation process breaks up the larger pieces in a few minutes of acid attack. It seems that the centres of the individual microcrystals in particular are not so strongly pinned as they were originally, since the transparent discs which

which are thought to be due to a crumpling and looseness in the layers are only found in these centre regions. It would seem that in some cases the bonding between the microcrystals has been broken by the intercalation reaction and that, in addition, some of the pinning between the layers has been loosened. The pinning at the edges of each microcrystal has, however, remained intact. This differentiation between different types of bonding between the layers is seen again when the oxidation of graphite to its oxide is considered, although in this case even the bonds at the edges are finally broken down and the layers can separate completely. In graphite, van der Waals bonding, twinning, impurity atoms and c-axis screws can all act as pinning agents. From the evidence given in this work (Results, I,D) of the adsorption of a line of impurity atoms along microcrystal edges and round the edge of the whole crystal, it is possible that these are the agents that preserve the integrity of the microcrystal when the intercalation process takes place, and that the other pinning points are broken by the intercalating and oxidising effect of the acid, leading to the looseness which may be imaged as transparent discs.

The work reported here shows many effects which are dissimilar to those reported in the literature for other intercalation compounds. The work of Heerschap, ~~Amelinckx~~

Amelinckx and Delavignette (1964) and Beles and Turnbull (1963 and 1965) on the bromine residue compound reported the presence of partial dislocations which had been forced further apart by the presence of areas of intercalate. Since polycrystalline graphite was the material used most regularly in this work these partial dislocation effects were never seen, as this type of graphite is not suitable for studying dislocation networks. On the occasions when purer graphite was used, dislocations were seen only rarely, since the transparent discs obscure completely any other markings on the crystals. It is interesting to note that when polycrystalline synthetic graphite was used to study the bromine compound (Wood, 1964) the dislocation effects were not seen and in fact there was very little difference between the residue compound and the parent graphite. This confirms the suggestion that the non-appearance of the partial dislocations is due to the fact that the material studied was polycrystalline synthetic graphite. Another difference between the bisulphate and the bromine residue compounds is that transparent discs are not reported for the latter. In view of the fact that the discs are thought to arise by the sudden removal of the acid, it may be that the absence of discs in the bromine compound is due to smoother removal of the gaseous bromine.

II. TRAPPED INTERCALATED MATERIAL.

Hennig (1961) reports that one third of the bisulphate ion and one half of the free acid originally present in the lamellar compound is retained after the formation of the residue compound, and that the ratio of anion to acid in the latter is 1:4. From an electron microscope study, it is impossible to gain quantitative information about the amount of intercalate present, but the comparative rarity of the areas containing dense material suggests that there may not be as much retained as Hennig's results indicate. These dense areas are certainly no more common than the areas containing solid deposits of uranyl nitrate, and the analytical figures indicate that this is present in small quantities only. By comparison with Hennig's figures on a more qualitative basis, however, it is probable that the dense discs are formed from bisulphate and the mobile dense particles are composed of free sulphuric acid, since the former are much less common than the latter.

In the Results, I, D, it was stated that the dense discs could be due to the direct image of small round particles with a tapered edge or to a moiré effect, giving an indirect image of areas which still contain bisulphate ions. For the bisulphate regions to appear in either of these ways implied crystallinity or regularity to a certain extent and if the intercalate was present to

to the extent suggested by Hennig (1951) it is surprising that the powder diffraction pattern should not show extra lines corresponding to the retention of this regularly placed material. It is also concluded that Hennig's suggestion that the trapped bisulphate is present in a totally disordered fashion may not be valid, but that small areas of bisulphate crystal probably exist, and that these are seen in the electron microscope, probably by a double diffraction process.

The free sulphuric acid, on the other hand, is present in a highly mobile, disordered state. From the figures given (Results, I, D) for the boiling point of the acid, it seems that it is physically trapped by tightly clamped areas of graphite which prevent it from evaporating when the residue compound is subjected to an increase of temperature and a decrease of pressure in the electron microscope. The particles of acid can move around inside the microcrystals, or along channels and acid can also be adsorbed along cracks or faults.

III. GROSS OXIDATION OF GRAPHITE BY A MIXTURE OF SULPHURIC AND NITRIC ACIDS.

While short term reaction with this reagent produces oxidation only with respect to the electronic levels of graphite, the long term reaction produces all the typical signs of gross oxidation (Results, II, A). In this respect the effects for the reaction of polycrystalline synthetic graphite are exactly the same as those found by Dawson and Follett (1963) for air oxidation of the same material. Since the rate is smaller by a factor of some thousands, it is possible to follow the production of channels from fine punctate cracks which are probably microcracks between crystallites. This is **in** agreement with the suggestion of Lang and Magnier (1963) that oxidation attack is dependent on the number of microcracks present.

Another factor which is important for the mechanism of oxidation is the impurity content of the graphite. Like air oxidation, the acid reaction is catalysed by the presence of heavy metals, and evidence has also been given (Results, II, D) for the preferential adsorption of material from the acid along the edges of the crystallites. Since polycrystalline graphite

graphite already contains more impurity than does natural material , it is probable that the channels are always formed by a catalytic process. Since the impurities present are concentrated along the grain boundaries (Bauer, 1961) the effects of catalysts and micro-pores on the oxidation rate are inseparable. The reason for the large amount of impurity present in these areas is that they contain a high concentration of defects and this combination of defect and impurity concentrations influencing the reaction is in general agreement with the conclusions of the work on gaseous oxidation (Hennig, 1962; Hughes, and Thomas, 1962; Hughes, Williams and Thomas, 1962; Thomas, Hughes and Williams, 1963 and Hughes, Thomas, Marsh and Reed, 1964).

The importance of these two factors is again seen when the differences in rate and mechanism of oxidation are examined for polycrystalline synthetic graphite and purified natural graphites. The latter is much more resistant to attack and can remain in acid for up to 9 weeks with no signs of oxidation whereas the former contains fine channels after only a few days reaction. Although the purified natural graphite does contain a smaller amount of impurity (Experimental, I, iv) addition of catalyst

catalyst does not bring its rate of oxidation up to that of the polycrystalline material. The fact that the purified natural graphite is almost single crystal in nature is reflected in the lack of channels arising from micropores.

Any channels which do occur after the oxidation of the natural graphite are of the type with a catalyst particle at the head. These differ from the ones described for air oxidation by Hennig (1962) and Presland and Hedley (1962 and 1963) in that they do not taper. The fact that tapering has not appeared after fifteen weeks' reaction is another reflection of the small rate of reaction of the acid attack since tapering is caused by further attack at one end of the channel.

It can therefore be concluded that the oxidation of graphite by acid is similar in all respects to that by oxygen and that the only difference is that the rate is very much smaller. For the air reaction, a surface oxide is postulated as an intermediate by Strickland-Constable (1965) and Marsh, O'Hair and Wynne-Jones (1965). An intermediate of this type remains in the channels in the early stages of the reaction with acid: it has a granular

granular appearance and has a diffraction pattern identical to that of graphite. It may therefore, be a substance of the type C_3O_2 , described by Smith, Young, Smith and Carter (1963). With oxidation using an intercalating reagent such as sulphuric acid, there is an excellent chance of such an intermediate being seen in the electron microscope, since the reagent will penetrate the crystal completely. Any intermediate can then be formed in pores which may not be reached by the water used for cleaning and evaporation will be prevented by the tight clamping of some areas of the graphite on the reversal of the intercalation reaction.

The attack by atomic oxygen is described by Marsh, O'Hair and Reed (1965) as producing widespread pitting and conical hillocks, and none of these features is seen after attack by acid. The accelerating effect of impurities (Results, II, A, iii) is not consistent with the report of Lang, Magnier and Brie (1965) that the oxidation by atomic oxygen shows no increase in rate on the addition of catalysts. The oxidation with acid is thus similar only to that by molecular oxygen.

IV. STRUCTURAL CHANGES DURING THE FORMATION OF GRAPHITE OXIDE.

A good deal can be learned of these changes by considering the appearance and disappearance of the transparent discs (Results, IV, B) as the oxidation proceeds. On the assumption that these discs are an indication of crumpling in the layers (Discussion, I), stages i) and ii) of the oxide show an increasing disorder of this type. The stage ii) oxide, in addition to containing a large number of atatic discs, also shows many extra spacings in its diffraction pattern. These two facts suggest that there is a large amount of crumpling in the layers and that this is pinned in some way, to prevent movement. The pinning is probably due to the fact that there is now a considerable amount of oxygen bound to the lattice, and most of this will be found round the crystallites since these regions contain a high defect concentration and will be more susceptible to oxidation. The dense ridges seen in these regions are more highly oxidised than the centre of the crystallites, since they have an appearance similar to the oxidation intermediate of the reaction with sulphuric and nitric acids and they are also the fore-runners of channels. It is also possible that

that enough oxygen is incorporated into the lattice at this stage to attract adsorbed water inside the crystallites, thus pushing the layers even further apart and preventing movement when the sample is examined in the electron microscope.

By stage iii), the discs have completely disappeared, since there is no longer any collapse of the layers when the compound is immersed in water. In fact, the final oxide, which contains a large amount of oxygen, will expand even further as it is hydrated and only a small amount of over-all folding will occur as the material dries out. It was suggested above that there is preferential oxidation round the edges of the crystallites, producing first of all ridges and then channels. The folded regions in the intermediate stages may also represent areas with a high concentration of oxygen in the form of COOH or epoxy groups. This is confirmed by the fact that in the final stage the pits are always associated with the edge of a crystallite or a fold, and these have been formed by further local attack at regions already partially oxidised.

The final oxide thus contains sheets which have become separated as the pinning joining the layers is attacked and broken. As a result, the layers.

layers lose their overall rigidity (Clauss, Plass, Boehm and Hoffmann, 1957) and the aromatic sheets have given way to alkane rings which are probably kept planar because of keto-enol tautomerism. The simultaneous comparative diffraction data (Results, IV, C, iii) confirm this suggestion for the structure of the sheets.

The gradual loss of order of the layers relative to each other is reflected in the disappearance of moiré patterns (Results, IV, B) which are formed by double diffraction from two crystallites and a disappearance of the ABAB stacking in graphite will mean that this effect is lost. This is confirmed by the loss of the 1011 and 11 $\bar{2}$ 2 lines in the diffraction pattern as the oxide is formed (Results, IV, C and Matuyama, 1954). As more is incorporated into the lattice, forcing the layers apart and forming the graphite oxide, the stacking order is destroyed.

V. COMPARISON OF THE TWO LIQUID OXIDANTS.

The mixture of sulphuric and nitric acids attacks the graphite at defects and crystallite boundaries and this attack is catalytic in nature. It thus produces pits and channels but it does not alter the structure of the lattice in any way. The other reagent, on the other hand, attacks the sheets themselves as well as causing the same gross oxidation effects. A large amount of oxygen is incorporated into the sheets themselves and this increases enormously the rate of gross oxidation, since pits and channels are a common feature after only six hours in the reagent. In addition, the order between the sheets has been destroyed and the material is no longer graphite. The difference between the two processes can be summarised thus: the sulphuric and nitric acid reagent produces local oxidation only while the other oxidant also oxidises the sheets themselves to produce graphite oxide.

References

- Adamson, I.Y.R.A. (1963) - B.Sc. Thesis, Glasgow.
- Agar, A.W., Frank, F.C. & Keller, A. (1959) Phil.Mag., 4, 32.
- Alexanian, C. (1961) J. Chim. Phys., 58, 133.
- Amelinckx, S. (1956) Phil. Mag., 1, 269.
- " (1963) "The Interaction of Radiation with Solids." Proc. Int. Summer School on Solid State Physics, Mol, 683.
- Amelinckx, S. & Delavignette, P. (1960a) Phil.Mag., 5, 533.
- " " (1960b) Nat., 185, 603.
- " " (1960c) Phys.Rev.Let., 5, 50.
- " " (1960d) J.Appl.Phys., 31, 2126.
- " " (1961) "Direct Observation of Imperfections in Crystals" p.295.
- " " (1963) "Electron Microscopy and Strength of Crystals" Interscience p.441.
- Armour Research Foundation of Illinois Institute of Technology (1949) Analyt. Chem., 21, 1151.
- Bacon, G.E. (1950) Acta Cryst., 3, 137.
- " (1951) Acta Cryst., 4, 558.
- " (1952) Acta Cryst., 5, 392.
- " (1958a) Ind. Carbon and Graphite, 183.
- " (1958b) Aere Report M/R 2702.
- Bacon, G.E. & Franklin, R.E. (1951) Acta Cryst., 4, 561.
- Bacon, G.E. & Warren, B.E. (1956) Acta Cryst., 9, 1029.
- Bacon, R. & Sprague, R. (1961a) "Direct Observation of Imperfections in Crystals." 357.
- " " (1961b) Proc. 5th Conf. on Carbon.p.466.

- Baker, C. (1962) 5th Int. Congress Electron Microscopy, Philadelphia, I, I-11.
- Baker, C., Chou, Y.T., & Kelly, A. (1961) Phil. Mag., 6, 1305.
- Baker, C., Gillin, L.M. & Kelly, A. (1965) 2nd Ind. Carbon and Graphite Conference, London.
- Bassett, G.A., Menter, J.W. & Pashley, D.W. (1958) Proc. Roy. Soc. A, 246, 345.
- Bauer, E. (1961) J. Chim. Phys., 58, 47.
- Beckett, R.J. & Croft, R.C. (1952) J. Phys. Chem., 56, 929.
- Bernal, J.D. (1924) Proc. Roy. Soc. A, 106, 749.
- Berthelot, M. & Petit, P. (1870) Ann. Chim. Phys., 19, 401.
- Boehm, H.P., Clauss, A. & Hofmann, U. (1961) J.Chim.Phys., 58, 141.
- Boehm, H.P. & Hofmann, U. (1955) Z.Anorg.Chem., 278, 58.
- Bollmann, W. (1960) Phil. Mag., 5, 621.
- " (1961a) Proc. 5th Conf. Carbon, Phil.II, 303.
- " (1961b) Proc. Eur. Reg. Conf. Electron Microscopy, Delft., 330.
- " (1961c) Proc. Int. Conf. Properties of Reactor Materials, 132.
- " (1962) Phil. Mag., 7₂, 1513.
- Bollmann, W. & Hennig, G.R. (1964) Carbon, 1, 525.
- Bonfiglioli, G. & Mojoni, A. (1964) J. Appl. Phys., 35, 683.
- Boswell, F.W.C. (1961) Proc. Eur. Conf. Electron Microscopy, Delft, 409.
- Bottomley, M.J., Parry, G.S., Ubbelohde, A.R. & Young, D.A. (1963) J. Chem. Soc., 5674.
- Bragg, W.L. (1913) Proc. Roy. Soc.A, 248, 468.

iii.

- Bradley, D.E. (1954) Brit. J.Appl.Phys., 5, 65.
- " (1959) Brit. J.Appl.Phys., 10, 198.
- Brodie, B.C. (1859) Phil. Trans. Roy. Soc., 149, 249.
- Carter, J.L. & Krumhausl, J.A. (1953) J.Chem.Phys., 21,2238.
- Clauss, A., Plass, R., Boehm, H-P. & Hofmann, U. (1957)
Z. Anorg. U. Allgem. Chem., 291, 205.
- Cosslett, V.E. (1951) "Practical Electron Microscopy."
- Coulson, C.A. (1947) Nat., 159, 265.
- Coulson, C.A. & Taylor, R. (1952) Proc. Phys.Soc.A., 65, 815.
- Cowley, J.W. & Ibers, J.A. (1956) Acta Cryst., 9, 421.
- Croft, R.C. (1952) J. Appl. Chem., 2, 557.
- " (1953) Nat., 172, 725.
- " (1956a) Austral. J. Chem., 9, 184.
- " (1956b) Austral. J. Chem., 9, 194.
- " (1956c) Austral. J. Chem., 9, 201.
- " (1956d) Austral. J. Chem., 9, 206.
- " (1957a) Research (London), 10, 23.
- " (1957b) Proc. 3rd Conf. on Carbon, 315.
- " (1960) Quart. Rev., XIV, 1, 1.
- Croft, R.C. & Thomas, R.G. (1951) Nat., 168, 32.
- Damiano, V.V. (1962) 5th Int. Congress Electron Microscopy,
Philadelphia, I, B-6.
- Dawson, I.M. & Follett, E.A.C. (1959) Proc. Roy. Soc. A., 253,390.
- " " (1961) Atomic Energy Report.
- " " (1962) 5th Int. Congress
Electron Microscopy, Philadelphia, I, 1-8.

- Dawson, I.M. & Follett, E.A.C. (1963) Proc. Roy.Soc.A., 274, 386.
- Dawson, I.M., Follett, E.A.C. & Donaldson, D.M. (1961)
Proc. Eur. Reg. Conf. E.M., Delft., 337.
- De Boer, J.H. & Van Doorn, A.B.C. (1958) Industrial Carbon
and Graphite, Soc. Chem. Ind., London, p.302.
- De la Cruz, F. & Cowley, J.M. (1963) Acta Cryst., 16, 531.
- Delavignette, P & Amelinckx, S. (1960) Phil.Mag., 5, 729.
- " " (1961) Proc. Eur. Reg. Conf.
Electron Microscopy, Delft, 404.
- Dowell, W.C.T., Farrant, J.L. & Rees, A.L.G. (1954) Proc. Int.
Conf. Electron Microscopy, London, 279.
- " " " (1958) 4th Int.
Conf. Electron Microscopy, Berlin, 367.
- Duval, X. (1961) J. Chim. Phys., 58, 3.
- Dzurus, M.L. & Hennig, G.R. (1957) J. Chem. Phys., 27, 275.
- Ewald, P.P. (1924) Sitzungsber Munch. Akad., 4, 7.
- Eeles, W.T. & Turnbull, J.A. (1963) Nat., 198, 877.
- " " (1965) Proc. Roy. Soc. A., 283, 179.
- Finch, G.I., Quarrell, A.G. & Wilman, H. (1935) Trans. Far. Soc.,
31, 1051.
- Finch, G.I. & Wilman, H. (1936) Proc. Roy. Soc. A., 155, 345.
- Follett, E.A.C. (1963) Unpublished work.
- Frankl, D.R. (1963) J. Appl. Phys., 34 (12), 3514.
- Franklin, R.E. (1950) J. Chim. Phys., 47, 573.
- " (1951a) Acta Cryst., 4, 253.
- " (1951b) Compt. Rend., 232, 232.
- " (1951c) Proc. Roy. Soc. A., 209, 196.

- Friedel, J. (1964) "Dislocations"
- Freise, E.J. (1962) Nat., 193, 671.
- Freise, E.J. & Kelly, A. (1961) Proc. Roy. Soc. A., 264, 269.
- " " (1963) Phil. Mag., 8, 1519.
- Fujita, F.E. & Izui, K. (1963) Proc. 5th Conf. on Carbon, II, 297.
- Ganguli, N. (1936) Phil. Mag., 21, 355.
- Gevers, R. (1963) "The Interaction of Radiation with Solids",
p.471.
- Goodman, J.F. (1957) Nat., 80, 425.
- Greer, E.N. & Topley, B. (1932) Nat., 129, 904.
- Grenall, A. (1958) Nat., 182, 448.
- Grenall, A. & Sosin, A. (1960) Proc. 4th Conf. on Carbon, 371.
- Hadzi, D. & Novak, A. (1955) Trans. Far. Soc., 51, 1614.
- Hall, C.E. (1953) "Introduction to Electron Microscopy."
- "Handbook of Chemistry and Physics"- Chemical Rubber
Publishing Co.
- Hashimoto, H. & Oyeda, R. (1957) Acta Cryst., 10, 143.
- Hauser, E.A. & Lynn, J.E. (1940) "Experiments in Colloid
Chemistry." McGraw-Hill.
- Hedges, J.M. & Mitchell, J.W. (1953a) Phil. Mag., 44, 223.
- " " (1953b) Phil. Mag., 44, 357.
- Heershap, M., Delavignette, P. & Amelinckx, S. (1964)
Carbon, 1, 235.

- Hennig, G. R. (1951) J. Chem. Phys., 19, 922.
- " (1952) J. Chem. Phys., 20, 1438.
- " (1956) Proc. 1st & 2nd Conf. on Carbon, 103.
- " (1959a) Prog. Inorg. Chem., 1, 125.
- " (1959b) Proc. 3rd Conf. on Carbon, 265.
- " (1960a) Proc. 4th Conf. on Carbon, 221.
- " (1960b) Proc. 4th Conf. on Carbon, 145.
- " (1961) J. Chim. Phys., 58, 12.
- " (1962) J. Inorg. Nucl. Chem., 24, 1129.
- " (1964a) J. Chem. Phys., 40, 2877.
- " (1964b) Appl. Phys. Letters., 4, 52.
- " (1964c) Appl. Phys. Letters., 4, 55.
- Hennig, G. R. & Kantar, M.A. (1960) Proc. 4th Conf. on Carbon, 141.
- Hennig, G.R. & McClelland, J.D. (1955) J. Chem. Phys., 23, 1431.
- Henry, N.F.M., Lipson, H. & Wooster, W.A. (1951) - "The Interpretation of X-Ray Diffraction Photographs"-Macmillan.
- Heindle, R.A. & Mohler, N.F. (1955) J. Amer. Ceramic Soc., 38, 89.
- Hesketh, R.V. (1964) J. Appl. Phys., 35, 3604.
- Hillier, J. (1954) Nat. Bur. Stand. Circ., 527, 413.
- Hirsch, P.B., Horne, R.W. & Whelan, M.J. (1956) Phil. Mag., 1, 677.
- Hirsch, P.B., Howie, H. & Whelan, M.J. (1960)
- Hirsch, P.B., Silcox, J., Smallman, R.E., & Westmacott, K.H. (1958) Phil. Mag., 3, 897.
- Hofmann, U. & Frenzel, A. (1930) Ber., 63, 1248.
- Hofmann, U. & Holst, R. (1939) Ber., 72, 754.

- Hofmann, U. & König, E. (1937) Zeit. F. Anorg. U. Allgem. Chem.
234, 311.
- Hofmann, U. & Rüdorff, W. (1938) Trans. Far. Soc., 34, 1017.
- Hooker, C.N., Ubbelohde, A.R. & Young, D.A. (1963)
Proc. Roy. Soc. A., 276, 83.
- Hove, J.E. (1955) Phys. Rev., 100, 645.
- Howie, H. (1961) "Direct Observation of Imperfections in
Crystals." p.269.
- Howie, H. & Whelan, M.J. (1961) Proc. Eur. Conf. Electron
Microscopy, Delft, 194.
- Hughes, Glenda E.E. & Thomas, J.M. (1962) Nat., 193, 838.
- Hughes, Glenda E.E., Thomas, J.M., Marsh, H. & Reed, R. (1964)
Carbon, 1, 339.
- Hughes, Glenda E.E., Williams, B.R. & Thomas, J.M. (1962)
Trans. Far. Soc., 58, 2011.
- Hull, A.W. (1917) Phys. Rev., 10, 661.
- Hummers, W.S. & Offeman, R.E. (1958) J. Amer. Chem. Soc., 80, 1, 1339.
- Izui, K. & Fujita, F.E. (1963) J. Phys. Soc. Japan, 18, 467.
- Jacquet, M. & Guérin, H. (1962) Bull. Soc. Chim. Franc., 5S, 411.
- Jenkins, G.M., Turnbull, J.A. & Williamson, G.K. (1962)
5th Int. Con. Electron Microscopy, Philadelphia, I, GG-11.
- Kay, D. (1961) "Techniques for Electron Microscopy."
- Kmetko, E.A. (1951) Phys. Rev., 82, 456.
- " (1953) J. Chem. Phys., 21, 2152.
- Kranitz, M. & Seal, M. (1962) 5th Int. Cong. Electron
Microscopy, Philadelphia, I, F.F.-7.
- Krishnan, K.S. & Ganguli, N. (1939) Z. Krist. A., 100, 530.

- Labaton, V. (1965) Personal Communication.
- Laidler, D. & Taylor, A. (1940) Nat., 146, 130.
- Lang, F.M. & Magnier, P. (1963) J. Chim. Phys., 60, 251.
- Lang, F.M., Magnier, P. & Brie, M. (1965) Second Ind. Carbon and Graphite Conf., London.
- Lang, F.M., Magnier, P., Sella, C. & Trillat, J.J. (1962) Compt. Rend., 254, 4114.
- Lind, R. (1964) Personal Communication.
- Lipson, H. & Stokes, A.R. (1942a) Nat., 149, 328.
- " " (1942b) Proc.Roy.Soc.A., 181, 101.
- Lukesh, J.S. (1950) Phys. Rev., 80, 226.
- " (1951a) J. Chem. Phys., 19, 384.
- " (1951b) J. Chem. Phys., 19, 1203.
- McDonnel, F.R.M., Pink, R.C. & Ubbelohde, A.R. (1951) J. Chem. Soc., 191.
- Maire, J. (1951) Compt. Rend., 232, 61.
- Maire, J. & Mathieu-Sicaud, A. (1952) Bull. Soc. Franc. de Mineralogie, 75, 599
- Maire, J. & Mering, J. (1959) Proc. 3rd Conf. on Carbon, 337.
- Marsh, H., O'Hair, T.E. & Reed, R. (1965) Trans.Far.Soc., 61, 285.
- Marsh, H., O'Hair, T.E. & Wynne-Jones, W.F.K. (1965) Trans. Far. Soc., 61, 274.
- Matuyama, E. (1952) Nat., 170, 1123.
- " (1954) J. Phys. Chem., 58, 215.
- Mellor, J.W. (1930) "A Comprehensive Treatise on Inorganic and Theoretical Chemistry", Vol.X., Longmans, Green & Co.

- Menter, J.W. (1956) Proc. Roy. Soc. A., 236, 119.
- " (1958) 4th Int. Conf. Electron Microscopy,
Berlin, 320.
- Meyer, L. (1938) Trans. Far. Soc., 34, 1056.
- Mitchell, J.W. (1961) "Direct Observation of Imperfections
in Crystals" p.3.
- Mitsuishi, T., Nagasaki, H. & Uyeda, R. (1951) Proc. Imp.
Acad. Japan, 27, 86.
- Mrozowski, S. (1950a) Phys. Rev., 77, 838.
- " (1950b) Phys. Rev., 78, 644.
- " (1952a) Phys. Rev., 85, 609.
- " (1952b) Phys. Rev., 86, 822.
- " (1953) J. Chem. Phys., 21, 492.
- Nicholson, R.B. (1963) - "Electron Microscopy and Strength
of Crystals" - Thomas G. & Washburn, J., Ed., p.861.
(Interscience)
- Oberlin, M. & Mering, J. (1961) Compt. Rend., 253, 2549.
- " " (1964) Carbon, 1, 471.
- Oberlin, M., Rappeneau, J. & Yvars, M. (1964) Carbon, 1, 481.
- Pashley, D.W., Menter, J.W. & Bassett, G.A. (1957) Nat., 179, 752.
- Phillips, V.A. & Cannon, P. (1960) Nat., 187, 313.
- Pinsker, Z.G. (1953) - "Electron Diffraction."
- Presland, A.E.B. & Hedley, J.A. (1962) 5th Int. Cong. Electron
Microscopy, Philadelphia, I, I-10.
- " " (1963) AERE/EMR/PR/1538/2.
- Rang, J. (1953) Z. Phys., 136, 465.
- Read, W.T. (1953) - "Dislocations in Crystals."

- Reynolds, W.N. & Thrower, P.A. (1964) Carbon, 1, 185.
- Reynolds, W.N., Thrower, P.A. & Sheldon, B.E. (1961) Nat., 189, 824.
- Riedmiller, R. (1936) Zeit. Fur. Phys., 102, 408.
- Riley, H.L. (1945a) Fuel, 24, 8.
- " (1945b) Fuel, 24, 43.
- Rüdorff, W. (1939) Z. Physik. Chem., B45, 42.
- Rüdorff, W. & Hofmann, U. (1938) Zeit. Fur. Anorg. und
Allgem. Chem., 238, 1.
- Rüdorff, W. & Rüdorff, G. (1947a) Z. Anorg. u. Allgem. Chem., 253, 281.
- " " (1947b) Chem. Ber., 80, 417.
- Ruess, G.L. (1946a) Monatsh., 76, 168.
- " (1946b) Monatsh., 76, 381.
- Ruff, O. & Brettschneider, O. (1934) Z. Anorg. u. Allgem. Chem.,
217, 1.
- Ruiz, J. Cano & Macewan, D.M.C. (1955) Nat., 176, 1222.
- Ruska, E. & Borries, B.V. "Elmiskop I - Siemens Electron
Microscope"
- Schaufhäutl, P. (1841) J. Prakt. Chem., 21, 155.
- Schmidt, L., Boehm, H.P. & Hofmann, U. (1958) Z. Anorg. Chem.,
296, 246.
- Seki, Y. (1953) J. Phys. Soc. Japan, 8, 149.
- Sella, M.C., Miloche, M. & Trillat, J.J. (1962) Compt. Rend.,
255, 10.
- Sella, C. & M.F., & Trillat, J.J. (1962) 5th Int. Cong.
Electron Microscopy, Philadelphia, I, G-3.
- Siems, R., Delavignette, P. & Amelinckx, S. (1962)
5th Int. Cong. on Electron Microscopy, Philadelphia, I, B-2.
- Smith, R.N., Young, D.A., Smith, E.N. & Carter, C.C. (1963)
Inorg. Chem., 2, 829.

- Staudenmaier, L. (1898) Ber., 31, 1481.
- " (1899) Ber., 32, 1394.
- " (1900) Ber., 33, 2824.
- Strickland-Constable, R.F. (1965) 2nd Conf. on Ind. Carbon and Graphite, London.
- Structure Reports (1949) 12, 236.
- Taylor, A. & Laidler, D. (1940) Nat., 146, 130.
- Thiele, H. (1932) Z. Anorg. u. Allgem. Chem., 207, 340.
- Thomas, J.M., Hughes, Glenda E.E. & Williams, B.H. (1963) Phil. Mag., 85, 8₂, 1513.
- Thomas, J.M. & Roscoe, C. (1965) 2nd Conf. on Ind. Carbon and Graphite, London.
- Thomson, G.P. & Cochrane, W. (1939) "Theory and Practice of Electron Diffraction."
- Trezbiatowski, W. (1937) Roczniki Chem., 17, 73.
- Tsuzuku, T. (1957) Proc. 3rd Conf. on Carbon, 433.
- Turnbull, J.A. & Eeles, W.T. (1965) 2nd Conf. on Ind. Carbon and Graphite, London.
- Tyler, W.W. & Wilson, A.C. (1953) Phys. Rev., 89, 870.
- Ubbelohde, A.R. (1957) Nat., 180, 380.
- " (1961) J. Chim. Phys., 58, 107.
- " (1964) Carbon, 2, 23.
- Ubbelohde, A.R. & Lewis, F.A. (1960) "Graphite and its Crystal Compounds."
- Walker, P. (1965) Personal Communication.
- Wallace, P.R. (1947) Phys. Rev., 71, 622.

- Warren, B.E. (1934) J. Chem. Phys., 2, 551.
- Watanabe, M. Someya, T. & Nagahuma, Y. (1962) 5th Int.
Cong. Electron Microscopy, Philadelphia, A-8.
- Watt, J.D. & Franklin, R.E. (1957) Nat., 180, 1190.
- " " (1958) Ind. Carbon & Graphite,
321.
- Whelan, M.J. & Hirsch, P.B. (1957a) Phil. Mag., 2, 1121.
- " " (1957b) Phil. Mag., 2, 1303.
- Whelan, M.J., Hirsch, P.B., Horne, R.W. & Bollman, W.
(1957). Proc. Roy. Soc. A., 240, 524.
- Williamson, G.K. (1961) Prop. of Reactor Materials, 144.
- Williamson, G.K. & Baker, C. (1958) Proc. Roy. Soc. A.,
249, 114.
- " " (1960a) Proc. Roy. Soc. A.,
257, 457.
- " " (1960b) Proc. Eur. Reg. Conf.
Electron Microscopy, Delft, 326.
- " " (1961a) Phil. Mag., 6, 313.
- " " (1961b) Proc. 5th Conf.
Carbon, II, 521.
- Wood, C.A. (1964). Ph.D. Thesis, Glasgow.
- Zworkykin, E.E., Morton, G.A., Ramberg, E.G., Hillier,
J. & Vance, A.W. (1945) "Electron Optics and the
Electron Microscope".